

A Additional Tables

Table 14: *Photometry available for the WC sample. The horizontal lines divide the individual spectral subtypes, from top to bottom: unknown-WC4-WC5-WC6-WC7-WC8*

M31 WR	LGGS	<i>U</i>	<i>B</i>	<i>V</i>	<i>R</i>	<i>I</i>	<i>U</i> - <i>B</i>	<i>B</i> - <i>V</i>	<i>V</i> - <i>R</i>	<i>R</i> - <i>I</i>	
99	J004416.20+412103.5	18.134	19.091	19.473	18.970	19.187	-0.957	-0.382	0.503	0.217	
133	J004513.68+413742.5	21.256	21.306	20.913	20.648	20.853	-0.050	0.393	0.265	0.205	
WC4	3	J003919.53+402211.6	18.757	19.555	19.170	18.920	19.174	-0.798	0.385	0.250	0.254
	12	J004019.47+405224.9	19.767	20.328	20.554	20.448	19.993	-0.561	-0.226	0.106	-0.455
	15	J004022.43+405234.6	19.332	19.907	20.179	19.987	19.870	-0.575	-0.272	0.192	-0.117
	23	J004034.69+404432.9	19.729	20.264	20.710	20.606	20.522	-0.535	-0.446	0.104	-0.084
	54	J004213.21+405051.8	20.850	21.004	21.105	20.931	20.884	-0.154	-0.101	0.174	-0.047
	61	J004247.12+405657.1	20.289	20.753	20.691	20.478	20.406	-0.464	0.062	0.213	-0.072
	140	J004530.61+414639.2	21.223	21.961	21.417	20.666	21.003	-0.738	0.544	0.751	0.337
WC5	4	J003933.46+402018.9	18.467	19.115	19.151	19.034	18.772	-0.648	-0.036	0.117	-0.262
	19	J004029.27+403916.6	20.603	20.942	21.211	21.026	20.852	-0.339	-0.269	0.185	-0.174
	35	J004109.59+404856.2	18.141	18.937	18.968	18.918	18.913	-0.796	-0.031	0.050	-0.005
	62	J004249.84+410215.7	21.898	21.839	21.634	21.318	21.502	0.059	0.205	0.316	0.184
	98	J004415.77+411952.5	23.016	22.990	22.774	22.380	?	0.026	0.216	0.394	?
	111	J004435.15+412545.2	21.566	21.710	21.638	21.411	21.063	-0.144	0.072	0.227	-0.348
	113	J004436.52+412202.0	20.463	20.678	20.926	20.709	20.458	-0.215	-0.248	0.217	-0.251
	138	J004522.78+420318.2	22.369	22.155	21.940	21.706	21.712	0.214	0.215	0.234	0.006
	146	J004539.35+414439.8	21.580	21.807	21.499	21.211	21.313	-0.227	0.308	0.288	0.102
	150	J004551.12+421015.4	20.370	20.591	20.890	20.670	20.511	-0.221	-0.299	0.220	-0.159
WC6	2	J003911.04+403817.5	19.934	20.235	20.587	20.379	20.148	-0.301	-0.352	0.208	-0.231
	7	J003939.97+403450.4	20.024	20.496	20.670	20.401	20.719	-0.472	-0.174	0.269	0.318
	13	J004020.44+404807.7	19.378	19.855	20.193	20.035	19.867	-0.477	-0.338	0.158	-0.168
	26	J004043.28+403525.2	22.802	22.620	22.095	21.609	21.904	0.182	0.525	0.486	0.295
	29	J004058.49+410414.8	21.883	21.995	21.892	21.570	21.898	-0.112	0.103	0.322	0.328
	30	J004059.13+403652.0	20.804	21.160	20.731	20.297	20.575	-0.356	0.429	0.434	0.278
	33	J004107.31+410417.0	21.502	21.603	21.307	21.025	21.292	-0.101	0.296	0.282	0.267
	47	J004144.47+404517.1	18.843	19.715	19.475	19.395	19.563	-0.872	0.240	0.080	0.168
	51	J004154.62+404713.8	22.115	22.280	21.700	20.922	21.213	-0.165	0.580	0.778	0.291
	52	J004203.94+412554.5	18.795	19.464	19.325	19.173	19.320	-0.669	0.139	0.152	0.147
	55	J004214.36+412542.3	20.992	20.924	20.708	20.315	20.556	0.068	0.216	0.393	0.241
	58	J004240.81+410241.6	20.810	20.818	20.417	19.994	20.173	-0.008	0.401	0.423	0.179
	64	X004256.05+413543.7	?	?	?	?	?	?	?	?	?
	71	X004308.25+413736.3	?	?	?	?	?	?	?	?	?
	73	J004316.44+414512.4	19.572	20.190	19.964	19.707	19.947	-0.618	0.226	0.257	0.240
	77	J004327.92+414207.3	20.127	20.726	20.474	20.246	20.418	-0.599	0.252	0.228	0.172
	84	J004341.72+412304.2	19.921	20.313	20.643	20.388	19.851	-0.392	-0.330	0.255	-0.537
	91	J004406.39+411921.0	20.780	21.023	21.331	21.046	21.387	-0.243	-0.308	0.285	0.341
	93	J004408.58+412121.2	20.008	20.018	20.004	19.664	19.666	-0.010	0.014	0.340	0.002
	94	J004410.17+413253.1	18.624	19.097	19.505	19.239	18.722	-0.473	-0.408	0.266	-0.517
	96	J004412.44+412941.7	18.858	19.250	19.671	19.535	19.309	-0.392	-0.421	0.136	-0.226
	103	J004425.10+412050.0	16.812	17.656	17.547	17.482	17.556	-0.844	0.109	0.065	0.074
	104	J004425.43+412044.7	19.103	19.565	19.494	19.354	19.452	-0.462	0.071	0.140	0.098
	116	J004444.00+412739.9	21.025	20.962	20.822	20.418	20.402	0.063	0.140	0.404	-0.016
	124	J004455.63+413105.1	19.903	20.089	20.336	20.122	20.080	-0.186	-0.247	0.214	-0.042
	126	J004500.96+413058.8	19.197	19.817	19.770	19.655	19.722	-0.620	0.047	0.115	0.067
	132	J004511.27+413815.3	19.527	19.967	20.304	20.192	19.840	-0.440	-0.337	0.112	-0.352
	139	J004524.26+415352.5	20.457	20.790	21.156	20.974	20.795	-0.333	-0.366	0.182	-0.179
	141	J004531.16+420658.1	19.703	19.699	20.007	19.793	19.616	0.004	-0.308	0.214	-0.177
	143	J004537.10+414201.4	19.482	19.935	19.943	19.749	19.660	-0.453	-0.008	0.194	-0.089
	151	J004551.35+414242.0	19.776	20.164	20.625	20.528	20.056	-0.388	-0.461	0.097	-0.472
WC7	22	J004034.17+404340.4	20.746	20.671	19.895	19.464	19.923	0.075	0.776	0.431	0.459
	43	J004134.99+410552.3	19.866	20.161	20.383	20.250	20.029	-0.295	-0.222	0.133	-0.221
	59	J004242.03+412314.9	20.984	20.982	20.939	20.728	20.530	0.002	0.043	0.211	-0.198
	102	J004422.24+411858.4	20.197	20.567	20.742	20.500	20.727	-0.370	-0.175	0.242	0.227
	121	J004451.98+412911.6	19.601	20.092	20.556	20.547	20.188	-0.491	-0.464	0.009	-0.359
	123	J004453.52+415354.3	20.030	20.442	20.721	20.498	20.880	-0.412	-0.279	0.223	0.382
	129	J004509.18+414021.4	20.066	20.444	20.389	19.839	20.137	-0.378	0.055	0.550	0.298
	130	J004510.39+413646.6	17.582	18.300	18.422	18.397	18.283	-0.718	-0.122	0.025	-0.114
WC8	49	J004147.24+410647.5	17.865	18.614	18.827	18.778	18.650	-0.749	-0.213	0.049	-0.128
	56	J004234.42+413024.2	18.761	19.504	19.654	19.583	19.736	-0.743	-0.150	0.071	0.153
	80	J004331.17+411203.5	19.347	20.056	19.927	19.723	19.680	-0.709	0.129	0.204	-0.043
	136	J004517.89+415209.5	17.148	18.087	18.106	18.067	18.037	-0.939	-0.019	0.039	-0.030

Table 15: Overview of the number of levels and transitions of the individual model atoms in different ionization stages. Note that not all models used for the final fit contain all the mentioned atoms listed here. However, if an element was included to the calculation, it was always with the full set of ionization stages, levels and transitions displayed here.

Element	Ion	Levels	Transitions	Element	Ion	Levels	Transitions
He	I	35	595	Al	V	10	45
He	II	26	325	Al	VI	10	45
He	III	1	0	Al	VII	4	6
C	II	3	3	Ne	II	1	0
C	III	40	780	Ne	III	18	153
C	IV	25	300	Ne	IV	35	595
C	V	29	406	Ne	V	54	1431
C	VI	1	0	Ne	VI	49	1176
N	II	38	703	Ne	VII	36	630
N	III	56	1540	Ne	VIII	77	2926
N	IV	38	703	Ne	IX	23	253
N	V	20	190	Ne	X	15	105
N	VI	14	91	Ne	XI	1	0
N	VII	10	45	Mg	II	1	0
O	II	36	630	Mg	III	43	903
O	III	33	528	Mg	IV	17	136
O	IV	29	406	Mg	V	20	190
O	V	54	1431	Mg	VI	21	210
O	VI	16	120	Mg	VII	20	190
O	VII	15	105	Mg	VIII	1	0
O	VIII	1	0	P	I	1	0
Si	III	24	276	P	II	57	1596
Si	IV	55	1485	P	III	47	1081
Si	V	52	1326	P	IV	12	66
Si	VI	10	45	P	V	11	55
Si	VII	9	36	P	VI	1	0
Si	VIII	1	0	S	I	33	528
Cl	III	1	0	S	II	32	496
Cl	IV	24	276	S	III	23	253
Cl	V	18	153	S	IV	25	300
Cl	VI	23	253	S	V	10	45
Cl	VII	20	190	S	VI	22	231
G	III	1	0	S	VII	1	0
G	IV	18	77	Na	III	1	0
G	V	22	107	Na	IV	14	91
G	VI	29	194	Na	V	11	55
G	VII	19	87	Na	VI	29	406
G	VIII	14	49	Na	VII	12	66
G	IX	15	56	Na	VIII	24	276
G	X	28	170	Na	IX	17	136
G	XI	26	161	Na	X	1	0
G	XII	13	37	Mg	II	1	0
G	XIII	15	50	Mg	III	43	903
G	XIV	14	49	Mg	IV	17	136
G	XV	1	0	Mg	V	20	190
Al	I	10	45	Mg	VI	21	210
Al	II	10	45	Mg	VII	20	190
Al	III	10	45	Mg	VIII	1	0
Al	IV	10	45				

Table 16: Full overview for the derived parameter for the sample stars in the present analysis.

Star	WC	$T_{2/3}$ [kK]	T_{eff} [kK]	$\log L$ [L_{\odot}]	M_* [M_{\odot}]	R_* [R_{\odot}]	R_t [R_{\odot}]	T	\mathcal{R}	v_{∞} [km s^{-1}]	$\log \dot{M}$ [$M_{\odot} \text{ yr}^{-1}$]	D	v_{rad} [km s^{-1}]	E_{B-V} [mag]	He	C	N	O	Si
2	6	62.0	89.1	5.4	12.8	2.11	2.19	12.0	17.6	2000	-4.62	10	300	0.1	3.7E-01	6.0E-01	-	3.0E-02	1.0E-03
7	6	64.5	70.8	5.3	11.5	2.98	3.98	10.0	15.0	2000	-5.03	30	200	0.07	4.8E-01	5.0E-01	-	2.0E-02	6.5E-04
12	4	98.2	188.4	5.6	16.9	0.59	0.49	18.5	24.1	2800	-4.83	100	150	0.1	4.1E-01	5.0E-01	-	8.0E-02	1.0E-02
13	6	59.0	70.8	5.6	16.7	4.21	3.98	10.0	15.0	2300	-4.50	10	200	0.1	3.4E-01	6.0E-01	-	5.0E-02	5.0E-03
15	4	64.6	70.8	5.6	17.7	4.21	4.47	10.0	14.5	2200	-4.83	30	350	0.08	7.9E-01	1.5E-01	6.0E-03	5.0E-02	5.0E-03
19	5	64.3	66.8	5.4	13.1	3.75	5.25	9.5	13.8	2500	-5.07	50	250	0.12	5.0E-01	4.5E-01	-	5.0E-02	6.2E-04
23	4	67.2	70.8	5.4	13.0	3.34	6.03	10.0	13.2	2000	-4.98	10	300	0.05	4.4E-01	5.0E-01	-	6.0E-02	1.0E-03
43	7	64.6	79.4	5.6	17.0	3.34	2.75	11.0	16.6	2300	-4.65	30	250	0.12	4.6E-01	5.0E-01	-	4.0E-02	1.0E-03
54	4	97.9	177.8	5.55	15.3	0.63	0.60	18.0	23.2	2600	-4.80	50	100	0.13	1.9E-01	7.0E-01	-	1.0E-01	5.0E-03
55	6	59.2	70.8	5.45	14.3	3.54	3.24	10.0	15.9	2200	-4.74	30	150	0.18	6.8E-01	3.0E-01	-	2.0E-02	2.0E-03
93	6	55.0	70.8	5.85	25.5	5.61	4.07	10.0	14.9	2200	-4.35	10	-50	0.15	8.9E-01	1.0E-01	2.0E-03	1.0E-03	1.0E-02
94	6	56.8	75.0	5.9	27.2	5.29	2.82	10.5	16.5	2300	-4.36	30	-150	0.1	7.9E-01	2.0E-01	-	1.0E-02	2.0E-03
96	6	56.7	66.8	5.9	27.1	6.67	3.63	9.5	15.4	2400	-4.47	50	-150	0.12	7.3E-01	2.5E-01	-	2.0E-02	1.0E-03
102	7-8	46.4	59.6	5.3	12.2	4.21	3.98	8.5	15.0	1100	-4.82	10	-100	0.1	8.3E-01	1.5E-01	-	1.0E-02	5.0E-03
113	5	56.1	79.4	5.5	15.7	2.98	2.82	11.0	16.5	1800	-4.61	10	-50	0.15	8.7E-01	1.0E-01	2.5E-02	5.0E-03	1.0E-03
121	7	52.8	59.6	5.2	10.5	3.75	6.61	8.5	12.8	1400	-4.92	4	-200	0.09	6.8E-01	3.0E-01	-	2.0E-02	1.0E-03
123	7	53.1	63.1	5.1	9.3	2.98	4.27	9.0	14.7	1200	-5.05	10	-150	0.05	6.3E-01	3.5E-01	-	9.0E-03	5.0E-03
124	6	53.9	56.2	5.62	17.8	6.82	7.24	8.0	12.4	2000	-4.83	25	-150	0.14	6.3E-01	3.5E-01	-	2.0E-02	2.0E-03
132	6	58.6	63.1	5.7	19.7	5.94	5.43	9.0	13.7	1900	-4.76	25	-150	0.14	5.1E-01	4.5E-01	-	4.0E-02	2.0E-03
138	5-6	87.5	177.8	5.2	10.2	0.42	0.55	18.0	23.6	1800	-5.12	40	-300	0.2	4.7E-01	5.0E-01	-	2.0E-02	1.0E-03
139	6	63.2	70.8	5.2	10.2	2.65	4.07	10.0	14.9	2000	-5.12	30	-200	0.1	4.8E-01	5.0E-01	-	2.0E-02	6.5E-04
150	5-6	82.2	177.8	5.4	13.0	0.53	0.54	18.0	23.7	1600	-5.05	50	-200	0.1	4.7E-01	5.0E-01	-	2.0E-02	1.0E-03
151	6	67.5	177.8	5.3	11.7	0.47	0.49	18.0	24.1	1800	-4.91	30	-250	0.05	5.7E-01	4.0E-01	-	2.0E-02	5.0E-03

Table 17: Velocities of the M31 WR stars. $v_{\text{rad}}(\text{M31})$ denotes the rotational velocity the stars have according to their position in M31, $v_{\text{rad}}(\text{projected})$ is how we would observe the rotation as radial velocity at the position of the individual stars, $v_{\text{rad}}(\text{measured})$ is the measured velocity from the spectra, and Δv_{rad} denotes the difference of $v_{\text{rad}}(\text{measured})$ and $v_{\text{rad}}(\text{projected})$. The given distance is the radial distance of the stars to the center of M31

Star	LGGS	distance [kpc]	$v_{\text{rad}}(\text{M31})$ [km s ⁻¹]	$v_{\text{rad}}(\text{projected})$ [km s ⁻¹]	$v_{\text{rad}}(\text{measured})$ [km s ⁻¹]	Δv_{rad} [km s ⁻¹]
WR2	J003911.04+403817.5	15.74	246.2	235.7	300.0	64.3
WR3	J003919.53+402211.6	14.69	251.1	244.6	250.0	5.4
WR4	J003933.46+402018.9	15.11	249.3	242.6	250.0	7.4
WR7	J003939.97+403450.4	12.51	251.8	244.7	200.0	-44.7
WR12	J004019.47+405224.9	11.14	255.8	242.9	150.0	-92.9
WR13	J004020.44+404807.7	10.07	259.3	250.2	200.0	-50.2
WR15	J004022.43+405234.6	10.82	256.9	244.3	350.0	105.7
WR19	J004029.27+403916.6	9.97	259.6	252.9	250.0	-2.9
WR22	J004034.17+404340.4	9.03	261.5	254.7	200.0	-54.7
WR23	J004034.69+404432.9	8.90	260.3	253.5	300.0	46.5
WR26	J004043.28+403525.2	11.60	254.4	246.1	250.0	3.9
WR29	J004058.49+410414.8	10.10	259.2	232.4	200.0	-32.4
WR30	J004059.13+403652.0	11.88	253.6	243.8	200.0	-43.8
WR33	J004107.31+410417.0	8.85	259.8	236.5	150.0	-86.5
WR35	J004109.59+404856.2	7.36	246.9	240.2	200.0	-40.2
WR43	J004134.99+410552.3	5.64	234.0	219.5	250.0	30.5
WR47	J004144.47+404517.1	11.35	255.1	238.8	250.0	11.2
WR49	J004147.24+410647.5	4.36	180.9	171.8	300.0	128.2
WR51	J004154.62+404713.8	11.32	255.2	236.2	200.0	-36.2
WR52	J004203.94+412554.5	11.72	254.0	-68.2	100.0	168.2
WR54	J004213.21+405051.8	11.34	255.1	228.5	100.0	-128.5
WR55	J004214.36+412542.3	10.08	259.3	-100.0	150.0	250.0
WR56	J004234.42+413024.2	10.05	259.4	-182.7	150.0	332.7
WR58	J004240.81+410241.6	7.70	249.3	202.7	50.0	-152.7
WR59	J004242.03+412314.9	4.65	192.7	-144.4	0.0	144.4
WR61	J004247.12+405657.1	12.05	253.1	194.7	100.0	-94.7
WR62	J004249.84+410215.7	9.19	261.7	193.7	0.0	-193.7
WR64	X004256.05+413543.7	10.39	258.3	-218.2	0.0	218.2
WR71	X004308.25+413736.3	9.99	259.5	-230.0	-150.0	80.0
WR73	J004316.44+414512.4	13.56	252.1	-223.2	-100.0	123.2
WR77	J004327.92+414207.3	10.39	258.3	-238.1	-150.0	88.1
WR80	J004331.17+411203.5	9.35	261.3	-51.0	-50.0	1.0
WR84	J004341.72+412304.2	5.21	215.9	-196.6	-200.0	-3.4
WR91	J004406.39+411921.0	10.64	257.5	-187.1	-50.0	137.1
WR93	J004408.58+412121.2	9.94	259.7	-206.5	-50.0	156.5
WR94	J004410.17+413253.1	5.89	236.9	-228.9	-150.0	78.9
WR96	J004412.44+412941.7	6.90	243.6	-230.1	-150.0	80.1
WR98	J004415.77+411952.5	11.77	253.9	-185.9	-100.0	85.9
WR99	J004416.20+412103.5	11.22	255.5	-197.2	0.0	197.2
WR102	J004422.24+411858.4	13.22	252.0	-174.3	-100.0	74.3
WR103	J004425.10+412050.0	12.67	251.8	-189.1	-100.0	89.1
WR104	J004425.43+412044.7	12.76	251.9	-188.3	-150.0	38.3
WR111	J004435.15+412545.2	11.71	254.1	-217.1	-50.0	167.1
WR113	J004436.52+412202.0	13.75	252.0	-193.7	-50.0	143.7
WR116	J004444.00+412739.9	12.10	252.9	-220.8	-100.0	120.8
WR121	J004451.98+412911.6	12.56	251.8	-222.5	-200.0	22.5
WR123	J004453.52+415354.3	10.33	258.5	-251.3	-150.0	101.3
WR124	J004455.63+413105.1	12.24	252.5	-227.7	-150.0	77.7
WR126	J004500.96+413058.8	13.05	251.9	-225.3	-200.0	25.3
WR129	J004509.18+414021.4	10.73	257.2	-245.3	-200.0	45.3
WR130	J004510.39+413646.6	12.02	253.2	-236.5	-250.0	-13.5
WR132	J004511.27+413815.3	11.62	254.3	-239.7	-150.0	89.7
WR133	J004513.68+413742.5	12.12	252.9	-237.0	-150.0	87.0
WR136	J004517.89+415209.5	10.31	258.6	-251.8	-300.0	-48.2
WR138	J004522.78+420318.2	12.98	251.9	-244.7	-300.0	-55.3
WR139	J004524.26+415352.5	10.76	257.1	-250.4	-200.0	50.4
WR140	J004530.61+414639.2	11.66	254.2	-244.6	-200.0	44.6
WR141	J004531.16+420658.1	14.11	251.6	-244.2	-300.0	-55.8
WR143	J004537.10+414201.4	13.67	252.0	-237.4	-200.0	37.4
WR146	J004539.35+414439.8	13.13	252.0	-239.8	-250.0	-10.2
WR150	J004551.12+421015.4	14.81	250.8	-243.8	-200.0	43.8
WR151	J004551.35+414242.0	15.29	248.4	-232.4	-250.0	-17.6

B Stellar data sheets

»For my part, I know nothing with any certainty, but the sight of the stars makes me dream in the same simple way as I dream about the black dots representing towns and villages on a map.«

– Vincent van Gogh

On the following pages, we will list all the individual sample stars which were analyzed in the above mentioned way. We will give an overview for each star about its derived stellar and wind parameter, the chemical composition, and the stellar feedback. Additionally a small map for every star is shown. If available for the individual star we will use a HST image, preferably in a somewhat bluer color. The HST maps show a small cut out from the image, centered on the pointing of the used fiber for the observation the star in question. The red circle denotes the fiber aperture (1"5 diameter) and the green circle illustrates the effect of moderate seeing adding 0"5 to the fiber aperture. The used camera and filter setting are indicated in the individual images. *TOTAL* as name for a filter refers to a stacked image created from all available filters for this camera that were used in the corresponding survey. If no HST image is available the image shown is a cutout from a DSS2 blue image of M31. The location of the star is indicated by a red box. This indication is rather rough and can only give an overview of the surrounding region.

All stellar parameter are taken from the best fitting model. However, the stellar feedback required some additional calculation. The mechanical energy is calculated via

$$L_{\text{mech}} = E_{\text{mech}}/\text{yr} = \dot{M} \cdot v_{\infty}^2$$

and given in erg/s and solar luminosities L_{\odot} . The chemical yield of a star is usually described as the total mass of one element that was used during a star's formation compared to the mass which is mixed into the ISM during its lifetime. For obvious reasons we can not use this definition here. Therefore we will address simply the mass of an individual element currently mixed into the ISM by the stellar wind as *current enrichment* q_{element} , calculated as

$$q_{\text{element}} = m_{\text{element}} \cdot \dot{M},$$

with m_{element} being the abundance of the individual element in mass fraction. The result is given in Earth masses $M_{\oplus} = 5.97 \cdot 10^{24}$ kg per year.

All further listed parameters are used in the usual manner. Note that v_{crit} denotes the critical rotational velocity, given as

$$v_{\text{crit}} = \sqrt{\frac{M_* \cdot G}{R_*}}.$$

An additional note on the used terminology: It has proven to be convenient during the fitting process to adopt a way of plotting the data such that all important informations, like photometry and stellar SED, as well as the entire spectral range is shown simultaneously. Those plots are called *Masterplots*. Those plots are added to the upcoming stellar data sheets as well and follow the above mentioned summary of stellar parameters. Those Masterplots contain four plots each:

- The first plot displays the spectral energy distribution (SED) of the star. Shown is the SED from the model atmosphere, once only the continuum (solid green line), once with the line spectrum superimposed (solid red line), and once with the line spectrum convoluted with a gaussian (FWHM=1000Å) similar to Fig.30 (solid brown line). The photometric measurements are displayed by the blue boxes with corresponding magnitude labeled.
- The lower three plots show the observed spectrum (solid blue line) compared to the best fitting model spectrum (solid red line), both in a normalized fashion.
- Note that for convenience the observation is shifted along wavelength scale according to the determined radial velocity. This means that interstellar or atmospheric absorptions, as well as nebula emission might be shifted out of their rest frame wavelength.
- Known spectral features are mark with their corresponding ion(s).
- For visibility reasons, all shown spectra contain zoomed out cut outs around the strong emission lines.

The stars are sorted according to their WR number in M31. Each of them has two pages dedicated. One contains the table with all derived stellar parameter, the HST/DSS2 map, and short comments to the star and on the fit. The other page displays the Masterplot.

B.1 M 31 WR 2

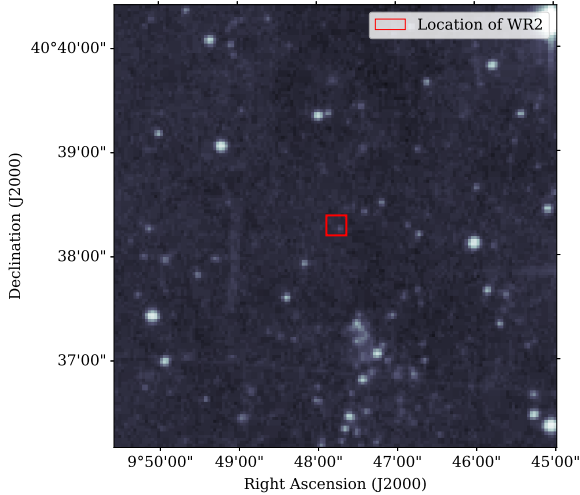


Figure 60: DSS image (blue) of the surrounding region of WR 2

- M 31 WR 2 is a WC6 star whose emission lines are very strong.
- The increased carbon abundances points at further developed state.
- It is not obvious in the photometry, but the red part of the spectrum shows signs of dilution for $\lambda > 7000\text{\AA}$.
- No HST image exists to investigate the stellar neighborhood. The DSS2 blue image is shown in Fig 60.
- No signs for rotation are found for this star.
- The overall quality of the spectral fit is very good for a WC star.
- Disagreements between the model spectrum and the observation can be seen, all of them are the usual problems as described above.
 - No reproduction of O VI $\lambda\lambda 3811, 34$
 - Overprediction of O III $\lambda 3961$, O IV $\lambda 3934$, and C IV $\lambda\lambda 4440 - 42$
 - The unknown emission at 4500\AA

Table 18: Summary for M 31 WR 2

(a) General overview

Star	WR2
LGGS	J003911.04+403817.5
Spectral type	WC6
E(B-V)	0.1

(b) Derived stellar parameter

T_{eff}	[K]	89125
$T_{2/3}$	[K]	61994
L	[$\log L_{\odot}$]	5.4
M_{*}	[M_{\odot}]	12.8
R_{*}	[R_{\odot}]	2.1
\dot{M}	[$\log M_{\odot}/\text{yr}$]	-4.621
D		10
R_t	[R_{\odot}]	2.1878
v_{∞}	[km/s]	2000
v_{rad}	[km/s]	300
v_{rot}	[km/s]	0
v_{crit}	[km/s]	1080

(c) Derived abundances

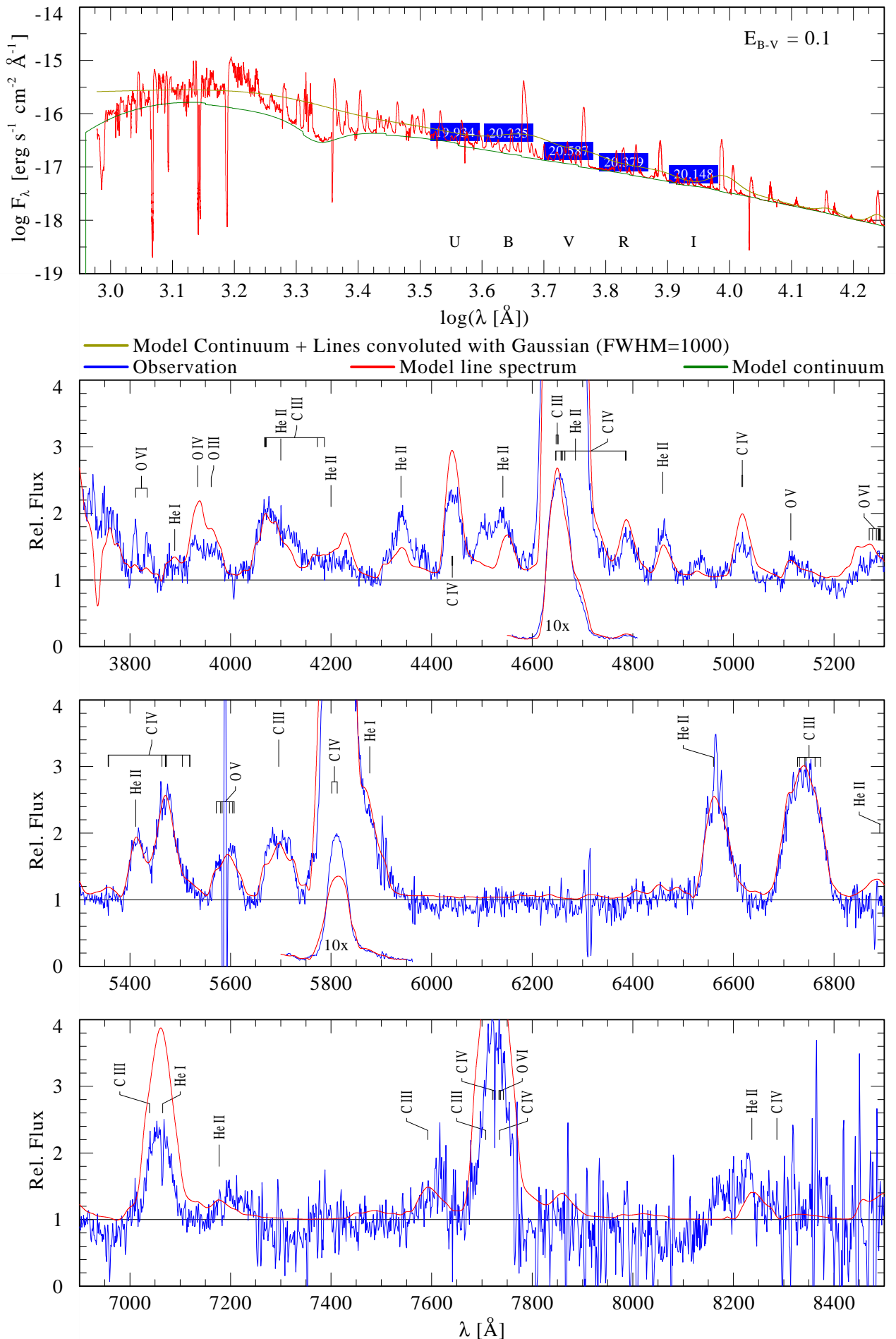
Element	mass fraction
Helium	3.7E-01
Carbon	6.0E-01
Oxygen	3.0E-02
Silicon	1.0E-03
Iron group	1.6E-03

(d) Ionizing photons, mechanical feedback, and current chemical enrichment

Ionization edge	Wavelength	$\log Q$
Hydrogen	911.6 \AA	49.22
Helium I	504.3 \AA	48.42
Helium II	227.9 \AA	37.70
Oxygen II	353.0 \AA	47.18
mechanical feedback		$6.07\text{E}+38 \text{ erg s}^{-1}$ $10^{4.20} L_{\odot}$
Chemical enrichment		
q_{He}	[M_{\oplus}/yr]	2.9E+00
q_{C}	[M_{\oplus}/yr]	4.8E+00
q_{O}	[M_{\oplus}/yr]	2.4E-01
q_{Si}	[M_{\oplus}/yr]	1.3E-02

Masterplot: **M31WR2 // LGS J003911.04+403817.5**

WC6



B.2 M 31 WR 7

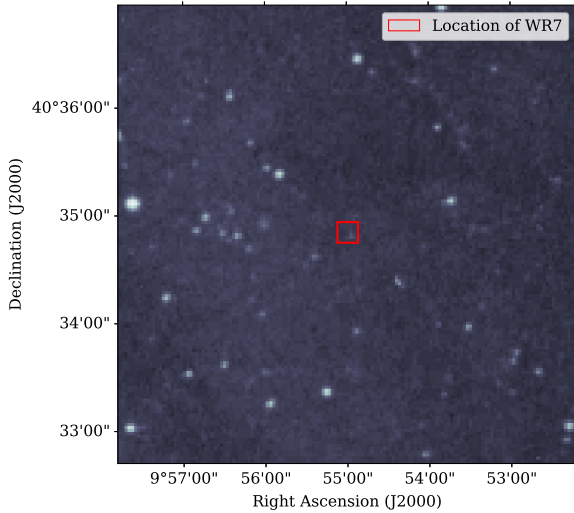


Figure 61: *DSS image (blue) of the surrounding region of WR 7*

- M 31 WR 7 is a WC6 star which resembles the spectrum of WR 2 nicely with the only difference that all emission lines in WR 7 are slightly weaker.
- The increased carbon abundances points at further developed state.
- It is not obvious in the photometry, but the red part of the spectrum shows signs of dilution for $\lambda > 6500\text{\AA}$.
- No HST image exists to investigate the stellar neighborhood. The DSS2 blue image is shown in Fig 61.
- The star shows signs of fast rotation leading to an overcritical rotation. See Sect. 9.4 for the solution for this issue.
- The overall quality of the spectral fit is good for a WC star.
- Disagreements between the model spectrum and the observation can be seen, all of them are the usual problems as described above.
 - No reproduction of O VI $\lambda\lambda 3811, 34$
 - The unknown emission at 4500\AA
- One could argue that in comparison to WR 2 the lines are slightly weaker, this might be an indication for dilution of the spectrum and those are in fact almost identical. However, the fact that WR 2 is fainter by 0.1 dex indicates that this is most likely not the case.

Table 19: *Summary for M 31 WR 7*

(a) *General overview*

Star	WR7
LGGS	J003939.97+403450.4
Spectral type	WC6
E(B-V)	0.07

(b) *Derived stellar parameter*

T_{eff}	[K]	70795
$T_{2/3}$	[K]	64544
L	[$\log L_{\odot}$]	5.3
M_{*}	[M_{\odot}]	11.5
R_{*}	[R_{\odot}]	3.0
\dot{M}	[$\log M_{\odot}/\text{yr}$]	-5.025
D		30
R_t	[R_{\odot}]	3.9811
v_{∞}	[km/s]	2000
v_{rad}	[km/s]	200
v_{rot}	[km/s]	1818
v_{crit}	[km/s]	861

(c) *Derived abundances*

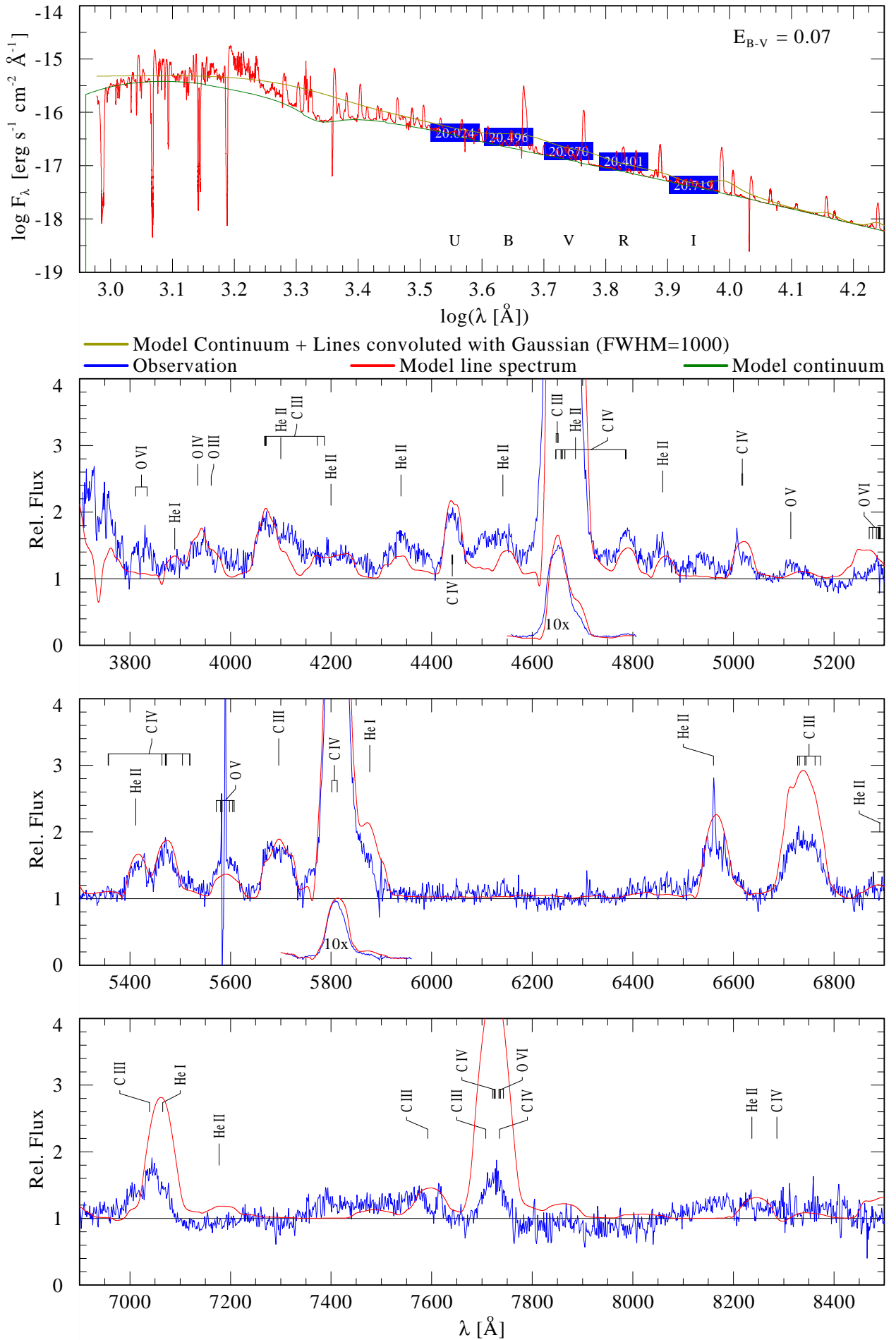
Element	mass fraction
Helium	4.8E-01
Carbon	5.0E-01
Oxygen	2.0E-02
Silicon	6.5E-04
Iron group	1.6E-03

(d) *Ionizing photons, mechanical feedback, and current chemical enrichment*

Ionization edge	Wavelength	$\log Q$
Hydrogen	911.6 \AA	49.14
Helium I	504.3 \AA	48.30
Helium II	227.9 \AA	37.81
Oxygen II	353.0 \AA	47.02
mechanical feedback		$2.39\text{E}+38 \text{ erg s}^{-1}$ $10^{3.79} L_{\odot}$
Chemical enrichment		
q_{He}	[M_{\oplus}/yr]	1.5E+00
q_{C}	[M_{\oplus}/yr]	1.6E+00
q_{O}	[M_{\oplus}/yr]	6.3E-02
q_{Si}	[M_{\oplus}/yr]	5.0E-03

Masterplot: [M31WR7](#) // [LGGs J003939.97+403450.4](#)

WC6



B.3 M 31 WR 12

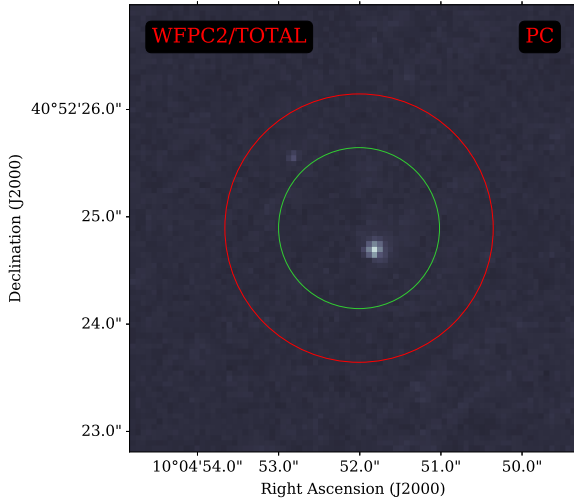


Figure 62: *HST* image of the surrounding region of WR 12. Camera and filter are noted in the image.

- WR 12 is bright and outstandingly hot. The emission lines are the second strongest in the entire sample, showing high terminal velocities and a thick wind.
- Notable are the found clumping of $D = 100$. The star is quite similar to WR 54, another WC 4.
- The determined reddening is low, but the obtained spectrum has a low S/N and shows numerous and strong nebula emission lines.
- With its strong emission lines, there is no doubt that this spectra does not suffer from contamination and the obtained HST image in Fig. 62 supports this.
- The stars shows signs of relatively slow rotation.
- The overall quality of the spectral fit is good for a WC star.
- Disagreements between the model spectrum and the observation can be seen, all of them are the usual problems as described above.
 - No reproduction of O VI $\lambda\lambda 3811, 34$, which is extremely strong for this star.
 - The diagnostic pair is relatively weak in the observation and overpredicted by the model
 - The unknown emission at 4500\AA is present in the observation
 - Overprediction of O III $\lambda 3961$, O IV $\lambda 3934$, and C IV $\lambda\lambda 4440 - 42$

Table 20: *Summary for M 31 WR 12*

(a) *General overview*

Star	WR12
LGGS	J004019.47+405224.9
Spectral type	WC4
E(B-V)	0.1

(b) *Derived stellar parameter*

T_{eff}	[K]	188365
$T_{2/3}$	[K]	98201
L	[$\log L_{\odot}$]	5.6
M_*	[M_{\odot}]	16.9
R_*	[R_{\odot}]	0.6
\dot{M}	[$\log M_{\odot}/\text{yr}$]	-4.825
D		100
R_t	[R_{\odot}]	0.4898
v_{∞}	[km/s]	2800
v_{rad}	[km/s]	150
v_{rot}	[km/s]	455
v_{crit}	[km/s]	2334

(c) *Derived abundances*

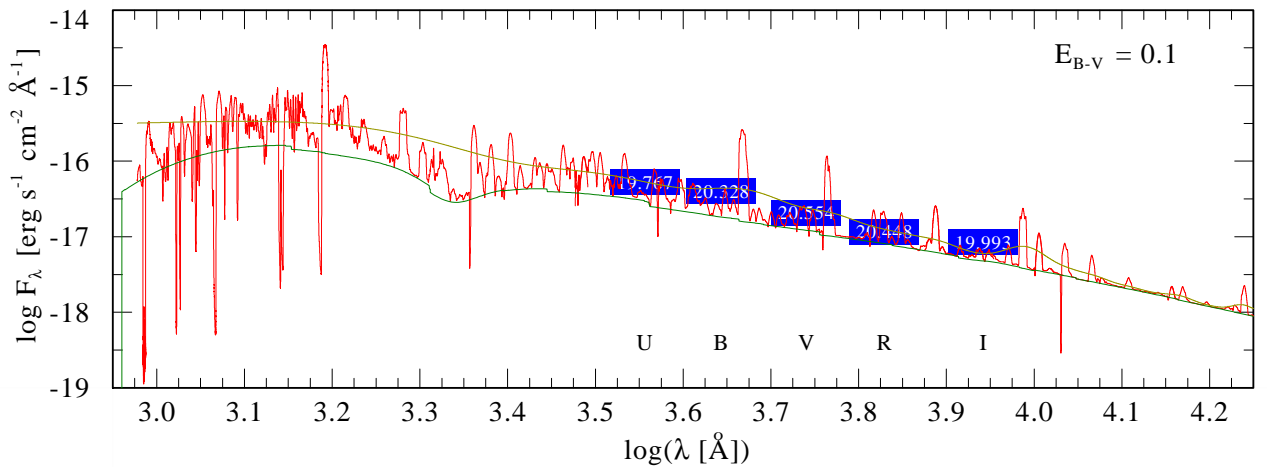
Element	mass fraction
Helium	4.1E-01
Carbon	5.0E-01
Oxygen	8.0E-02
Silicon	1.0E-02
Iron group	1.6E-03

(d) *Ionizing photons, mechanical feedback, and current chemical enrichment*

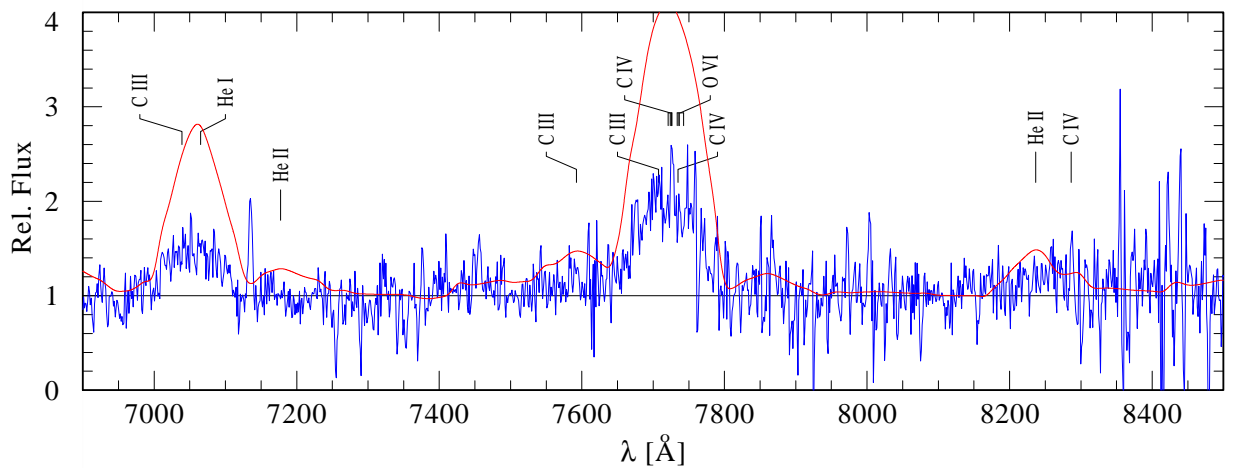
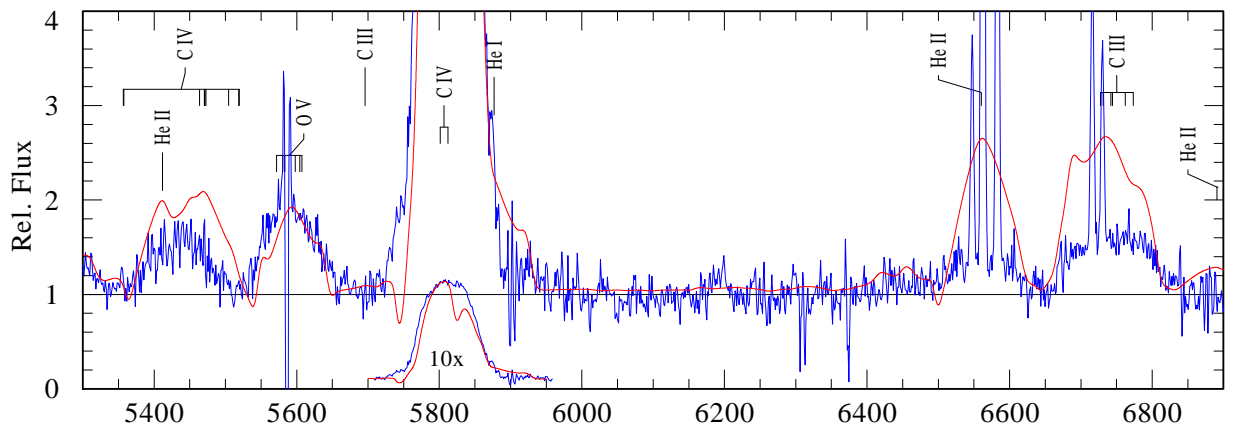
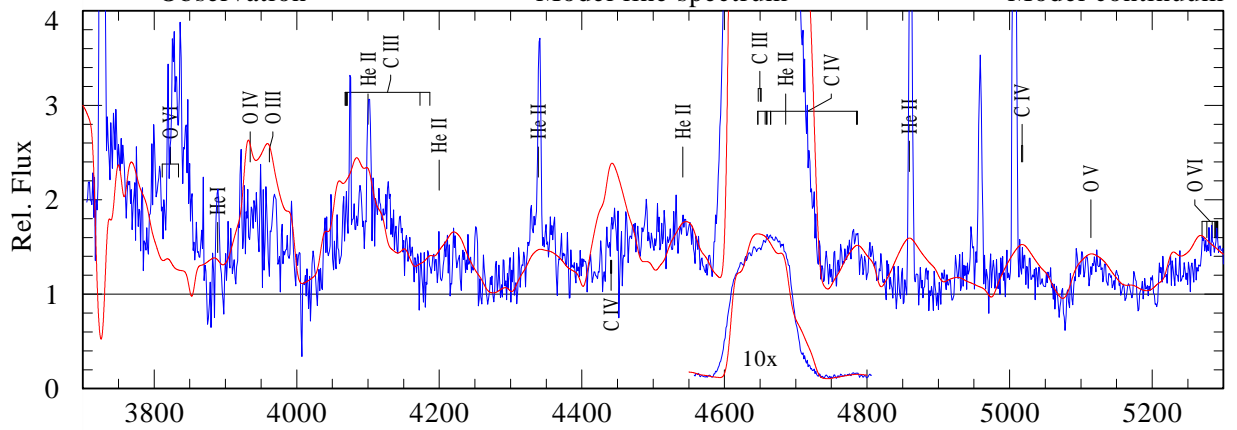
Ionization edge	Wavelength	$\log Q$
Hydrogen	911.6 \AA	49.40
Helium I	504.3 \AA	48.78
Helium II	227.9 \AA	38.96
Oxygen II	353.0 \AA	47.91
mechanical feedback		$7.44\text{E}+38 \text{ erg s}^{-1}$ $10^{4.29} L_{\odot}$
Chemical enrichment		
q_{He}	[M_{\oplus}/yr]	2.0E+00
q_{C}	[M_{\oplus}/yr]	2.5E+00
q_{O}	[M_{\oplus}/yr]	4.0E-01
q_{Si}	[M_{\oplus}/yr]	8.0E-03

Masterplot: **M31WR12 // LGG5 J004019.47+405224.9**

WC4



— Model Continuum + Lines convoluted with Gaussian (FWHM=1000)
 — Observation — Model line spectrum — Model continuum



B.4 M 31 WR 13

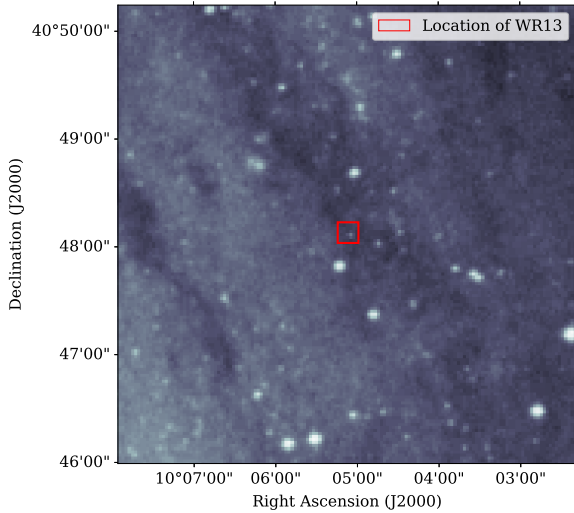


Figure 63: DSS image (blue) of the surrounding region of WR 13

- WR 13 is another WC6 stars that shows relatively strong emission lines
- It inhibits signs of a more developed state with an increased carbon abundance
- No HST images is available but the spectrum is undoubtedly not contaminated. The DSS2 blue image is shown in Fig 63.
- The roundish line profiles indicate a fast rotation which is found to be overcritical for the star. See Sect. 9.4 for the solution for this issue.
- The overall quality of the spectral fit is good for a WC star.
- Disagreements between the model spectrum and the observation can be seen, all of them are the usual problems as described above.
 - No reproduction of O VI $\lambda\lambda 3811, 34$, which is extremely strong for this star.
 - The diagnostic pair is relatively weak in the observation and overpredicted by the model
 - The unknown emission at 4500\AA is present in the observation
 - Overprediction of C IV $\lambda\lambda 4440 - 42$

Table 21: Summary for M 31 WR 13

(a) General overview

Star	WR13
LGGS	J004020.44+404807.7
Spectral type	WC6
E(B-V)	0.1

(b) Derived stellar parameter

T_{eff}	[K]	70795
$T_{2/3}$	[K]	58959
L	[$\log L_{\odot}$]	5.6
M_{*}	[M_{\odot}]	16.7
R_{*}	[R_{\odot}]	4.2
\dot{M}	[$\log M_{\odot}/\text{yr}$]	-4.5
D		10
R_t	[R_{\odot}]	3.9811
v_{∞}	[km/s]	2300
v_{rad}	[km/s]	200
v_{rot}	[km/s]	1818
v_{crit}	[km/s]	874

(c) Derived abundances

Element	mass fraction
Helium	3.4E-01
Carbon	6.0E-01
Oxygen	5.0E-02
Silicon	5.0E-03
Iron group	1.6E-03

(d) Ionizing photons, mechanical feedback, and current chemical enrichment

Ionization edge	Wavelength	$\log Q$
Hydrogen	911.6 \AA	49.40
Helium I	504.3 \AA	48.45
Helium II	227.9 \AA	36.73
Oxygen II	353.0 \AA	46.76
mechanical feedback		$1.06\text{E}+39 \text{ erg s}^{-1}$ $10^{4.44} L_{\odot}$
Chemical enrichment		
q_{He}	[M_{\oplus}/yr]	3.6E+00
q_{C}	[M_{\oplus}/yr]	6.3E+00
q_{O}	[M_{\oplus}/yr]	5.3E-01
q_{Si}	[M_{\oplus}/yr]	1.7E-02

B.5 M 31 WR 15

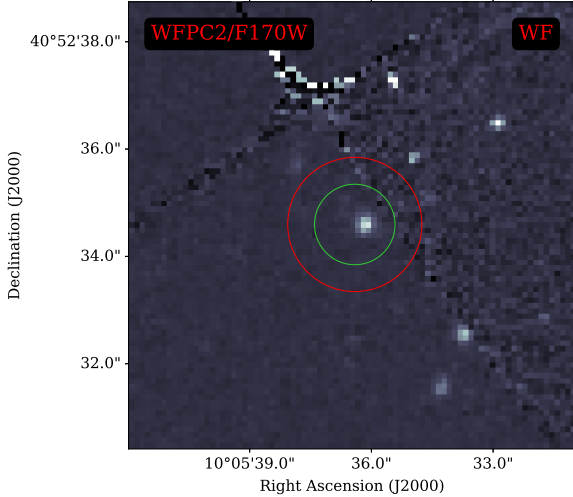


Figure 64: *HST* image of the surrounding region of WR 15. Camera and filter are noted in the image.

- WR 15 is a WC4 stars which shows quite an interesting spectrum.
- It shows clear signs of nitrogen in its spectrum. Together with the low carbon abundance, this points towards an early evolutionary state.
- $\text{N IV } \lambda\lambda 7103\text{--}7129$ is weak, but clearly visible. Note that red part of the spectrum shows signs of contamination. Therefore, the given nitrogen abundance is only an upper limit.
- Further note that this stars has a surprisingly low v_∞ for a WC4 which also supports the argumentation presented in Sect. 7.6.
- The stars shows sign of fast rotation which might explain the observed abundance patterns with increased mixing.
- The overall quality of the spectral fit is good for a WC star.
- Disagreements between the model spectrum and the observation can be seen, all of them are the usual problems as described above.
 - The diagnostic pair is slightly overpredicted by the model
- Due to the appearance of N, we suggest to classify this stars as WC4/WN

Table 22: *Summary for M 31 WR 15*

(a) *General overview*

Star	WR15
LGGS	J004022.43+405234.6
Spectral type	WC4
E(B-V)	0.08

(b) *Derived stellar parameter*

T_{eff}	[K]	70795
$T_{2/3}$	[K]	64602
L	[$\log L_\odot$]	5.6
M_*	[M_\odot]	17.7
R_*	[R_\odot]	4.2
\dot{M}	[$\log M_\odot/\text{yr}$]	-4.833
D		30
R_t	[R_\odot]	4.4668
v_∞	[km/s]	2200
v_{rad}	[km/s]	350
v_{rot}	[km/s]	1364
v_{crit}	[km/s]	899

(c) *Derived abundances*

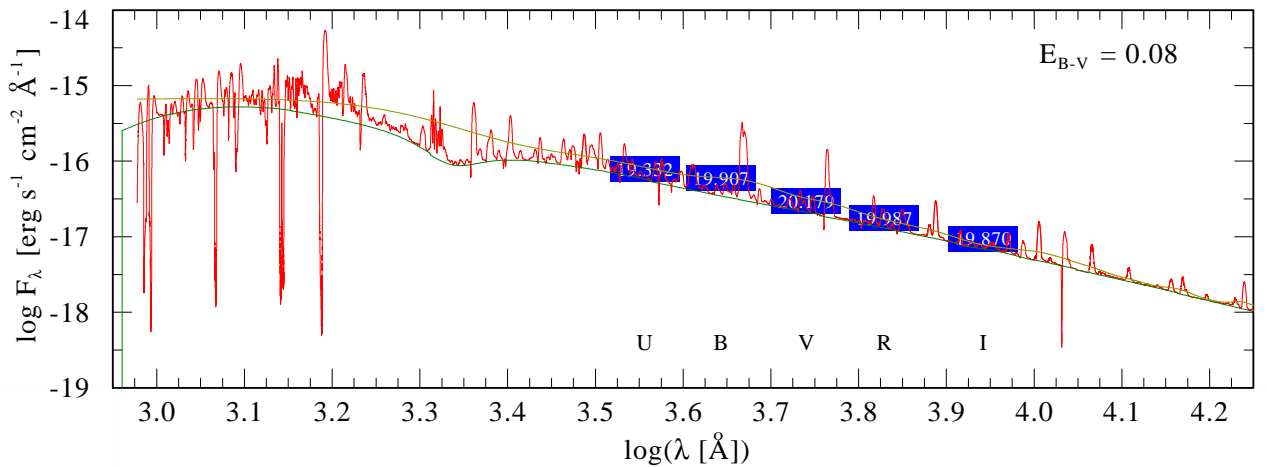
Element	mass fraction
Helium	7.9E-01
Carbon	1.5E-01
Oxygen	5.0E-02
Nitrogen	6.0E-03
Silicon	5.0E-03
Iron group	1.6E-03

(d) *Ionizing photons, mechanical feedback, and current chemical enrichment*

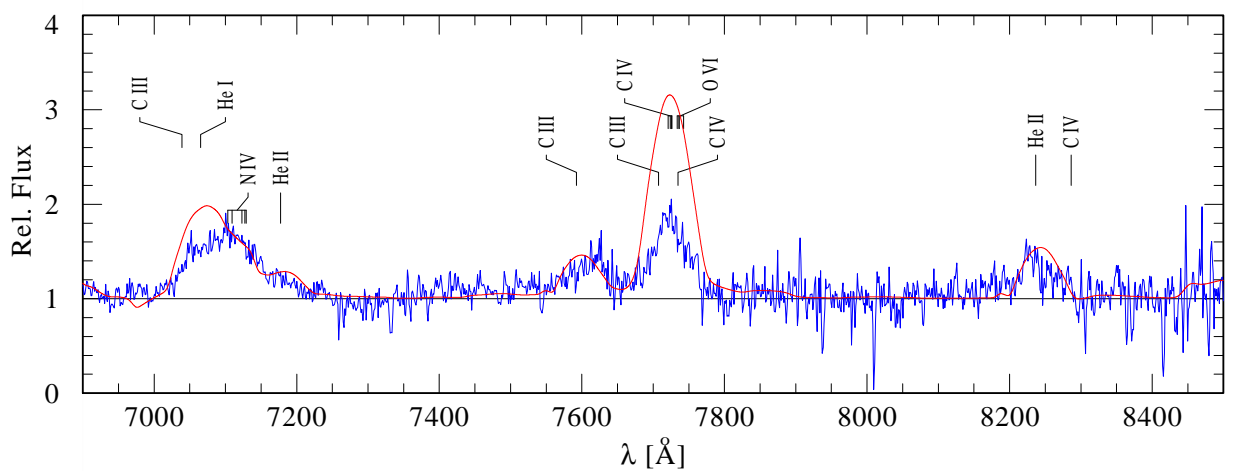
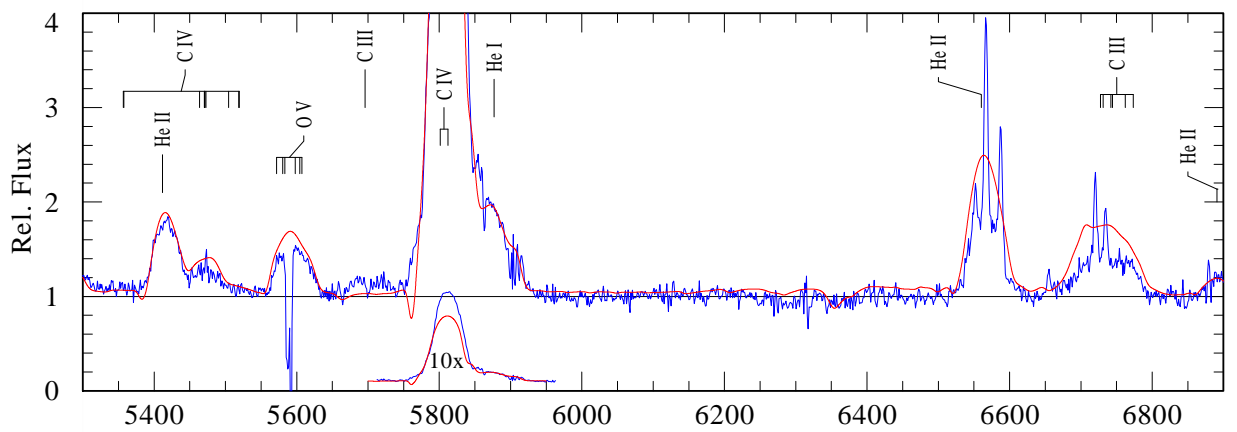
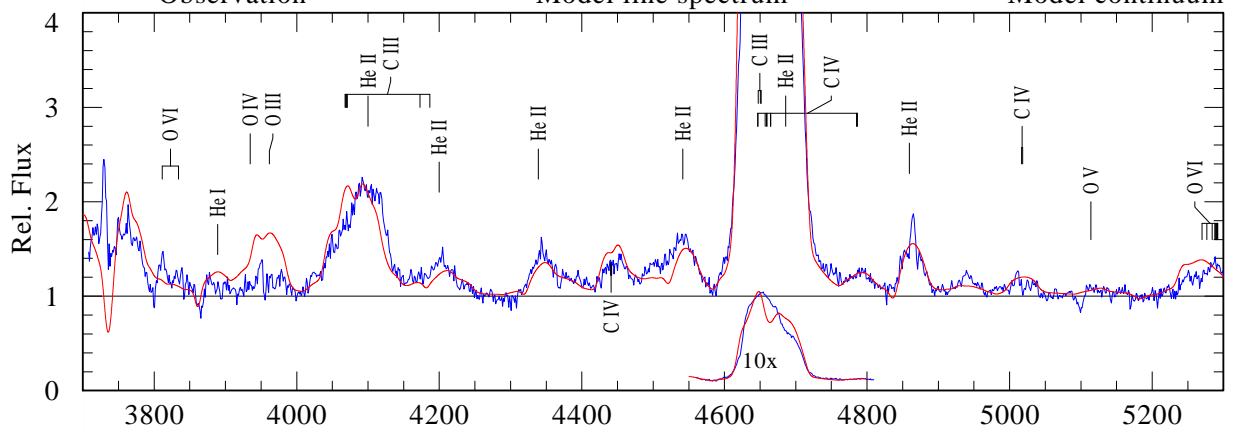
Ionization edge	Wavelength	$\log Q$
Hydrogen	911.6 Å	49.44
Helium I	504.3 Å	48.80
Helium II	227.9 Å	38.30
Oxygen II	353.0 Å	47.69
mechanical feedback		$4.51\text{E}+38 \text{ erg s}^{-1}$ $10^{4.07} L_\odot$
Chemical enrichment		
q_{He}	[M_\oplus/yr]	3.9E+00
q_{C}	[M_\oplus/yr]	7.3E-01
q_{N}	[M_\oplus/yr]	2.9E-02
q_{O}	[M_\oplus/yr]	2.4E-01
q_{Si}	[M_\oplus/yr]	7.8E-03

Masterplot: **M31WR15 // LGS J004022.43+405234.6**

WC4



— Model Continuum + Lines convoluted with Gaussian (FWHM=1000)
 — Observation — Model line spectrum — Model continuum



B.6 M 31 WR 19

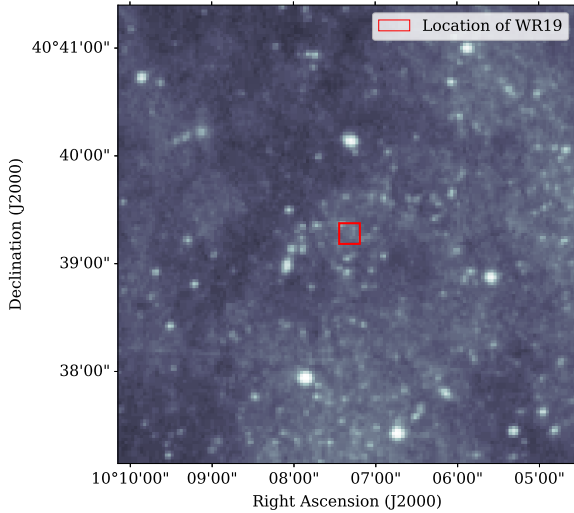


Figure 65: DSS image (blue) of the surrounding region of WR 19

- WR 19 is another WC5 stars with comparably weak lines.
- No HST images is available but this star appears to be in a region with increased stellar density, see Fig 65. However, the spectral fit as well as the luminosity show a reasonable solution for this stars as single star.
- The roundish line profiles indicate a fast rotation which is found to be overcritical for the star. See Sect. 9.4 for the solution for this issue.
- The overall quality of the spectral fit is intermediate for a WC star.
- Disagreements between the model spectrum and the observation can be seen, all of them are the usual problems as described above.
 - No reproduction of O VI $\lambda\lambda 3811, 34$, which is extremely strong for this star.
 - The diagnostic pair is relatively weak in the observation and overpredicted by the model
 - The unknown emission at 4500\AA is present in the observation
 - Overprediction of C IV $\lambda\lambda 4440 - 42$
 - Possible contamination for lines $> 6000\text{\AA}$.

Table 23: Summary for M 31 WR 19

(a) General overview

Star	WR19
LGGS	J004029.27+403916.6
Spectral type	WC5
E(B-V)	0.12

(b) Derived stellar parameter

T_{eff}	[K]	66834
$T_{2/3}$	[K]	64289
L	$[\log L_{\odot}]$	5.4
M_*	$[M_{\odot}]$	13.1
R_*	$[R_{\odot}]$	3.7
\dot{M}	$[\log M_{\odot}/\text{yr}]$	-5.069
D		50
R_t	$[R_{\odot}]$	5.2481
v_{∞}	$[\text{km/s}]$	2500
v_{rad}	$[\text{km/s}]$	250
v_{rot}	$[\text{km/s}]$	1364
v_{crit}	$[\text{km/s}]$	818

(c) Derived abundances

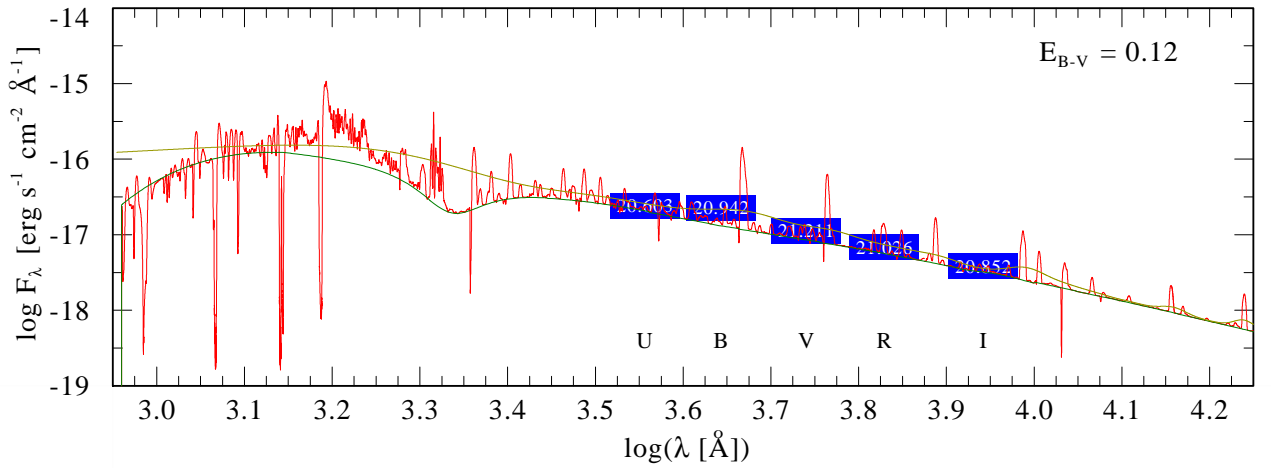
Element	mass fraction
Helium	5.0E-01
Carbon	4.5E-01
Oxygen	5.0E-02
Silicon	6.2E-04
Iron group	1.6E-03

(d) Ionizing photons, mechanical feedback, and current chemical enrichment

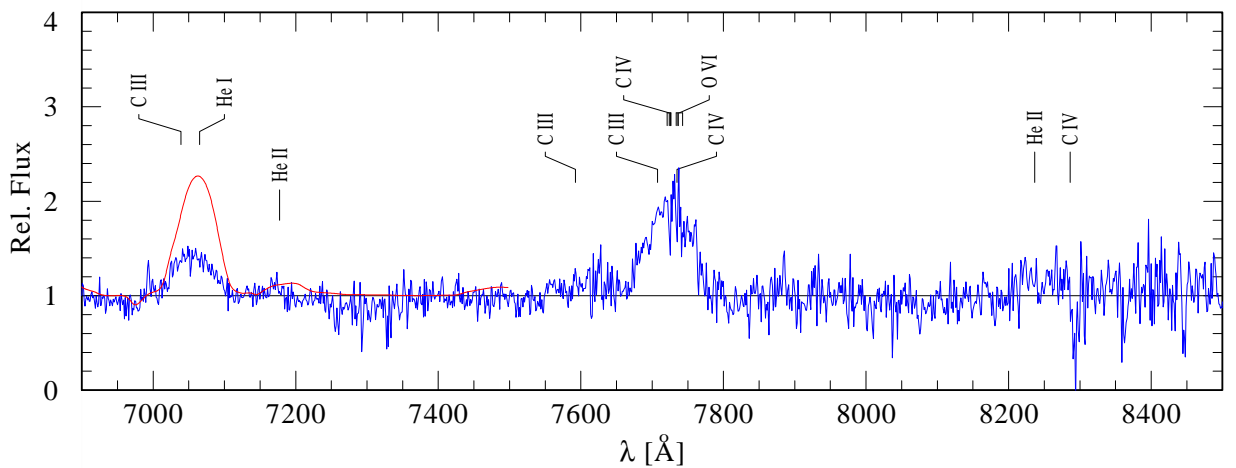
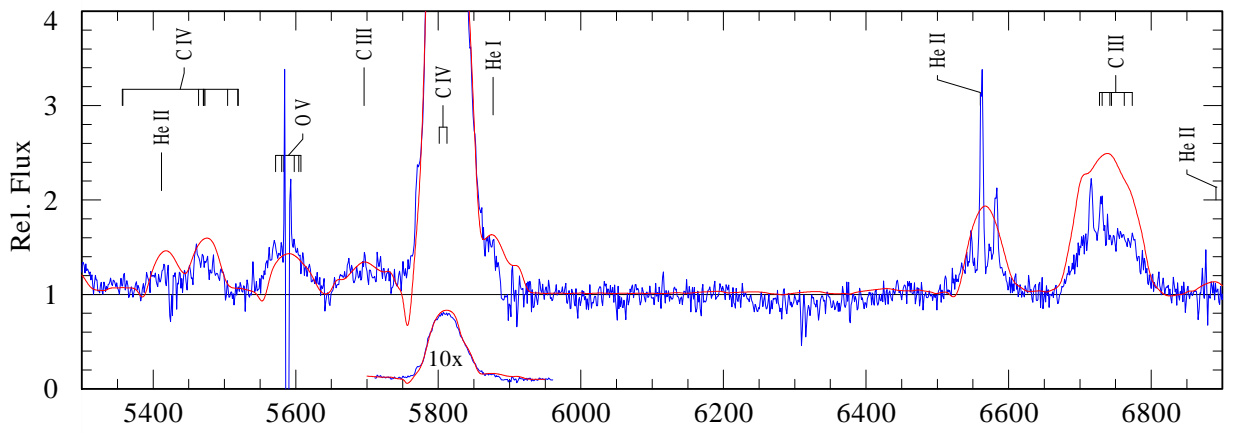
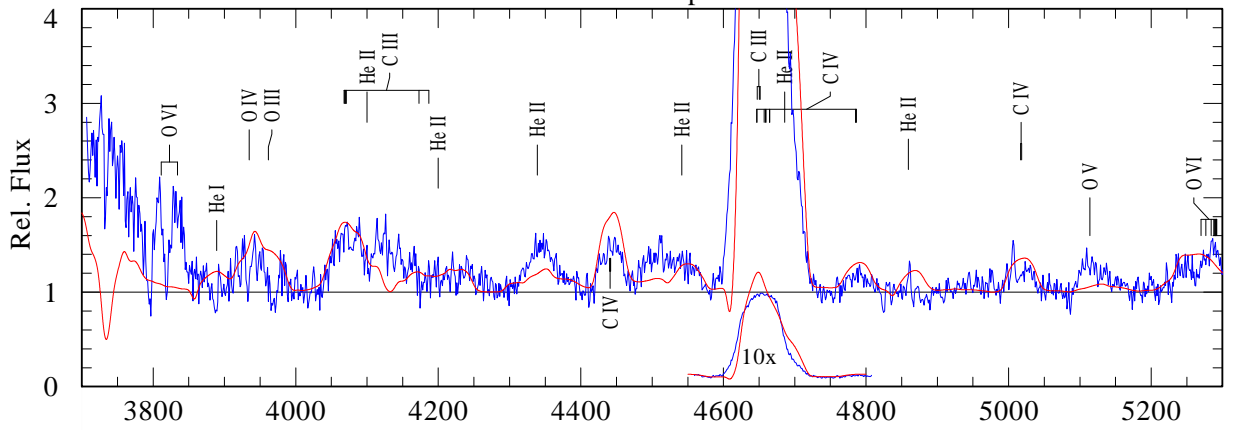
Ionization edge	Wavelength	$\log Q$
Hydrogen	911.6 \AA	49.23
Helium I	504.3 \AA	48.41
Helium II	227.9 \AA	37.91
Oxygen II	353.0 \AA	47.17
mechanical feedback		$3.38\text{E}+38 \text{ erg s}^{-1}$ $10^{3.94} L_{\odot}$
Chemical enrichment		
q_{He}	$[M_{\oplus}/\text{yr}]$	1.4E+00
q_{C}	$[M_{\oplus}/\text{yr}]$	1.3E+00
q_{O}	$[M_{\oplus}/\text{yr}]$	1.4E-01
q_{Si}	$[M_{\oplus}/\text{yr}]$	4.5E-03

Masterplot: **M31WR19 // LGS J004029.27+403916.6**

WC5



— Model Continuum + Lines convoluted with Gaussian (FWHM=1000)
— Observation — Model line spectrum — Model continuum



B.7 M 31 WR 23

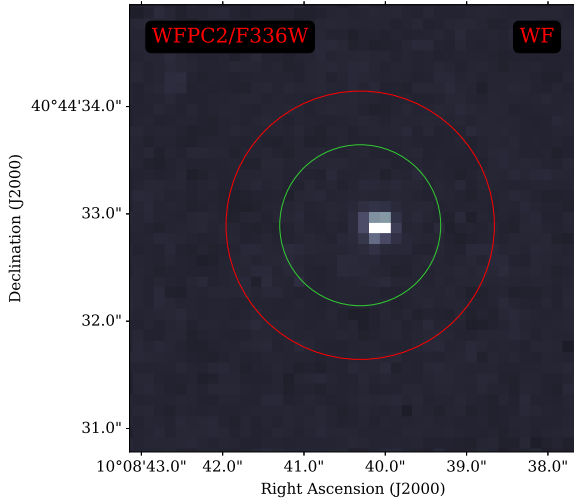


Figure 66: *HST* image of the surrounding region of WR 23. Camera and filter are noted in the image.

- WR 23 is WC4 star which unlike WR 15 does not show signs of an early evolutionary state but has a comparably low temperature.
- The dilution of the lines in the red increases for larger wavelength.
- The prominent lines are relatively weak for WC4 while the overall spectrum does not indicate any contamination.
- The star shows signs of fast rotation leading to an almost overcritical rotation. See Sect. 9.4 for the solution for this issue.
- The overall quality of the spectral fit is intermediate for a WC star.
- Disagreements between the model spectrum and the observation can be seen, all of them are the usual problems as described above.
 - No reproduction of O VI $\lambda\lambda 3811, 34$
 - Overprediction of O III $\lambda 3961$, O IV $\lambda 3934$, and C IV $\lambda\lambda 4440 - 42$
 - The unknown emission at 4500\AA

Table 24: *Summary for M 31 WR 23*

(a) *General overview*

Star	WR23
LGGS	J004034.69+404432.9
Spectral type	WC4
E(B-V)	0.05

(b) *Derived stellar parameter*

T_{eff}	[K]	70795
$T_{2/3}$	[K]	67234
L	[$\log L_{\odot}$]	5.4
M_{*}	[M_{\odot}]	13.0
R_{*}	[R_{\odot}]	3.3
\dot{M}	[$\log M_{\odot}/\text{yr}$]	-4.981
D		10
R_t	[R_{\odot}]	6.0256
v_{∞}	[km/s]	2000
v_{rad}	[km/s]	300
v_{rot}	[km/s]	2273
v_{crit}	[km/s]	863

(c) *Derived abundances*

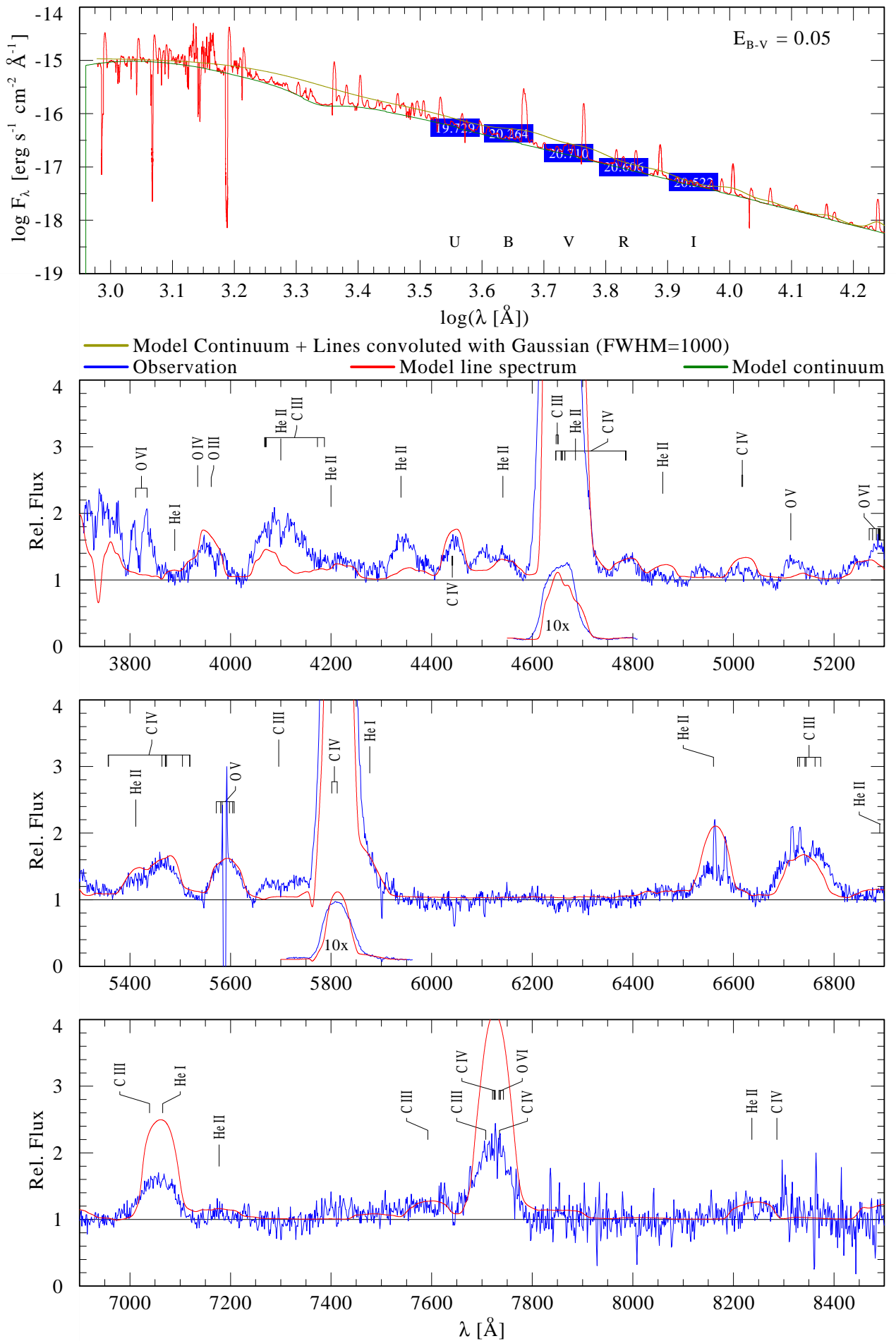
Element	mass fraction
Helium	4.4E-01
Carbon	5.0E-01
Oxygen	6.0E-02
Silicon	1.0E-03
Iron group	1.6E-03

(d) *Ionizing photons, mechanical feedback, and current chemical enrichment*

Ionization edge	Wavelength	$\log Q$
Hydrogen	911.6 \AA	49.27
Helium I	504.3 \AA	48.74
Helium II	227.9 \AA	39.85
Oxygen II	353.0 \AA	47.88
mechanical feedback		$2.65\text{E}+38 \text{ erg s}^{-1}$ $10^{3.84} L_{\odot}$
Chemical enrichment		
q_{He}	[M_{\oplus}/yr]	1.5E+00
q_{C}	[M_{\oplus}/yr]	1.7E+00
q_{O}	[M_{\oplus}/yr]	2.1E-01
q_{Si}	[M_{\oplus}/yr]	5.6E-03

Masterplot: **M31WR23 // LGS J004034.69+404432.9**

WC4



B.8 M 31 WR 43

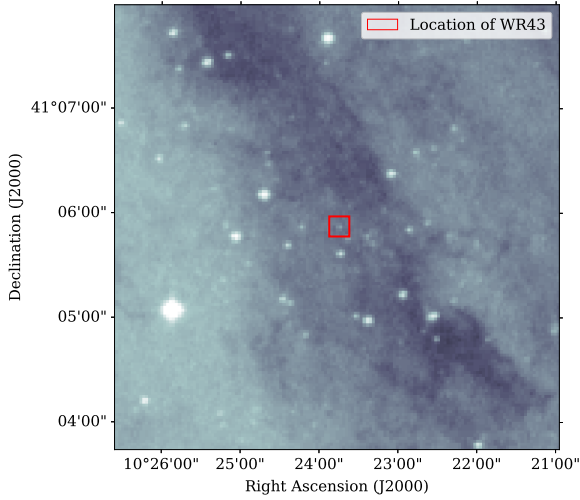


Figure 67: DSS image (blue) of the surrounding region of WR 43

- WR 43 is a
- It is not obvious in the photometry, but the red part of the spectrum shows signs of dilution for $\lambda > 6500\text{\AA}$. The spectrum shows small absorption lines in the red.
- No HST image exists to investigate the stellar neighborhood. The DSS2 blue image is shown in Fig 60.
- The overall quality of the spectral fit is average for a WC star.
- Disagreements between the model spectrum and the observation can be seen, all of them are the usual problems as described above.
 - No reproduction of O VI $\lambda\lambda 3811, 34$
 - Overprediction of O III $\lambda 3961$, O IV $\lambda 3934$, and C IV $\lambda\lambda 4440 - 42$
 - The diagnostic pair is overpredicted.

Table 25: Summary for M 31 WR 43

(a) General overview

Star	WR43
LGGS	J004134.99+410552.3
Spectral type	WC7
E(B-V)	0.12

(b) Derived stellar parameter

T_{eff}	[K]	79433
$T_{2/3}$	[K]	64564
L	[$\log L_{\odot}$]	5.6
M_*	[M_{\odot}]	17.0
R_*	[R_{\odot}]	3.3
\dot{M}	[$\log M_{\odot}/\text{yr}$]	-4.649
D		30
R_t	[R_{\odot}]	2.7542
v_{∞}	[km/s]	2300
v_{rad}	[km/s]	250
v_{rot}	[km/s]	2273
v_{crit}	[km/s]	988

(c) Derived abundances

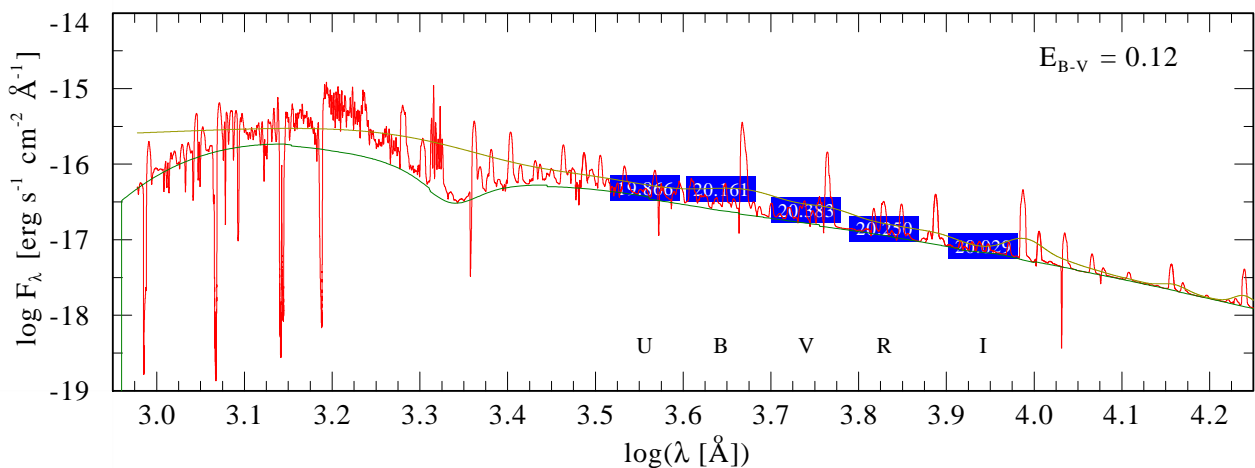
Element	mass fraction
Helium	4.6E-01
Carbon	5.0E-01
Oxygen	4.0E-02
Silicon	1.0E-03
Iron group	1.6E-03

(d) Ionizing photons, mechanical feedback, and current chemical enrichment

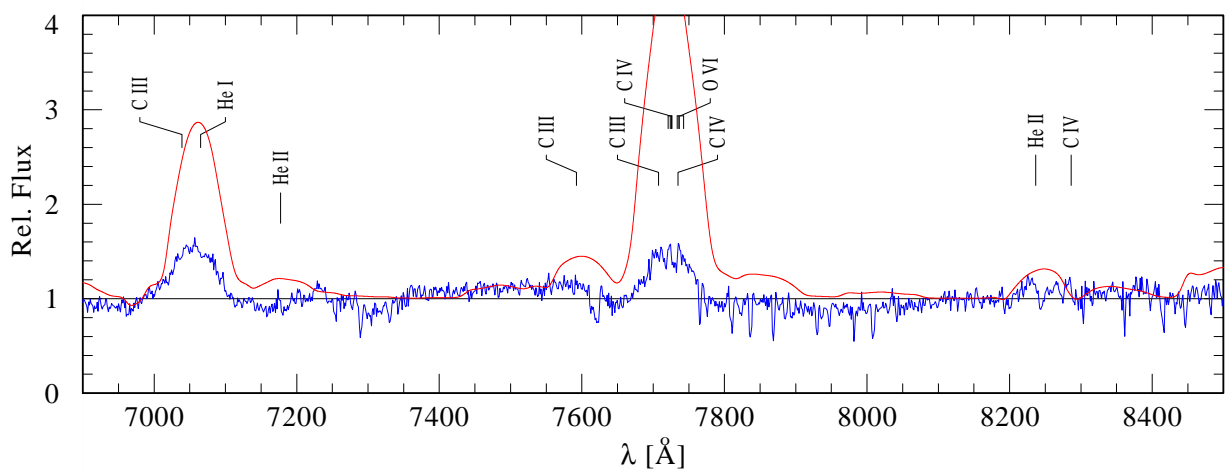
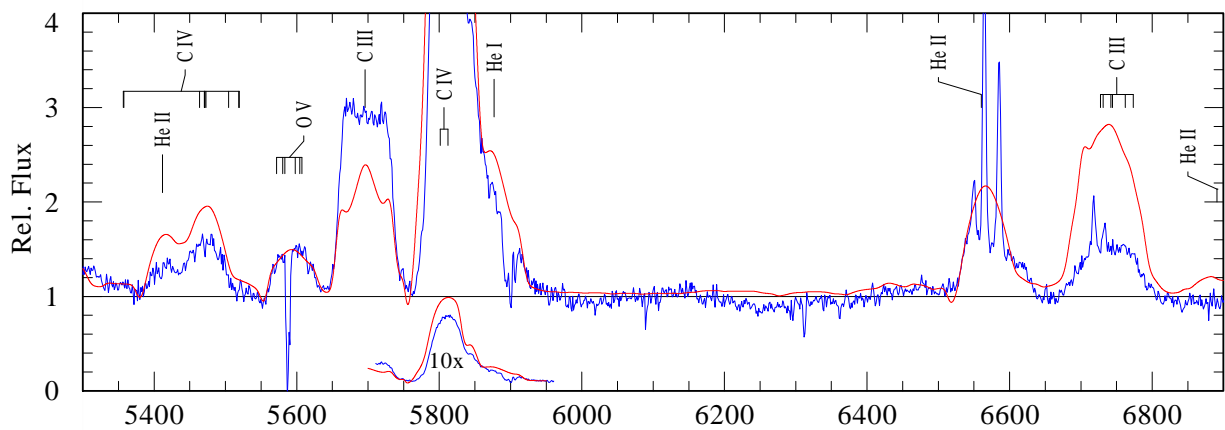
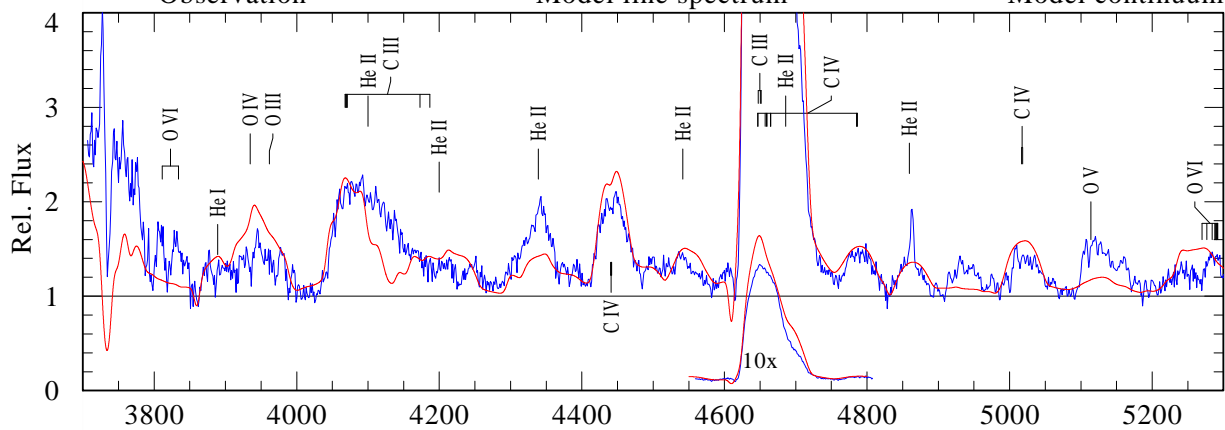
Ionization edge	Wavelength	$\log Q$
Hydrogen	911.6 \AA	49.41
Helium I	504.3 \AA	48.50
Helium II	227.9 \AA	37.01
Oxygen II	353.0 \AA	46.91
mechanical feedback		$7.53\text{E}+38 \text{ erg s}^{-1}$ $10^{4.29} L_{\odot}$
Chemical enrichment		
q_{He}	[M_{\oplus}/yr]	3.4E+00
q_{C}	[M_{\oplus}/yr]	3.7E+00
q_{O}	[M_{\oplus}/yr]	3.0E-01
q_{Si}	[M_{\oplus}/yr]	1.2E-02

Masterplot: **M31WR43 // LGS J004134.99+410552.3**

WC7



— Model Continuum + Lines convoluted with Gaussian (FWHM=1000)
 — Observation — Model line spectrum — Model continuum



B.9 M 31 WR 54

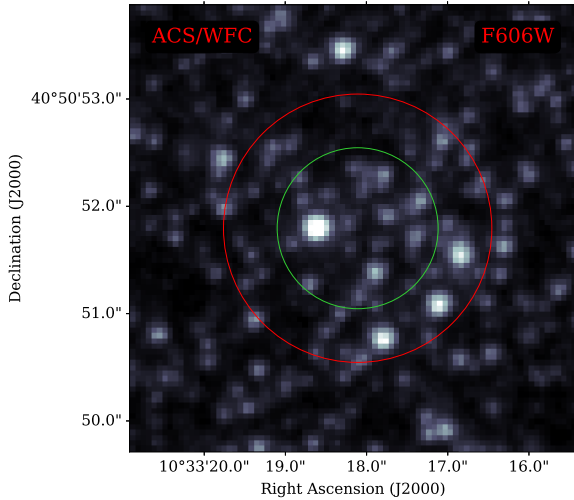


Figure 68: *HST* image of the surrounding region of WR 54. Camera and filter are noted in the image.

- WR 54 is the most extreme star in the sample. The WC 4 star has the highest observed carbon and oxygen abundance, is very hot for a WC and its emission are very strong.
- Lines that are usually overpredicted by the models in other stars are underpredicted here due to the extreme strong emissions.
- The HST image in Fig. 68 shows a crowded region around this star. Only an image with a red filter is available.
- The spectrum is very noisy over the entire spectral range.
- There are no signs of rotation visible.
- The overall quality of the spectral fit is very good for a WC star.
- Disagreements between the model spectrum and the observation can be seen, all of them are the usual problems as described above.
 - No reproduction of O VI $\lambda\lambda 3811, 34$
 - Overprediction of O III $\lambda 3961$, O IV $\lambda 3934$, and C IV $\lambda\lambda 4440 - 42$

Table 26: *Summary for M 31 WR 54*
(a) *General overview*

Star	WR54
LGGS	J004213.21+405051.8
Spectral type	WC4
E(B-V)	0.13

(b) *Derived stellar parameter*

T_{eff}	[K]	177828
$T_{2/3}$	[K]	97940
L	[$\log L_{\odot}$]	5.55
M_*	[M_{\odot}]	15.3
R_*	[R_{\odot}]	0.6
\dot{M}	[$\log M_{\odot}/\text{yr}$]	-4.804
D		50
R_t	[R_{\odot}]	0.6026
v_{∞}	[km/s]	2600
v_{rad}	[km/s]	100
v_{rot}	[km/s]	0
v_{crit}	[km/s]	2158

(c) *Derived abundances*

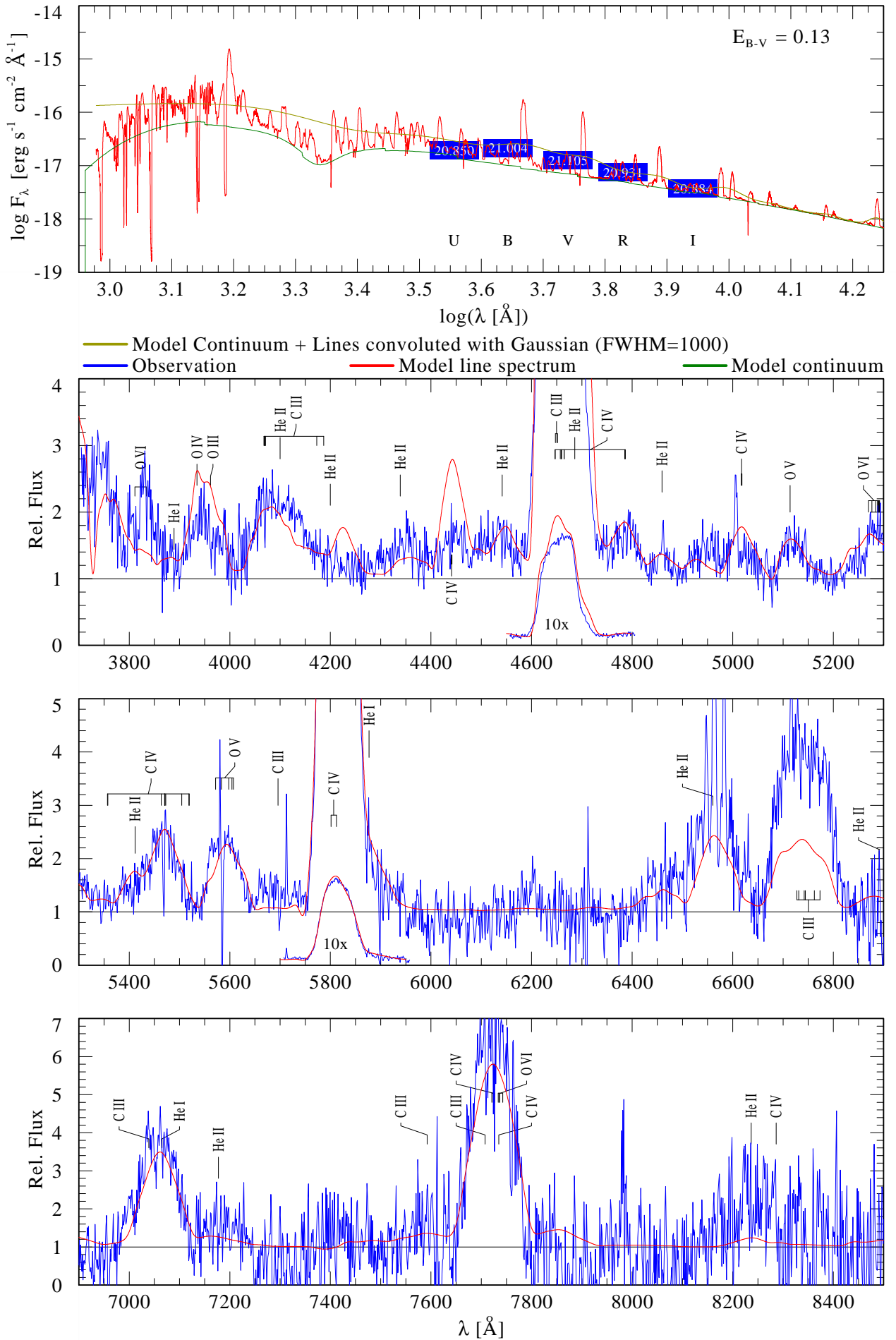
Element	mass fraction
Helium	1.9E-01
Carbon	7.0E-01
Oxygen	1.0E-01
Silicon	5.0E-03
Iron group	1.6E-03

(d) *Ionizing photons, mechanical feedback, and current chemical enrichment*

Ionization edge	Wavelength	$\log Q$
Hydrogen	911.6 Å	49.36
Helium I	504.3 Å	48.80
Helium II	227.9 Å	39.63
Oxygen II	353.0 Å	48.01
mechanical feedback		$6.73\text{E}+38 \text{ erg s}^{-1}$ $10^{4.24} L_{\odot}$
Chemical enrichment		
q_{He}	[M_{\oplus}/yr]	1.0E+00
q_{C}	[M_{\oplus}/yr]	3.7E+00
q_{O}	[M_{\oplus}/yr]	5.2E-01
q_{Si}	[M_{\oplus}/yr]	8.4E-03

Masterplot: **M31WR54 // LGS J004213.21+405051.8**

WC4



B.10 M 31 WR 55

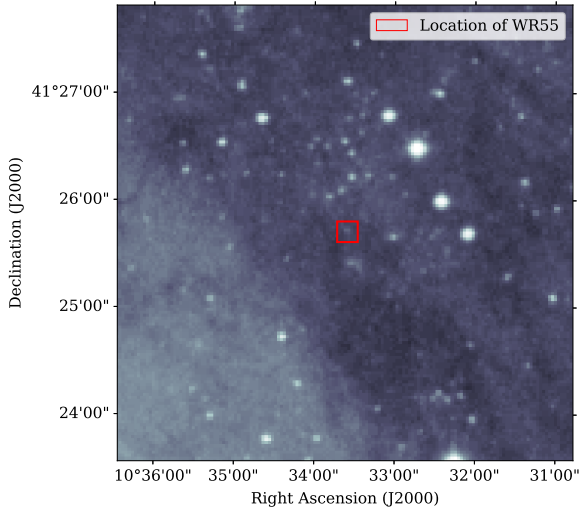


Figure 69: DSS image (blue) of the surrounding region of WR 55

- M 31 WR 55 is a WC6 star which resembles the spectrum of WR 7 with a lower carbon abundance.
- It is not obvious in the photometry, but the red part of the spectrum shows signs of dilution for $\lambda > 6500\text{\AA}$ and absorption features that might originate in a contaminating star.
- No HST image exists to investigate the stellar neighborhood. The DSS2 blue image is shown in Fig 69.
- The star shows signs of fast rotation leading to an overcritical rotation. See Sect. 9.4 for the solution for this issue.
- The overall quality of the spectral fit is good for a WC star.
- The radial velocity might indicate a run-away star. See Sect. 8.1 for details.
- The reddening for this star is quite high, but the nebula lines are weak.
- Disagreements between the model spectrum and the observation can be seen, all of them are the usual problems as described above.
 - The diagnostic pair is slightly overpredicted by the model

Table 27: Summary for M 31 WR 55
(a) General overview

Star	WR55
LGGS	J004214.36+412542.3
Spectral type	WC6
E(B-V)	0.18

(b) Derived stellar parameter

T_{eff}	[K]	70795
$T_{2/3}$	[K]	59218
L	[$\log L_{\odot}$]	5.45
M_{*}	[M_{\odot}]	14.3
R_{*}	[R_{\odot}]	3.5
\dot{M}	[$\log M_{\odot}/\text{yr}$]	-4.736
D		30
R_t	[R_{\odot}]	3.2359
v_{∞}	[km/s]	2200
v_{rad}	[km/s]	150
v_{rot}	[km/s]	2273
v_{crit}	[km/s]	881

(c) Derived abundances

Element	mass fraction
Helium	6.8E-01
Carbon	3.0E-01
Oxygen	2.0E-02
Silicon	2.0E-03
Iron group	1.6E-03

(d) Ionizing photons, mechanical feedback, and current chemical enrichment

Ionization edge	Wavelength	$\log Q$
Hydrogen	911.6 \AA	49.26
Helium I	504.3 \AA	48.32
Helium II	227.9 \AA	36.26
Oxygen II	353.0 \AA	46.55
mechanical feedback		$5.64\text{E}+38 \text{ erg s}^{-1}$ $10^{4.17} L_{\odot}$
Chemical enrichment		
q_{He}	[M_{\oplus}/yr]	4.1E+00
q_{C}	[M_{\oplus}/yr]	1.8E+00
q_{O}	[M_{\oplus}/yr]	1.2E-01
q_{Si}	[M_{\oplus}/yr]	9.8E-03

B.11 M 31 WR 93

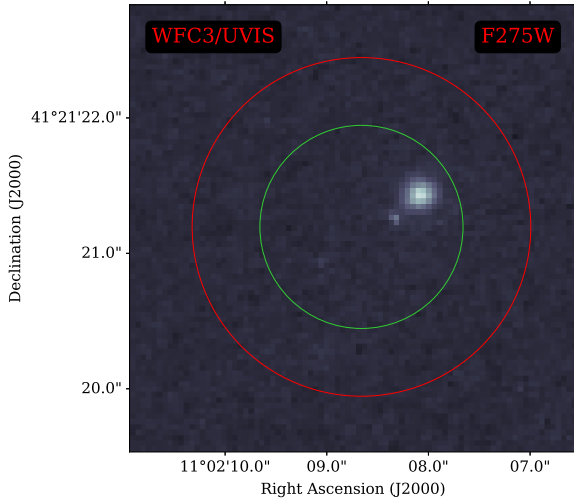


Figure 70: *HST* image of the surrounding region of WR 93. Camera and filter are noted in the image.

- WR 93 is a very bright WC6 star.
- Next to a reduced carbon abundance, the star also shows signs of nitrogen in its spectrum.
- The spectral analysis revealed a star that is not only very bright but also has a very strong stellar wind.
- It is not obvious in the photometry, but the red part of the spectrum shows signs of dilution for $\lambda > 7000\text{\AA}$.
- The HST image of the stellar neighborhood in Fig 70 shows no other source closeby.
- The star shows signs of fast rotation leading to an almost overcritical rotation. See Sect. 9.4 for the solution for this issue.
- The overall quality of the spectral fit is very good for a WC star.
- The spectral fit does not suffer from the same shortcomings as other fits, but it shows an overestimation for some He II lines.
- Despite of the relatively high reddening found for this star, the S/N ratio of the spectrum is high.
- We suggest to classify this star as WC6/WN

Table 28: *Summary for M 31 WR 93*

(a) *General overview*

Star	WR93
LGGS	J004408.58+412121.2
Spectral type	WC6
E(B-V)	0.15

(b) *Derived stellar parameter*

T_{eff}	[K]	70795
$T_{2/3}$	[K]	55032
L	[$\log L_{\odot}$]	5.85
M_{*}	[M_{\odot}]	25.5
R_{*}	[R_{\odot}]	5.6
\dot{M}	[$\log M_{\odot}/\text{yr}$]	-4.347
D		10
R_t	[R_{\odot}]	4.0738
v_{∞}	[km/s]	2200
v_{rad}	[km/s]	-50
v_{rot}	[km/s]	2273
v_{crit}	[km/s]	933

(c) *Derived abundances*

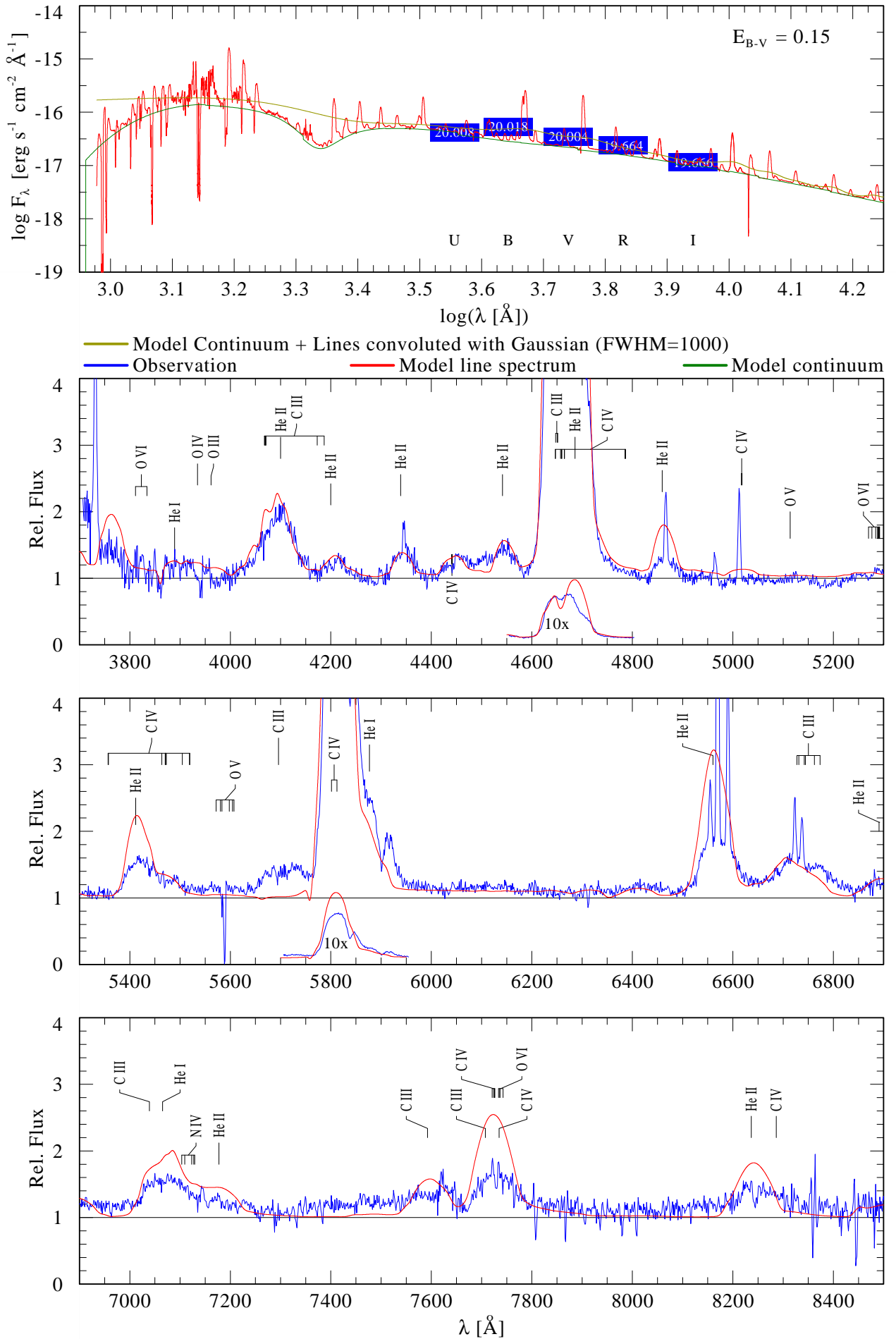
Element	mass fraction
Helium	8.9E-01
Carbon	1.0E-01
Oxygen	1.0E-03
Nitrogen	2.0E-03
Silicon	1.0E-02
Iron group	1.6E-03

(d) *Ionizing photons, mechanical feedback, and current chemical enrichment*

Ionization edge	Wavelength	$\log Q$
Hydrogen	911.6 \AA	49.68
Helium I	504.3 \AA	49.17
Helium II	227.9 \AA	39.14
Oxygen II	353.0 \AA	48.25
mechanical feedback		$1.38\text{E}+39 \text{ erg s}^{-1}$ $10^{4.56} L_{\odot}$
Chemical enrichment		
q_{He}	[M_{\oplus}/yr]	1.3E+01
q_{C}	[M_{\oplus}/yr]	1.5E+00
q_{N}	[M_{\oplus}/yr]	3.0E-02
q_{O}	[M_{\oplus}/yr]	1.5E-02
q_{Si}	[M_{\oplus}/yr]	2.4E-02

Masterplot: [M31WR93](#) // [LGS J004408.58+412121.2](#)

WC6



B.12 M 31 WR 94

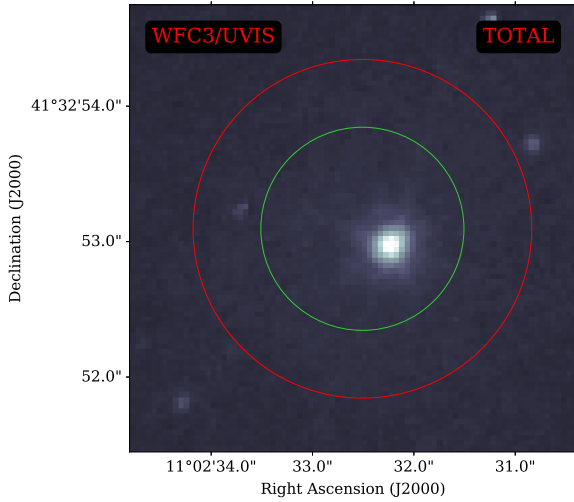


Figure 71: *HST* image of the surrounding region of WR 94. Camera and filter are noted in the image.

This star is like WR 93 interesting for its extremely strong stellar wind and overall feedback. It is among the brightest stars of the sample and has the second highest mass loss rate of all here analyzed stars. Together with its relatively fast wind, it transfers an enormous amount of kinetic energy into its surroundings. So far it is very similar to WR 93. But for WR 94, the effect of this strong feedback is actually visible, as this star has blown a bubble around itself with ≈ 30 pc diameter (see Fig. 72).

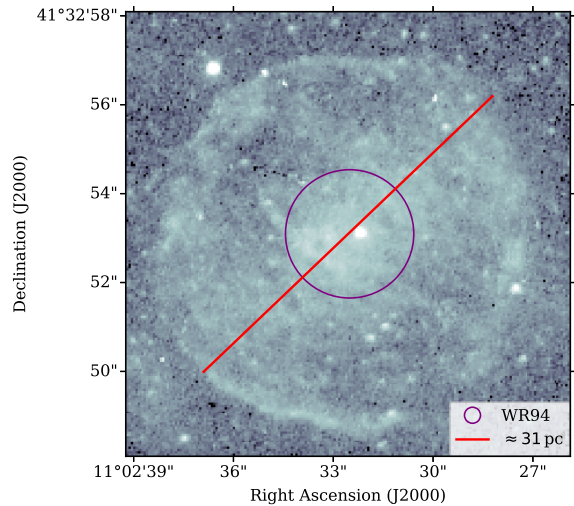


Figure 72: Wind blown bubble around WR 94, reported as H II region [AMB2011] HII 2671 by Azimlu et al. (2011). Background image is taken by *HST* ACS WFC with the filter F658N.

Photometry and spectrum of this star indicate a dilution in the red part of the spectrum. Furthermore, this is a very fast rotator. See Sect. 9.4 for the solution for this issue.

Table 29: Summary for M 31 WR 94
(a) General overview

Star	WR94
LGGS	J004410.17+413253.1
Spectral type	WC6
E(B-V)	0.1

(b) Derived stellar parameter

T_{eff}	[K]	74989
$T_{2/3}$	[K]	56783
L	[$\log L_{\odot}$]	5.9
M_*	[M_{\odot}]	27.2
R_*	[R_{\odot}]	5.3
\dot{M}	[$\log M_{\odot}/\text{yr}$]	-4.364
D		30
R_t	[R_{\odot}]	2.8184
v_{∞}	[km/s]	2300
v_{rad}	[km/s]	-150
v_{rot}	[km/s]	2727
v_{crit}	[km/s]	993

(c) Derived abundances

Element	mass fraction
Helium	7.9E-01
Carbon	2.0E-01
Oxygen	1.0E-02
Silicon	2.0E-03
Iron group	1.6E-03

(d) Ionizing photons, mechanical feedback, and current chemical enrichment

Ionization edge	Wavelength	$\log Q$
Hydrogen	911.6 Å	49.71
Helium I	504.3 Å	48.85
Helium II	227.9 Å	36.50
Oxygen II	353.0 Å	47.17
mechanical feedback		$1.45\text{E}+39 \text{ erg s}^{-1}$ $10^{4.58} L_{\odot}$
Chemical enrichment		
q_{He}	[M_{\oplus}/yr]	1.1E+01
q_{C}	[M_{\oplus}/yr]	2.9E+00
q_{O}	[M_{\oplus}/yr]	1.4E-01
q_{Si}	[M_{\oplus}/yr]	2.3E-02

B.13 M 31 WR 96

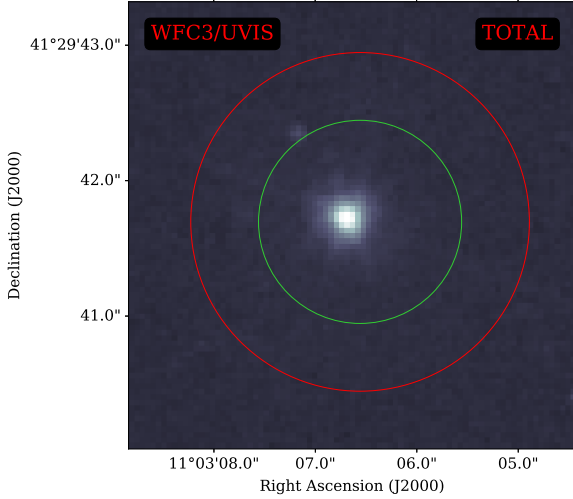


Figure 73: *HST* image of the surrounding region of WR 96. Camera and filter are noted in the image.

- WR 96 is a very bright WC6 star.
- The star shows a reduced carbon abundance.
- The spectral analysis revealed a star that is not only very bright but also has a very strong stellar wind.
- The red part of the spectrum shows signs of dilution for $\lambda > 7000\text{\AA}$. The photometry supports this finding as well as the appearance of small absorption lines.
- The HST image of the stellar neighborhood in Fig 73 shows no other source closeby.
- The star shows signs of fast rotation leading to an almost overcritical rotation. See Sect. 9.4 for the solution for this issue.
- The overall quality of the spectral fit is very good for a WC star.

Table 30: *Summary for M 31 WR 96*

(a) *General overview*

Star	WR96
LGGS	J004412.44+412941.7
Spectral type	WC6
E(B-V)	0.12

(b) *Derived stellar parameter*

T_{eff}	[K]	66834
$T_{2/3}$	[K]	56738
L	[$\log L_{\odot}$]	5.9
M_{*}	[M_{\odot}]	27.1
R_{*}	[R_{\odot}]	6.7
\dot{M}	[$\log M_{\odot}/\text{yr}$]	-4.471
D		50
R_t	[R_{\odot}]	3.6308
v_{∞}	[km/s]	2400
v_{rad}	[km/s]	-150
v_{rot}	[km/s]	2273
v_{crit}	[km/s]	882

(c) *Derived abundances*

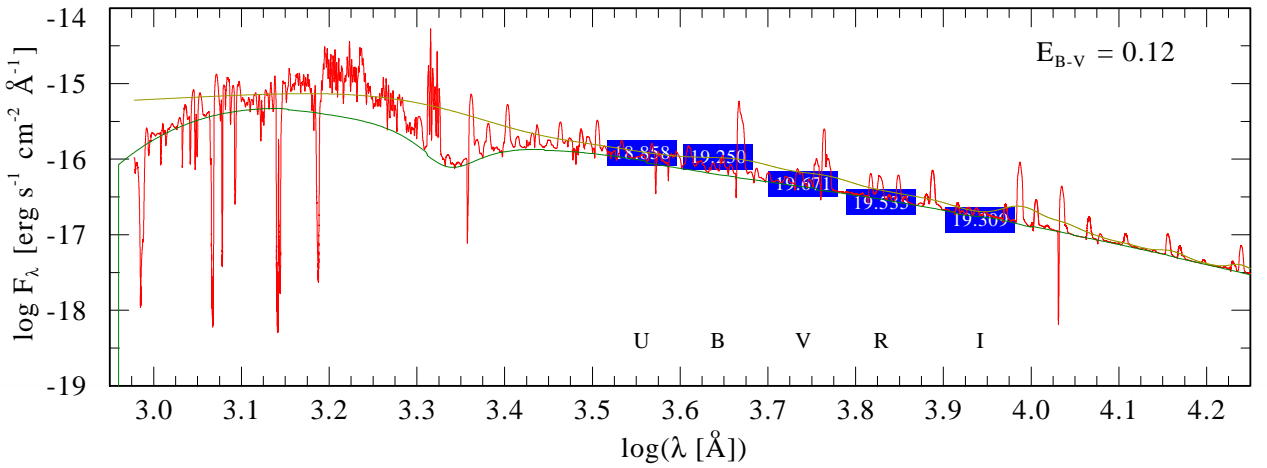
Element	mass fraction
Helium	7.3E-01
Carbon	2.5E-01
Oxygen	2.0E-02
Silicon	1.0E-03
Iron group	1.6E-03

(d) *Ionizing photons, mechanical feedback, and current chemical enrichment*

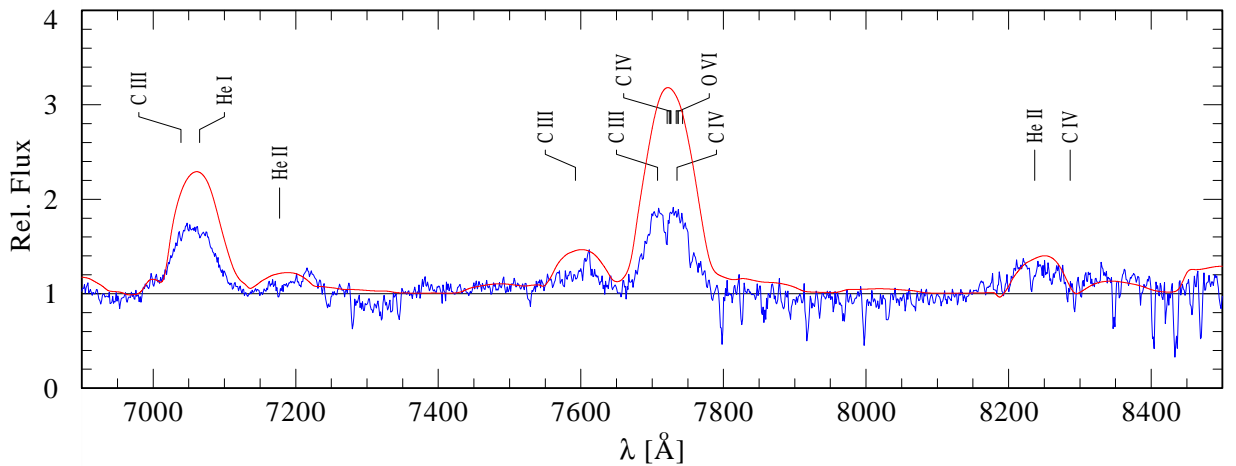
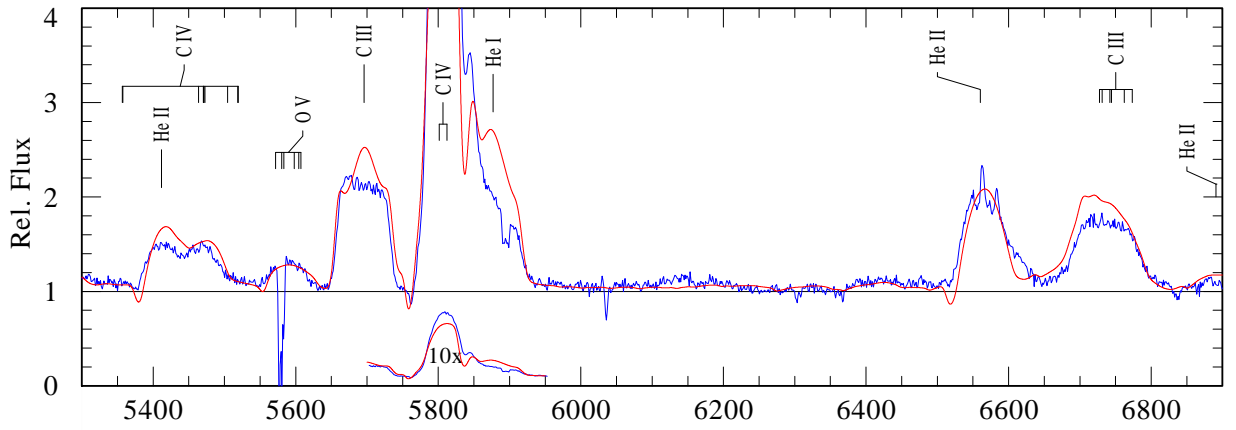
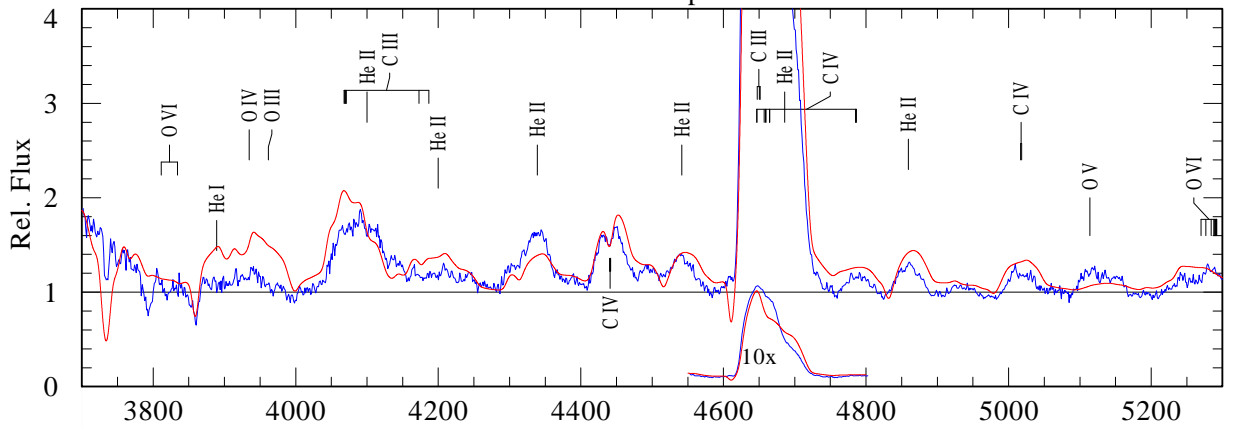
Ionization edge	Wavelength	$\log Q$
Hydrogen	911.6 \AA	49.69
Helium I	504.3 \AA	48.69
Helium II	227.9 \AA	36.52
Oxygen II	353.0 \AA	46.79
mechanical feedback		$1.23\text{E}+39 \text{ erg s}^{-1}$ $10^{4.51} L_{\odot}$
Chemical enrichment		
q_{He}	[M_{\oplus}/yr]	8.2E+00
q_{C}	[M_{\oplus}/yr]	2.8E+00
q_{O}	[M_{\oplus}/yr]	2.3E-01
q_{Si}	[M_{\oplus}/yr]	1.8E-02

Masterplot: [M31WR96 // LGS J004412.44+412941.7](#)

WC6



— Model Continuum + Lines convoluted with Gaussian (FWHM=1000)
 — Observation — Model line spectrum — Model continuum



B.14 M 31 WR 102

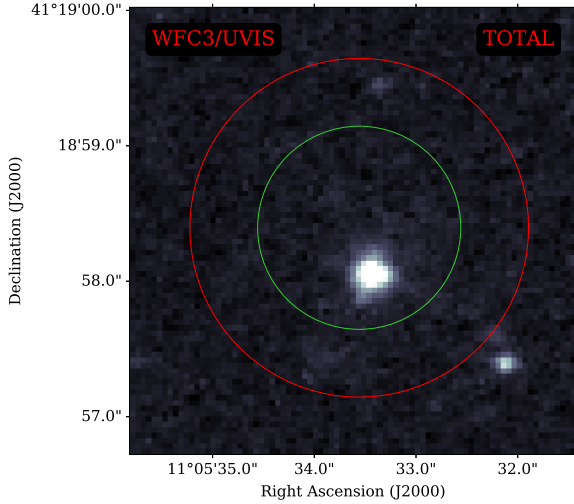


Figure 74: *HST* image of the surrounding region of WR 102. Camera and filter are noted in the image.

- WR 102 is a WC7-8 and therefore the latest type star analyzed here.
- The star has a very low terminal velocity which causes the spectrum to be dominated by narrow emission.
- The *HST* image of the stellar neighborhood in Fig 74 shows no other source closely but a slightly asymmetric appearance of the star.
- Dilution and absorption lines for $\lambda > 7000 \text{ \AA}$ indicate contamination.
- The overall quality of the spectral fit is very good for a WC star.
- Notable for this star is a strongly reduced carbon abundance.
- The star shows signs of slow rotation.
- It does not suffer from the same shortcomings as the other fits.

Table 31: *Summary for M 31 WR 102*

(a) *General overview*

Star	WR102
LGGS	J004422.24+411858.4
Spectral type	WC7-8
E(B-V)	0.1

(b) *Derived stellar parameter*

T_{eff}	[K]	59566
$T_{2/3}$	[K]	46368
L	[$\log L_{\odot}$]	5.3
M_{*}	[M_{\odot}]	12.2
R_{*}	[R_{\odot}]	4.2
\dot{M}	[$\log M_{\odot}/\text{yr}$]	-4.821
D		10
R_t	[R_{\odot}]	3.9811
v_{∞}	[km/s]	1100
v_{rad}	[km/s]	-100
v_{rot}	[km/s]	455
v_{crit}	[km/s]	745

(c) *Derived abundances*

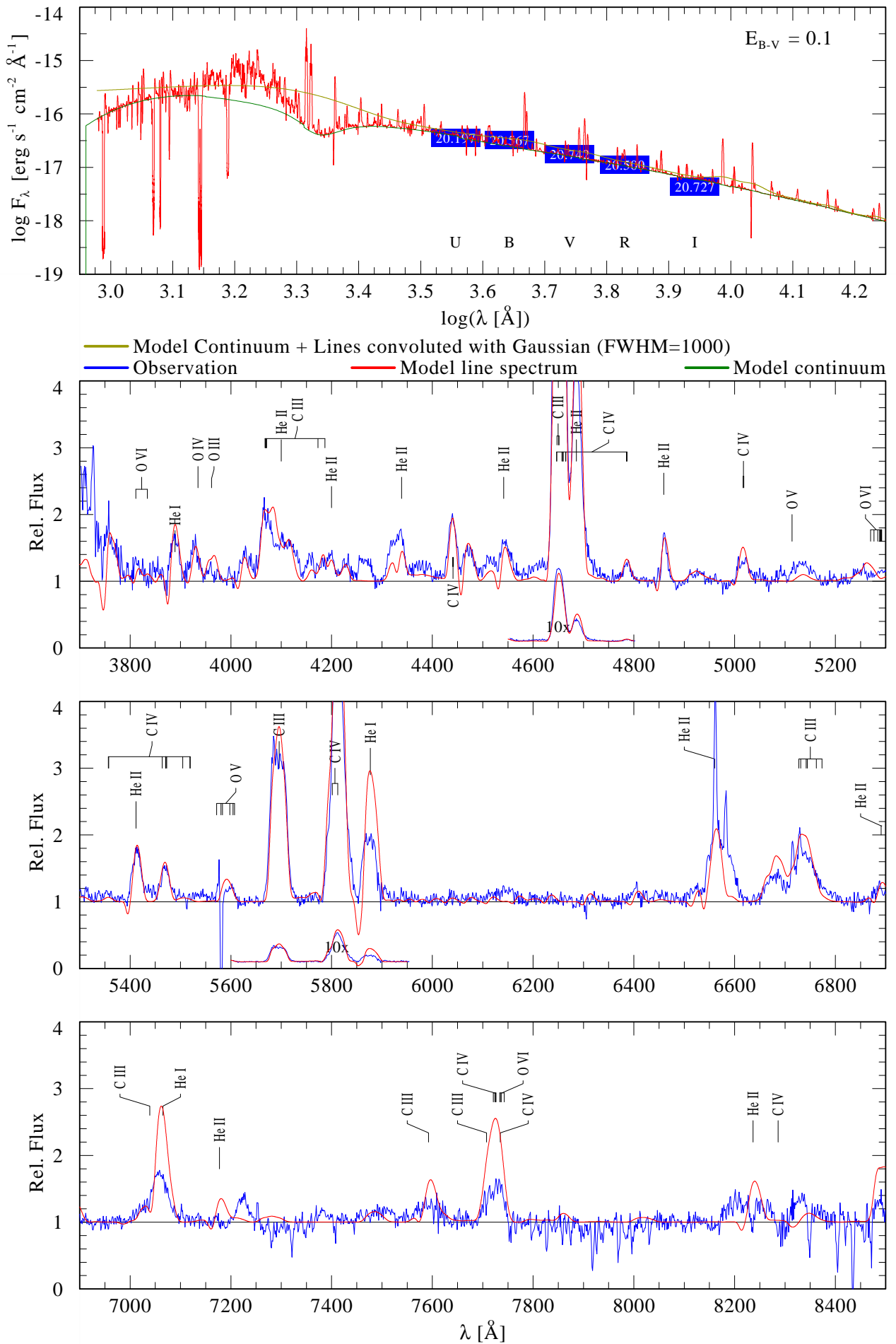
Element	mass fraction
Helium	8.3E-01
Carbon	1.5E-01
Oxygen	1.0E-02
Silicon	5.0E-03
Iron group	1.6E-03

(d) *Ionizing photons, mechanical feedback, and current chemical enrichment*

Ionization edge	Wavelength	$\log Q$
Hydrogen	911.6 \AA	49.08
Helium I	504.3 \AA	47.95
Helium II	227.9 \AA	34.57
Oxygen II	353.0 \AA	45.89
mechanical feedback		$1.16\text{E}+38 \text{ erg s}^{-1}$ $10^{3.48} L_{\odot}$
Chemical enrichment		
q_{He}	[M_{\oplus}/yr]	4.2E+00
q_{C}	[M_{\oplus}/yr]	7.5E-01
q_{O}	[M_{\oplus}/yr]	5.0E-02
q_{Si}	[M_{\oplus}/yr]	8.0E-03

Masterplot: **M31WR102 // LGGS J004422.24+411858.4**

WC7-8



B.15 M 31 WR 113

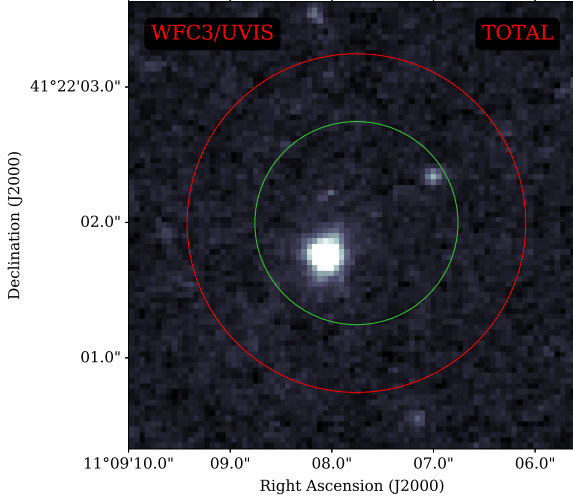


Figure 75: *HST* image of the surrounding region of WR 113. Camera and filter are noted in the image.

- WR 113 is a WC5 star and the third star in our sample which shows clear signs of nitrogen.
- The found nitrogen abundance is consistent with the low carbon abundance.
- The does not show signs of rotation.
- The *HST* image of the stellar neighborhood in Fig 75 shows no other source closely.
- The overall quality of the spectral fit is very good for a WC star.
- The spectral fit does not suffer from the same shortcomings as other fits. C IV $\lambda 5808$ is underpredicted by the model and N IV $\lambda 4060$ is overpredicted. ionNiv $\lambda 7100+$ is reproduced nicely.
- We suggest to classify this star as WC5/WN.

Table 32: *Summary for M 31 WR 113*

(a) *General overview*

Star	WR113
LGGS	J004436.52+412202.0
Spectral type	WC5
E(B-V)	0.15

(b) *Derived stellar parameter*

T_{eff}	[K]	79433
$T_{2/3}$	[K]	56124
L	[$\log L_{\odot}$]	5.5
M_{*}	[M_{\odot}]	15.7
R_{*}	[R_{\odot}]	3.0
\dot{M}	[$\log M_{\odot}/\text{yr}$]	-4.607
D		10
R_t	[R_{\odot}]	2.8184
v_{∞}	[km/s]	1800
v_{rad}	[km/s]	-50
v_{rot}	[km/s]	0
v_{crit}	[km/s]	1005

(c) *Derived abundances*

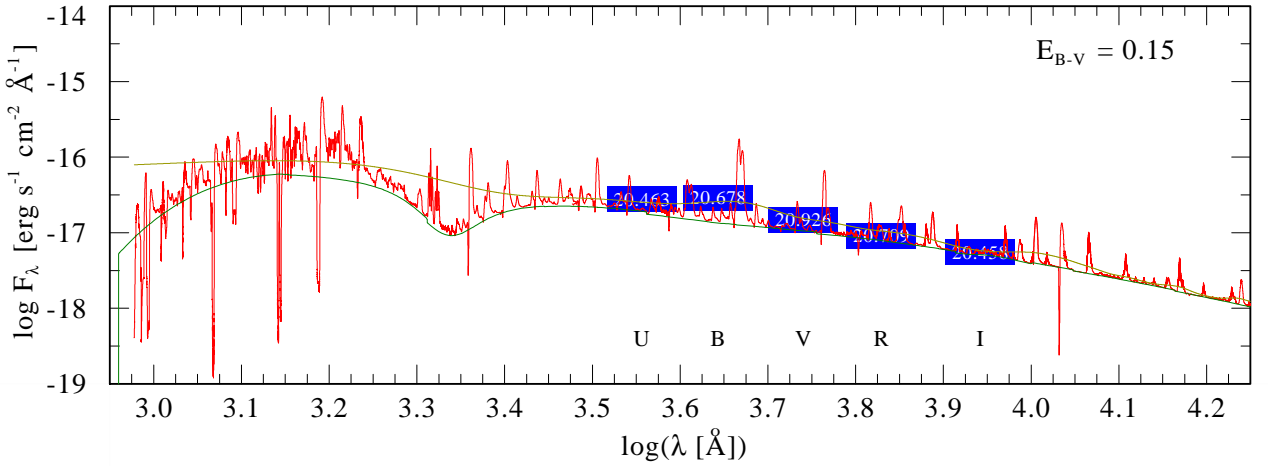
Element	mass fraction
Helium	8.7E-01
Carbon	1.0E-01
Oxygen	5.0E-03
Nitrogen	2.5E-02
Silicon	1.0E-03
Iron group	1.6E-03

(d) *Ionizing photons, mechanical feedback, and current chemical enrichment*

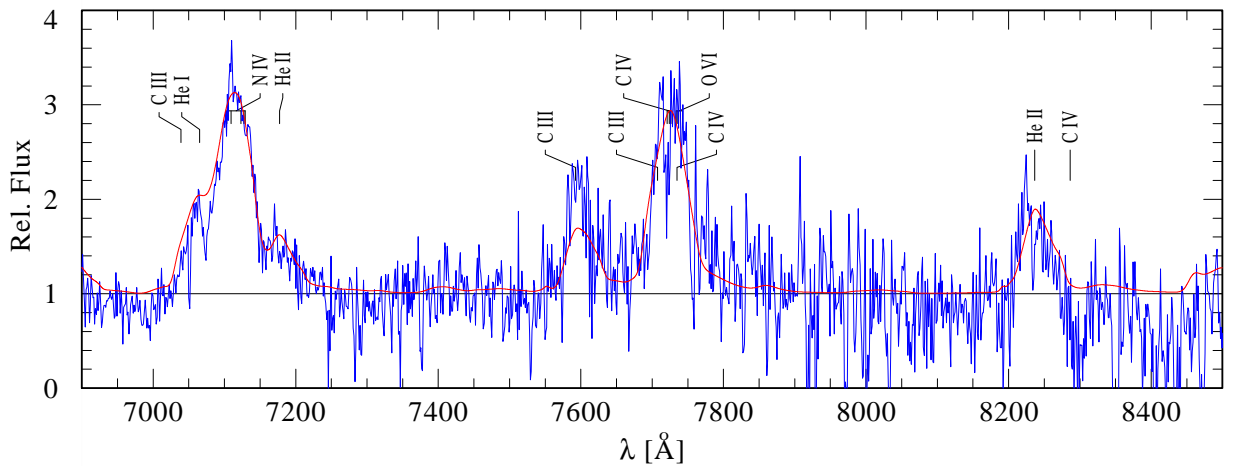
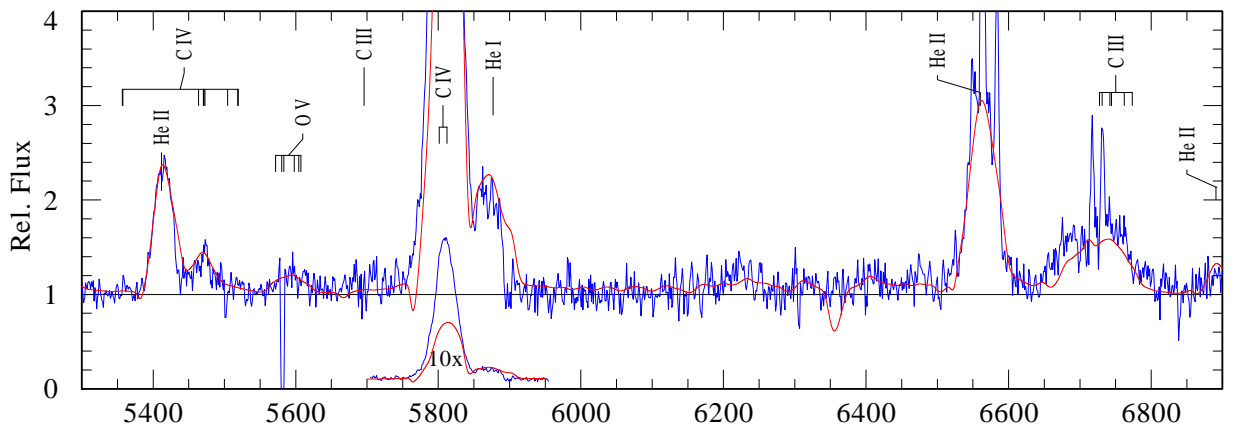
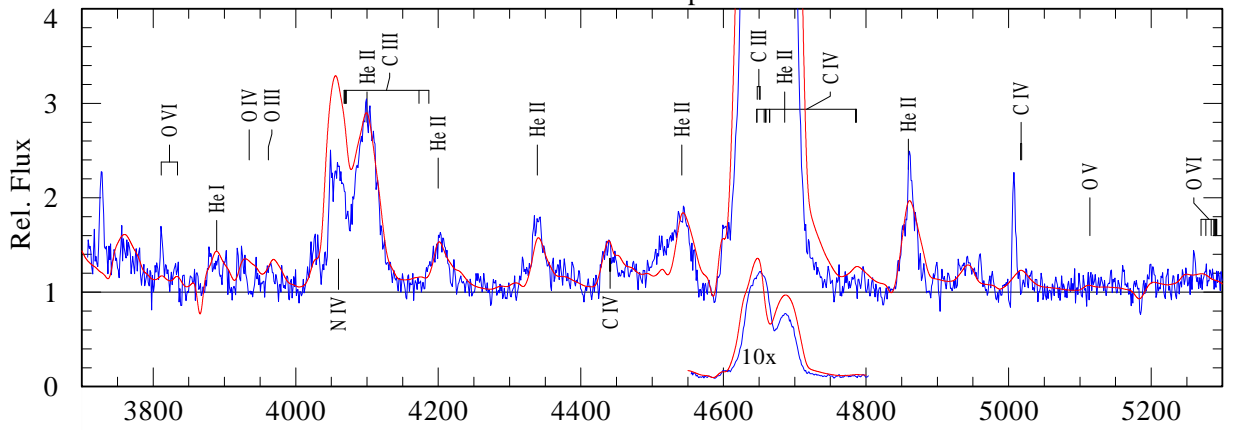
Ionization edge	Wavelength	$\log Q$
Hydrogen	911.6 Å	49.34
Helium I	504.3 Å	48.68
Helium II	227.9 Å	37.71
Oxygen II	353.0 Å	47.49
mechanical feedback		$5.08\text{E}+38 \text{ erg s}^{-1}$ $10^{4.12} L_{\odot}$
Chemical enrichment		
q_{He}	[M_{\oplus}/yr]	7.1E+00
q_{C}	[M_{\oplus}/yr]	8.2E-01
q_{N}	[M_{\oplus}/yr]	2.1E-01
q_{O}	[M_{\oplus}/yr]	4.1E-02
q_{Si}	[M_{\oplus}/yr]	1.3E-02

Masterplot: **M31WR113 // LGGS J004436.52+412202.0**

WC5



— Model Continuum + Lines convoluted with Gaussian (FWHM=1000)
— Observation — Model line spectrum — Model continuum



B.16 M 31 WR 121

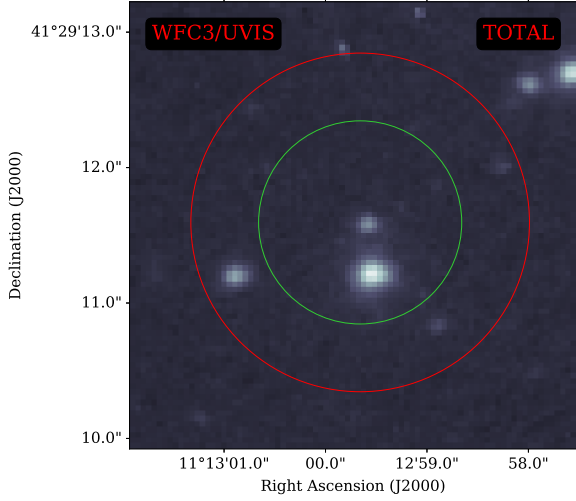


Figure 76: *HST* image of the surrounding region of WR 121. Camera and filter are noted in the image.

- WR 121 is a WC7 and quite luminous.
- The star has a very low terminal velocity which causes the spectrum to be dominated by narrow emission.
- The HST image of the stellar neighborhood in Fig 74 shows a handful of fainter blue source closeby.
- Dilution and absorption lines for $\lambda > 7000 \text{ \AA}$ indicate contamination.
- The overall quality of the spectral fit is good for a WC star.
- It does not suffer from the same shortcomings as the other fits.
- The overall quality of the spectral fit is very good for a WC star.
- The diagnostic pair is slightly overestimated. C III $\lambda 5696$ is underpredicted.

Table 33: *Summary for M 31 WR 121*

(a) *General overview*

Star	WR121
LGGS	J004451.98+412911.6
Spectral type	WC7
E(B-V)	0.09

(b) *Derived stellar parameter*

T_{eff}	[K]	59566
$T_{2/3}$	[K]	52819
L	[$\log L_{\odot}$]	5.2
M_{*}	[M_{\odot}]	10.5
R_{*}	[R_{\odot}]	3.7
\dot{M}	[$\log M_{\odot}/\text{yr}$]	-4.922
D		4
R_t	[R_{\odot}]	6.6069
v_{∞}	[km/s]	1400
v_{rad}	[km/s]	-200
v_{rot}	[km/s]	909
v_{crit}	[km/s]	734

(c) *Derived abundances*

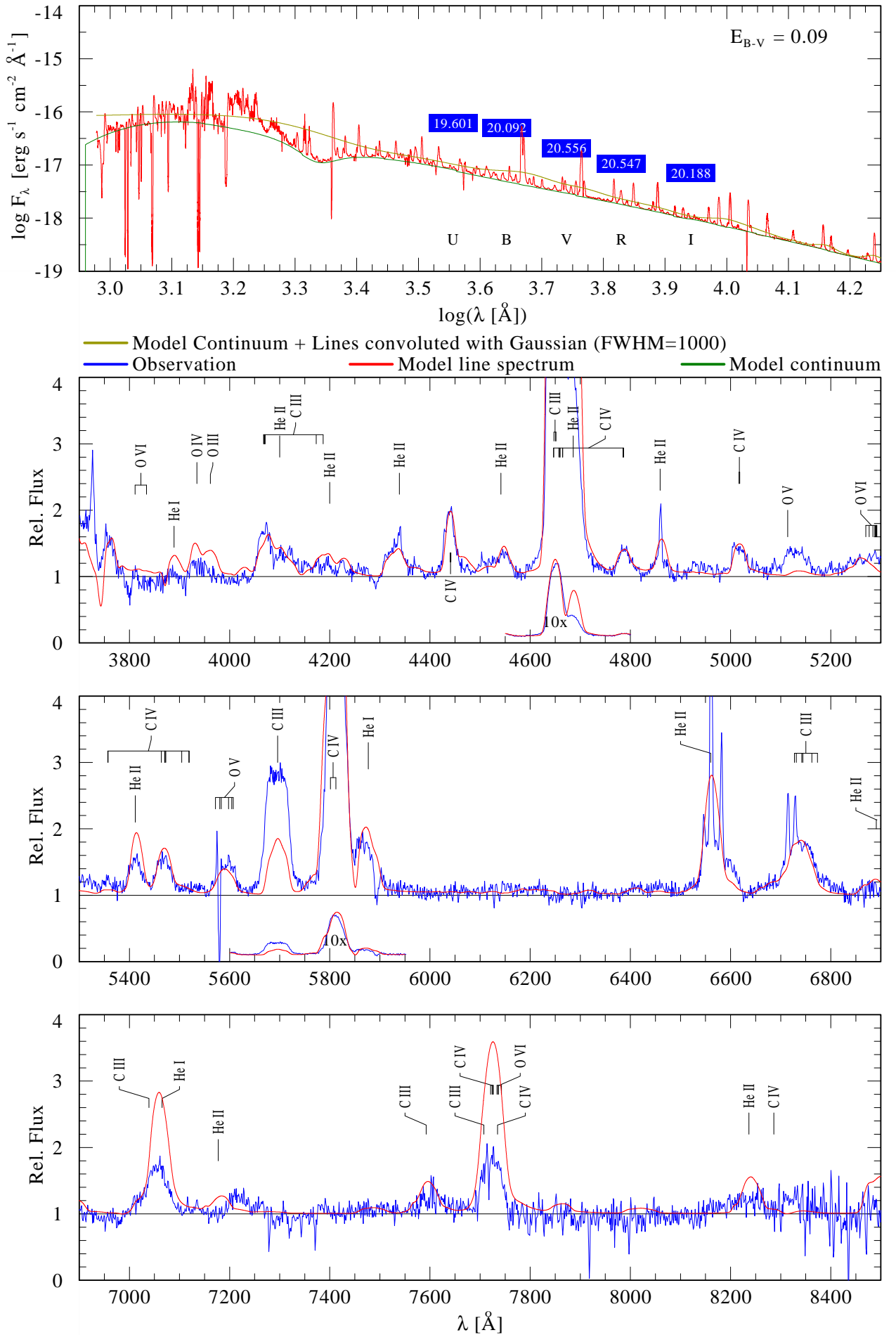
Element	mass fraction
Helium	6.8E-01
Carbon	3.0E-01
Oxygen	2.0E-02
Silicon	1.0E-03
Iron group	1.6E-03

(d) *Ionizing photons, mechanical feedback, and current chemical enrichment*

Ionization edge	Wavelength	$\log Q$
Hydrogen	911.6 \AA	49.05
Helium I	504.3 \AA	48.23
Helium II	227.9 \AA	37.39
Oxygen II	353.0 \AA	46.99
mechanical feedback		$1.49\text{E}+38 \text{ erg s}^{-1}$ $10^{3.59} L_{\odot}$
Chemical enrichment		
q_{He}	[M_{\oplus}/yr]	2.7E+00
q_{C}	[M_{\oplus}/yr]	1.2E+00
q_{O}	[M_{\oplus}/yr]	8.0E-02
q_{Si}	[M_{\oplus}/yr]	6.4E-03

Masterplot: M31WR121 // LGGS J004451.98+412911.6

WC7



B.17 M 31 WR 123

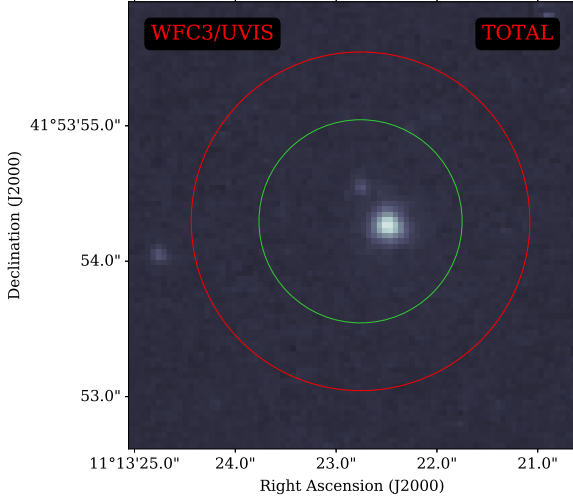


Figure 77: *HST* image of the surrounding region of WR 123. Camera and filter are noted in the image.

- WR 123 is a WC7 and comparably faint.
- The star has a very low terminal velocity which causes the spectrum to be dominated by narrow emission.
- The *HST* image of the stellar neighborhood in Fig 77 shows no bright source nearby.
- Dilution and absorption lines for $\lambda > 7000 \text{ \AA}$ indicate contamination.
- The overall quality of the spectral fit is good for a WC star.
- Disagreements between the model spectrum and the observation can be seen, all of them are the usual problems as described above.
 - The diagnostic pair is slightly overestimated. C III $\lambda 5696$ is underpredicted.
 - Underestimation of He II $\lambda 4338$

Table 34: *Summary for M 31 WR 123*

(a) *General overview*

Star	WR123
LGGS	J004453.52+415354.3
Spectral type	WC7
E(B-V)	0.05

(b) *Derived stellar parameter*

T_{eff}	[K]	63096
$T_{2/3}$	[K]	53072
L	[$\log L_{\odot}$]	5.1
M_{*}	[M_{\odot}]	9.3
R_{*}	[R_{\odot}]	3.0
\dot{M}	[$\log M_{\odot}/\text{yr}$]	-5.053
D		10
R_t	[R_{\odot}]	4.2658
v_{∞}	[km/s]	1200
v_{rad}	[km/s]	-150
v_{rot}	[km/s]	0
v_{crit}	[km/s]	774

(c) *Derived abundances*

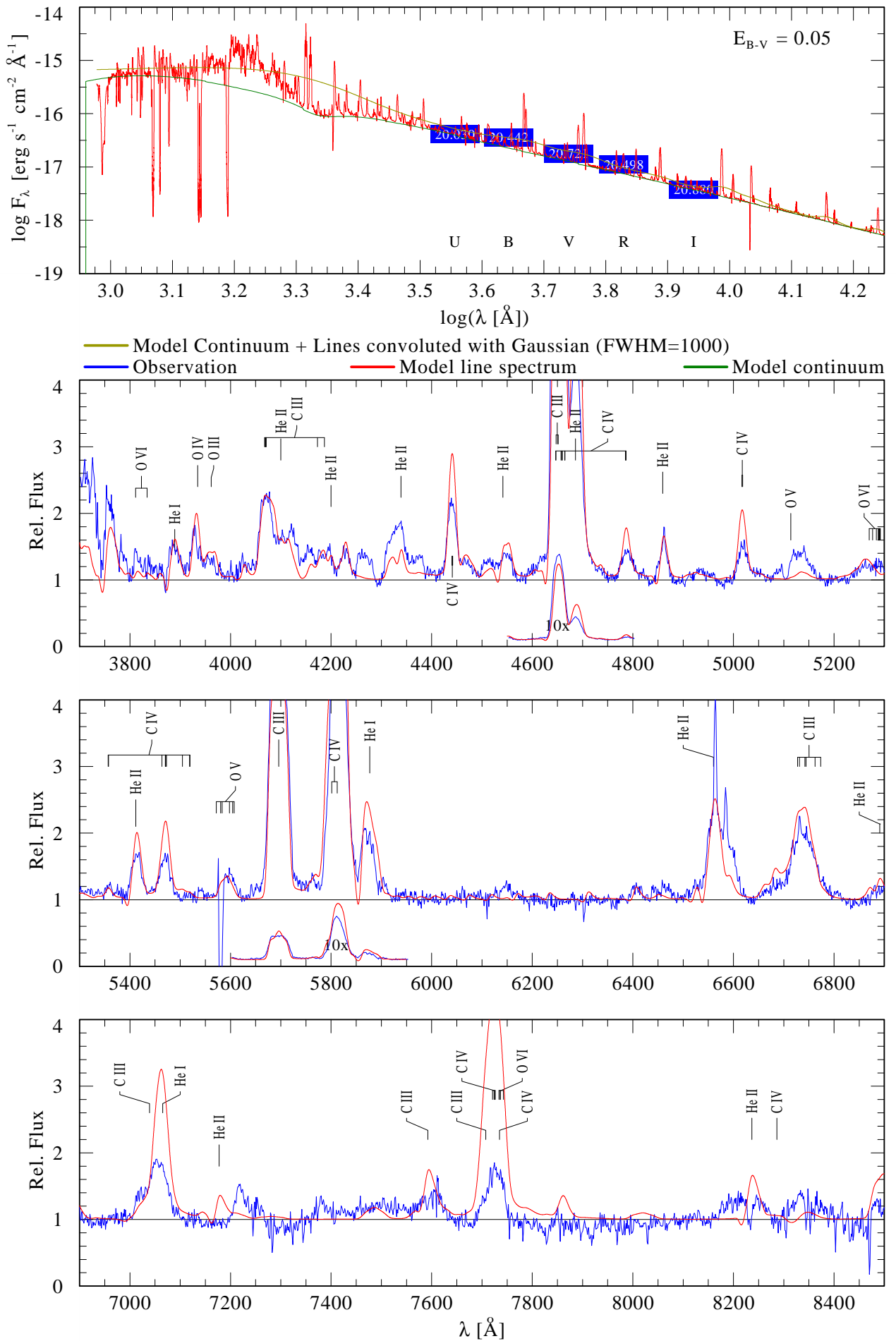
Element	mass fraction
Helium	6.3E-01
Carbon	3.5E-01
Oxygen	9.0E-03
Silicon	5.0E-03
Iron group	1.6E-03

(d) *Ionizing photons, mechanical feedback, and current chemical enrichment*

Ionization edge	Wavelength	$\log Q$
Hydrogen	911.6 \AA	48.91
Helium I	504.3 \AA	47.90
Helium II	227.9 \AA	35.63
Oxygen II	353.0 \AA	46.06
mechanical feedback		$8.08\text{E}+37 \text{ erg s}^{-1}$ $10^{3.32} L_{\odot}$
Chemical enrichment		
q_{He}	[M_{\oplus}/yr]	1.9E+00
q_{C}	[M_{\oplus}/yr]	1.0E+00
q_{O}	[M_{\oplus}/yr]	2.7E-02
q_{Si}	[M_{\oplus}/yr]	4.7E-03

Masterplot: **M31WR123 // LGGS J004453.52+415354.3**

WC7



B.18 M 31 WR 124

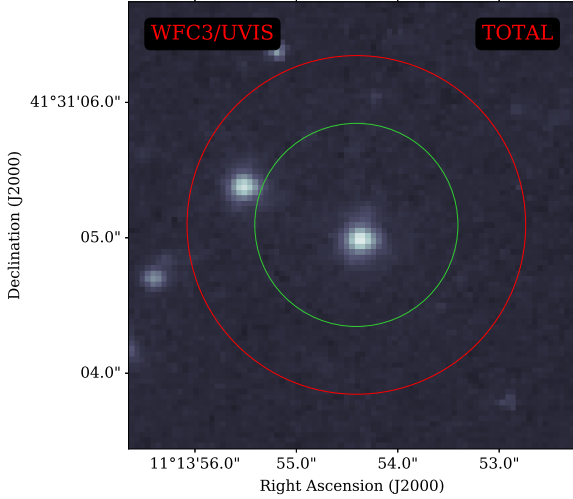


Figure 78: *HST* image of the surrounding region of WR 124. Camera and filter are noted in the image.

- WR 124 is a WC6 star with relatively weak lines.
- The reduced carbon abundance indicates an early evolutionary state.
- The star shows signs of slow rotation.
- The *HST* image of the stellar neighborhood in Fig 78 shows a similar bright source nearby that might have contaminated the spectrum.
- Dilution and absorption lines for $\lambda > 7000 \text{ \AA}$ indicate contamination.
- The overall quality of the spectral fit is average for a WC star.
- Disagreements between the model spectrum and the observation can be seen, all of them are the usual problems as described above.
 - The diagnostic pair and C III $\lambda 5696$ are overpredicted.

Table 35: Summary for M 31 WR 124
(a) General overview

Star	WR124
LGGS	J004455.63+413105.1
Spectral type	WC6
E(B-V)	0.14

(b) Derived stellar parameter

T_{eff}	[K]	56234
$T_{2/3}$	[K]	53950
L	[$\log L_{\odot}$]	5.62
M_{*}	[M_{\odot}]	17.8
R_{*}	[R_{\odot}]	6.8
\dot{M}	[$\log M_{\odot}/\text{yr}$]	-4.835
D		25
R_t	[R_{\odot}]	7.2444
v_{∞}	[km/s]	2000
v_{rad}	[km/s]	-150
v_{rot}	[km/s]	909
v_{crit}	[km/s]	708

(c) Derived abundances

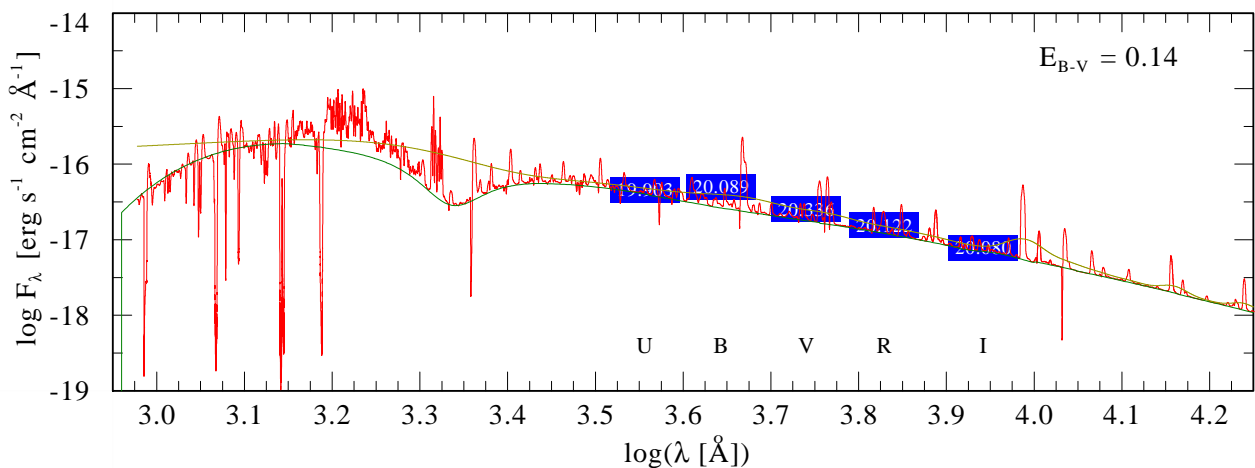
Element	mass fraction
Helium	6.3E-01
Carbon	3.5E-01
Oxygen	2.0E-02
Silicon	2.0E-03
Iron group	1.6E-03

(d) Ionizing photons, mechanical feedback, and current chemical enrichment

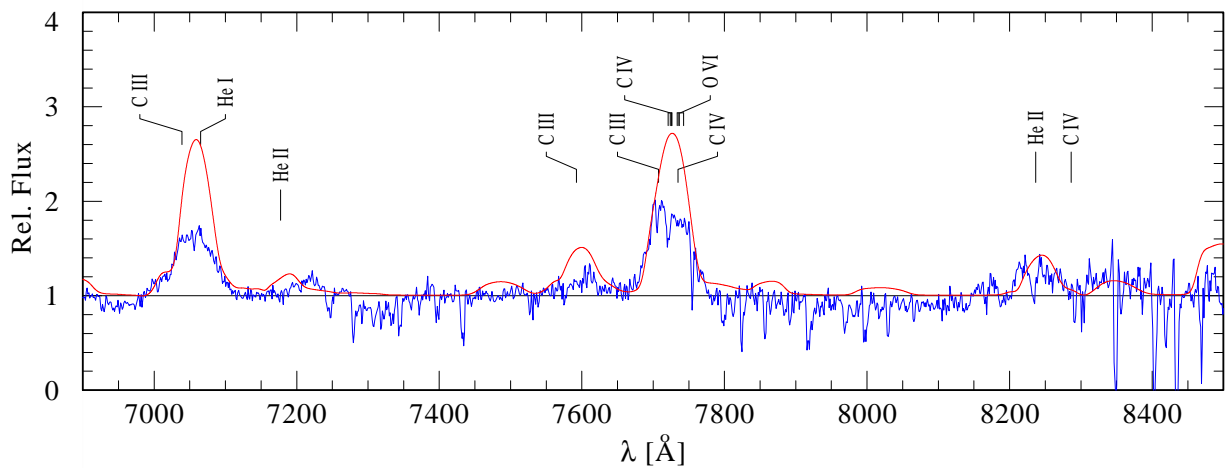
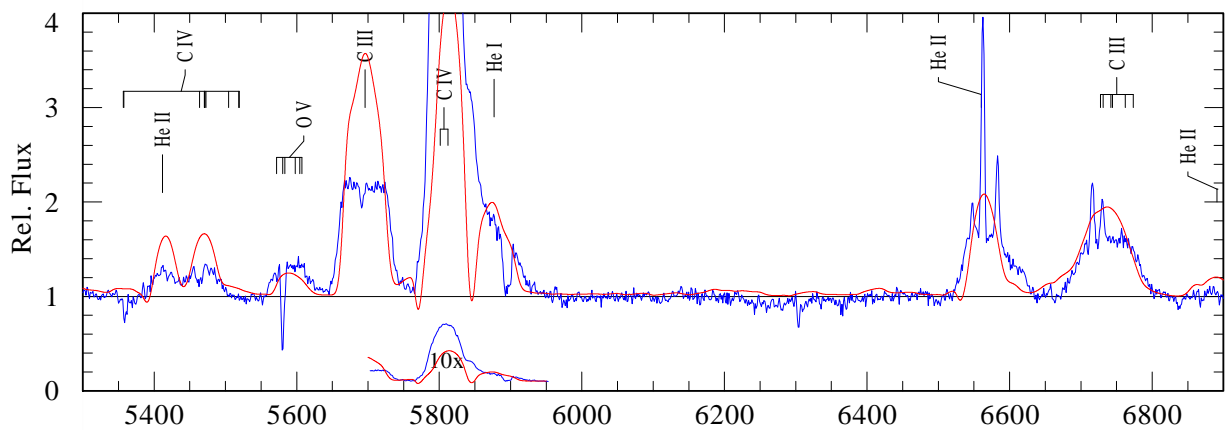
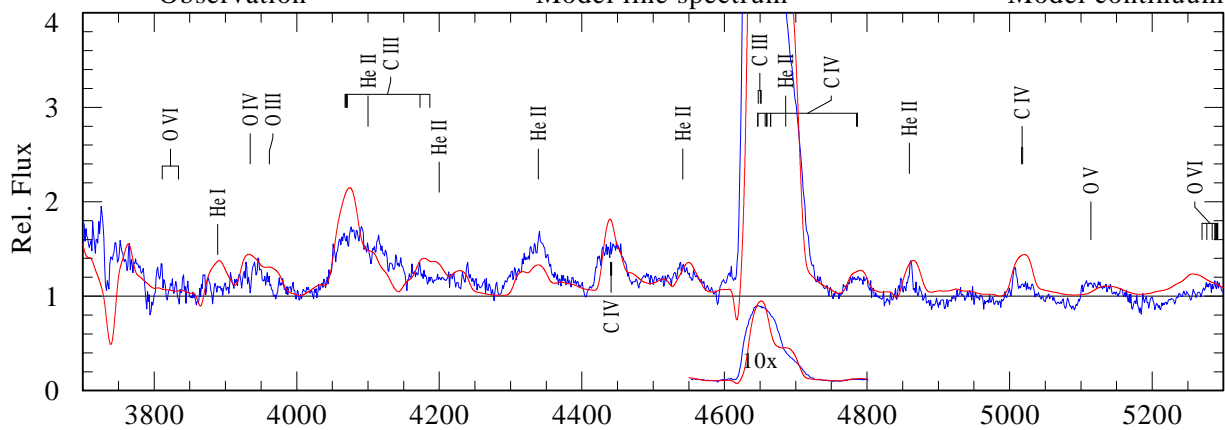
Ionization edge	Wavelength	$\log Q$
Hydrogen	911.6 \AA	49.45
Helium I	504.3 \AA	48.41
Helium II	227.9 \AA	36.60
Oxygen II	353.0 \AA	46.68
mechanical feedback		$3.71\text{E}+38 \text{ erg s}^{-1}$ $10^{3.98} L_{\odot}$
Chemical enrichment		
q_{He}	[M_{\oplus}/yr]	3.0E+00
q_{C}	[M_{\oplus}/yr]	1.7E+00
q_{O}	[M_{\oplus}/yr]	9.7E-02
q_{Si}	[M_{\oplus}/yr]	7.8E-03

Masterplot: **M31WR124 // LGGS J004455.63+413105.1**

WC6



— Model Continuum + Lines convoluted with Gaussian (FWHM=1000)
 — Observation — Model line spectrum — Model continuum



B.19 M 31 WR 132

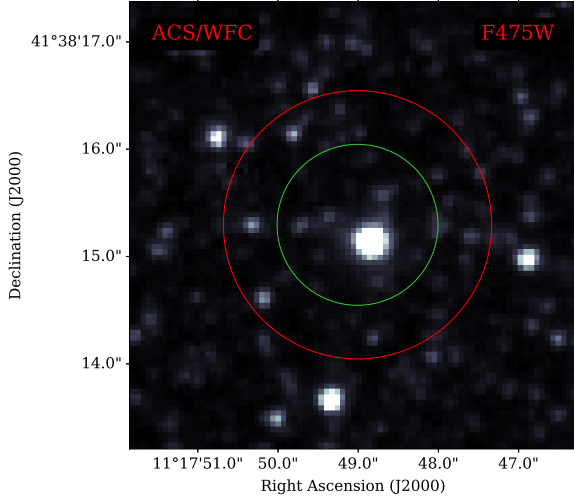


Figure 79: *HST* image of the surrounding region of WR 132. Camera and filter are noted in the image.

- WR 132 is a WC6 and comparably bright.
- The star has a relatively low terminal velocity.
- The *HST* image of the stellar neighborhood in Fig 79 shows some source nearby that are all fainter than the WR.
- Dilution and absorption lines for $\lambda > 7000 \text{ \AA}$ indicate contamination.
- The overall quality of the spectral fit is good for a WC star.
- Disagreements between the model spectrum and the observation can be seen, all of them are the usual problems as described above.
 - Overprediction of $\text{O III } \lambda 3961$, $\text{O IV } \lambda 3934$, and $\text{C IV } \lambda \lambda 4440 - 42$
 - The diagnostic pair is slightly overestimated.
 - Underestimation of $\text{He II } \lambda 4338$

Table 36: Summary for M 31 WR 132

(a) General overview

Star	WR132
LGGS	J004511.27+413815.3
Spectral type	WC6
E(B-V)	0.14

(b) Derived stellar parameter

T_{eff}	[K]	63096
$T_{2/3}$	[K]	58631
L	[$\log L_{\odot}$]	5.7
M_{*}	[M_{\odot}]	19.7
R_{*}	[R_{\odot}]	5.9
\dot{M}	[$\log M_{\odot}/\text{yr}$]	-4.76
D		25
R_t	[R_{\odot}]	5.4325
v_{∞}	[km/s]	1900
v_{rad}	[km/s]	-150
v_{rot}	[km/s]	909
v_{crit}	[km/s]	797

(c) Derived abundances

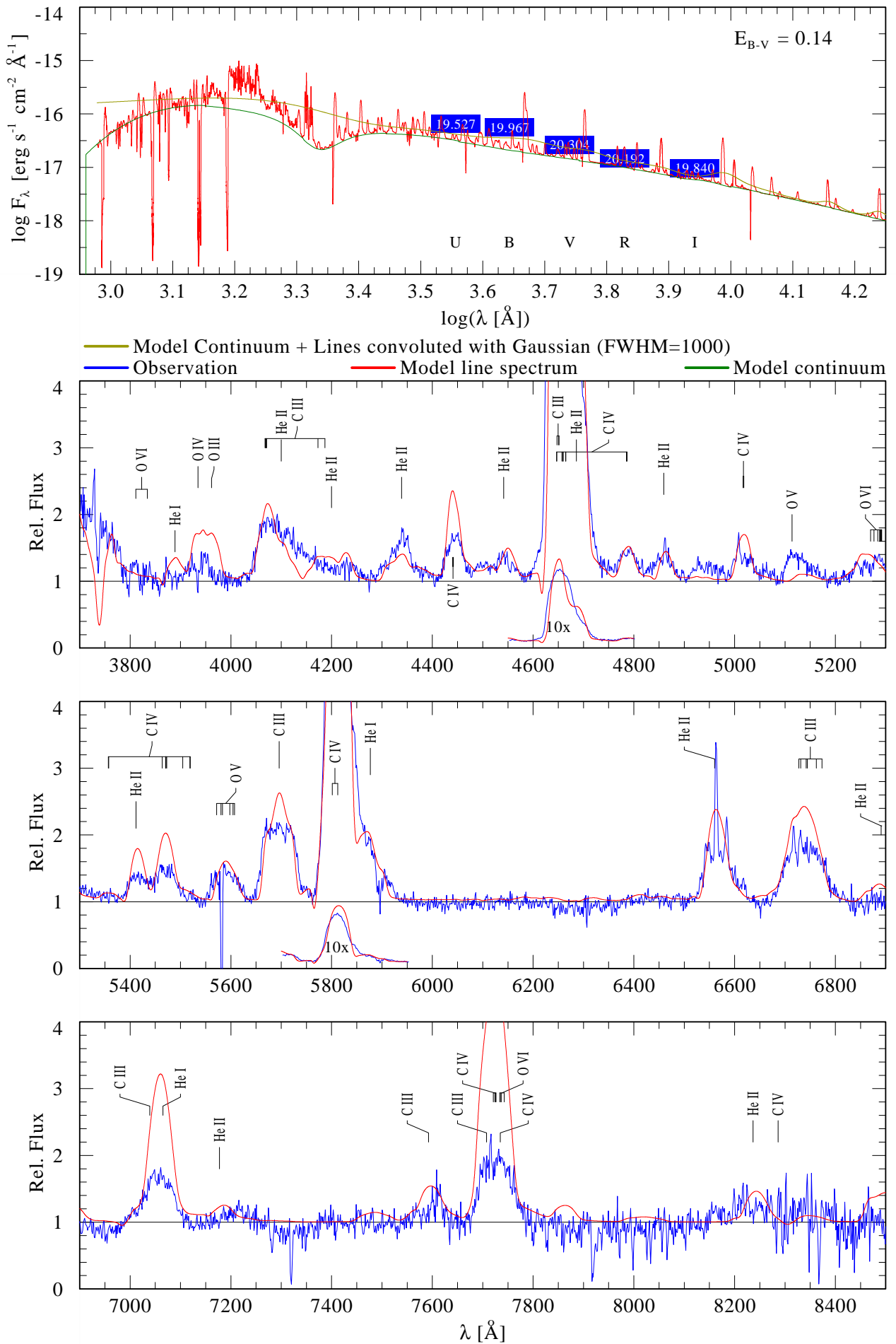
Element	mass fraction
Helium	5.1E-01
Carbon	4.5E-01
Oxygen	4.0E-02
Silicon	2.0E-03
Iron group	1.6E-03

(d) Ionizing photons, mechanical feedback, and current chemical enrichment

Ionization edge	Wavelength	$\log Q$
Hydrogen	911.6 \AA	49.54
Helium I	504.3 \AA	48.60
Helium II	227.9 \AA	37.18
Oxygen II	353.0 \AA	47.08
mechanical feedback		$3.98\text{E}+38 \text{ erg s}^{-1}$ $10^{4.01} L_{\odot}$
Chemical enrichment		
q_{He}	[M_{\oplus}/yr]	2.9E+00
q_{C}	[M_{\oplus}/yr]	2.6E+00
q_{O}	[M_{\oplus}/yr]	2.3E-01
q_{Si}	[M_{\oplus}/yr]	9.3E-03

Masterplot: M31WR132 // LGGS J004511.27+413815.3

WC6



B.20 M 31 WR 138

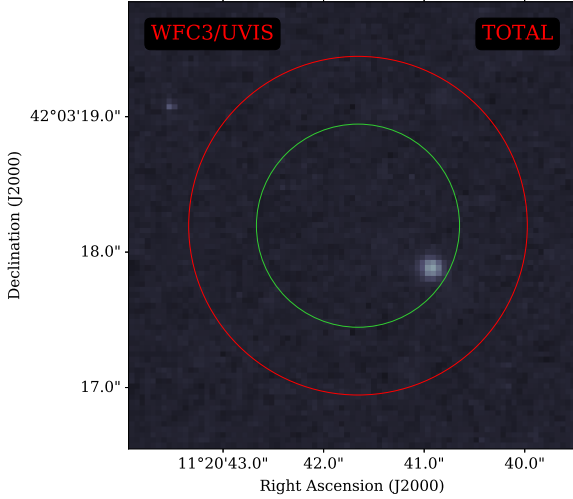


Figure 80: *HST* image of the surrounding region of WR 138. Camera and filter are noted in the image.

- WR 138 is a WC5-6 and comparably faint with a very noisy spectrum.
- The star has a relatively low terminal velocity for an early WC.
- Due to the low S/N, no signs of rotation are visible.
- The *HST* image of the stellar neighborhood in Fig 80 shows no source nearby.
- Dilution of the emission lines for $\lambda > 7000 \text{ \AA}$ indicates weak contamination.
- The overall quality of the spectral fit is good for a WC star.
- Disagreements between the model spectrum and the observation can be seen, all of them are the usual problems as described above.
 - No reproduction of O VI $\lambda\lambda 3811, 34$
 - Overprediction of O III $\lambda 3961$, O IV $\lambda 3934$, and C IV $\lambda\lambda 4440 - 42$
 - C III $\lambda 5696$ is underpredicted.
 - The diagnostic pair is slightly overestimated.
 - Underestimation of He II $\lambda 4338$

Table 37: Summary for M 31 WR 138

(a) General overview

Star	WR138
LGGS	J004522.78+420318.2
Spectral type	WC5-6
E(B-V)	0.20

(b) Derived stellar parameter

T_{eff}	[K]	177828
$T_{2/3}$	[K]	87492
L	$[\log L_{\odot}]$	5.2
M_*	$[M_{\odot}]$	10.2
R_*	$[R_{\odot}]$	0.4
\dot{M}	$[\log M_{\odot}/\text{yr}]$	-5.118
D		40
R_t	$[R_{\odot}]$	0.5495
v_{∞}	$[\text{km/s}]$	1800
v_{rad}	$[\text{km/s}]$	-300
v_{rot}	$[\text{km/s}]$	0
v_{crit}	$[\text{km/s}]$	2152

(c) Derived abundances

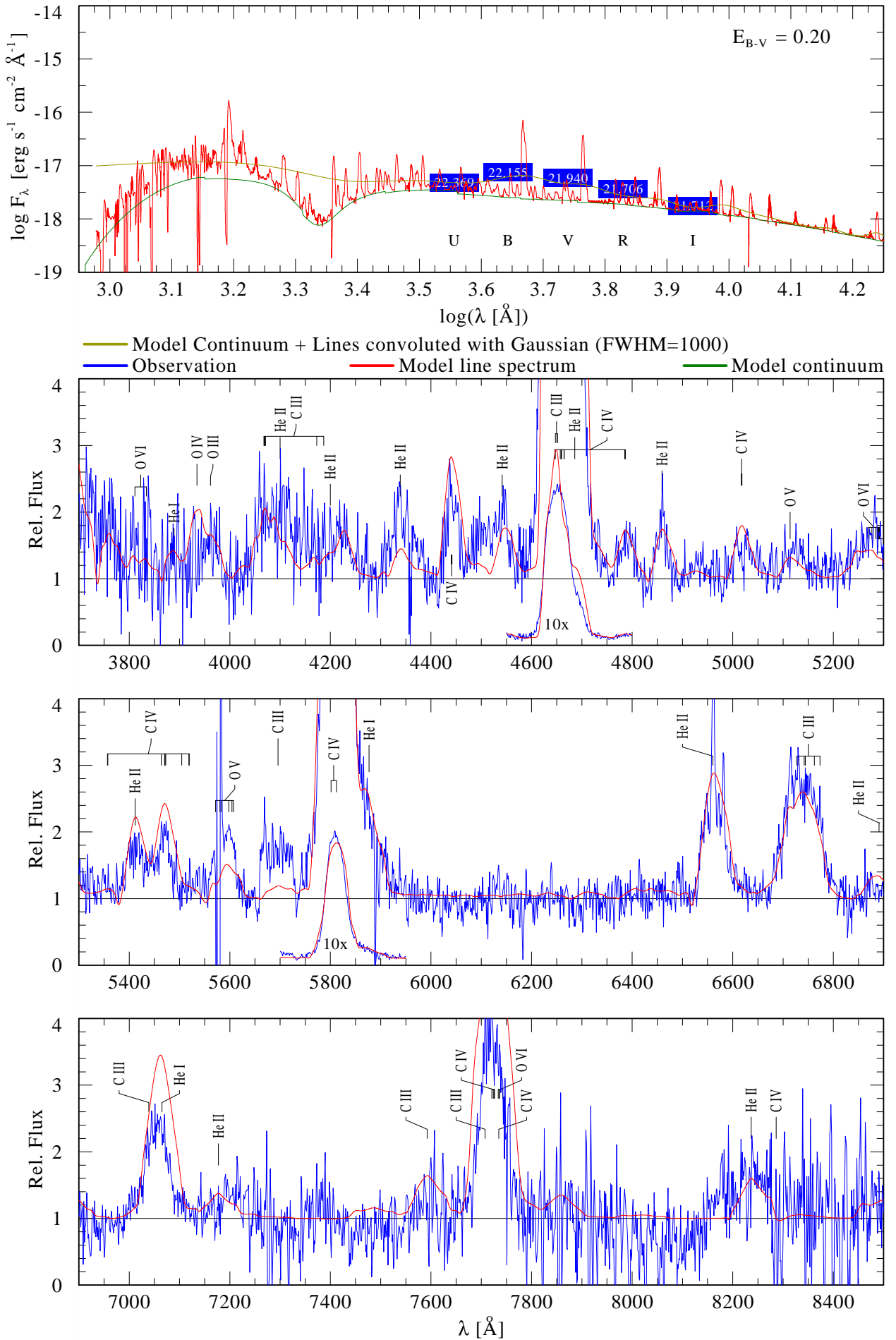
Element	mass fraction
Helium	4.7E-01
Carbon	5.0E-01
Oxygen	2.0E-02
Silicon	1.0E-03
Iron group	3.2E-03

(d) Ionizing photons, mechanical feedback, and current chemical enrichment

Ionization edge	Wavelength	$\log Q$
Hydrogen	911.6 \AA	49.02
Helium I	504.3 \AA	48.32
Helium II	227.9 \AA	38.65
Oxygen II	353.0 \AA	47.27
mechanical feedback		$1.57\text{E}+38 \text{ erg s}^{-1}$ $10^{3.61} L_{\odot}$
Chemical enrichment		
q_{He}	$[M_{\oplus}/\text{yr}]$	1.2E+00
q_{C}	$[M_{\oplus}/\text{yr}]$	1.3E+00
q_{O}	$[M_{\oplus}/\text{yr}]$	5.1E-02
q_{Si}	$[M_{\oplus}/\text{yr}]$	8.1E-03

Masterplot: **M31WR138 // LGGs J004522.78+420318.2**

WC5-6



B.21 M 31 WR 139

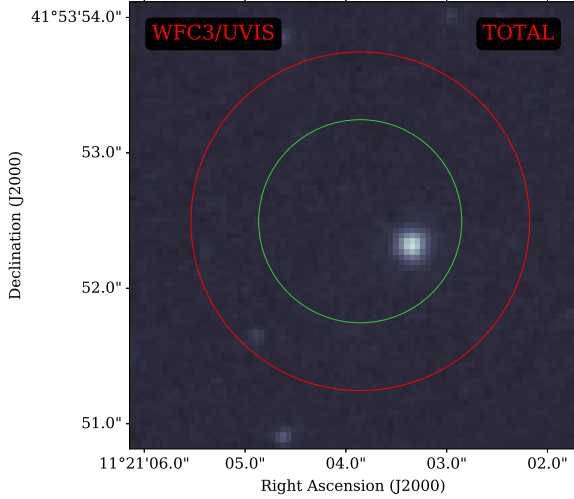


Figure 81: *HST* image of the surrounding region of WR 139. Camera and filter are noted in the image.

- WR 139 is a WC6 and shows a spectrum with a high S/N.
- The star shows signs of fast rotation leading to an almost overcritical rotation. See Sect. 9.4 for the solution for this issue.
- The HST image of the stellar neighborhood in Fig 81 shows no bright source nearby.
- Dilution and absorption lines for $\lambda > 7000 \text{ \AA}$ indicate contamination.
- The overall quality of the spectral fit is good for a WC star.
- Disagreements between the model spectrum and the observation can be seen, all of them are the usual problems as described above.
 - No reproduction of O VI $\lambda\lambda 3811, 34$
 - Overprediction of O III $\lambda 3961$, O IV $\lambda 3934$, and C IV $\lambda\lambda 4440 - 42$
 - C III $\lambda 5696$ is slightly overpredicted.
 - The diagnostic pair is slightly overestimated.
 - Underestimation of He II $\lambda 4338$

Table 38: *Summary for M 31 WR 139*

(a) *General overview*

Star	WR139
LGGS	J004524.26+415352.5
Spectral type	WC6
E(B-V)	0.1

(b) *Derived stellar parameter*

T_{eff}	[K]	70795
$T_{2/3}$	[K]	63168
L	[$\log L_{\odot}$]	5.2
M_{*}	[M_{\odot}]	10.2
R_{*}	[R_{\odot}]	2.7
\dot{M}	[$\log M_{\odot}/\text{yr}$]	-5.115
D		30
R_t	[R_{\odot}]	4.0738
v_{∞}	[km/s]	2000
v_{rad}	[km/s]	-200
v_{rot}	[km/s]	1818
v_{crit}	[km/s]	858

(c) *Derived abundances*

Element	mass fraction
Helium	4.8E-01
Carbon	5.0E-01
Oxygen	2.0E-02
Silicon	6.5E-04
Iron group	1.6E-03

(d) *Ionizing photons, mechanical feedback, and current chemical enrichment*

Ionization edge	Wavelength	$\log Q$
Hydrogen	911.6 \AA	49.04
Helium I	504.3 \AA	48.16
Helium II	227.9 \AA	37.21
Oxygen II	353.0 \AA	46.82
mechanical feedback		$1.95\text{E}+38 \text{ erg s}^{-1}$ $10^{3.70} L_{\odot}$
Chemical enrichment		
q_{He}	[M_{\oplus}/yr]	1.2E+00
q_{C}	[M_{\oplus}/yr]	1.3E+00
q_{O}	[M_{\oplus}/yr]	5.1E-02
q_{Si}	[M_{\oplus}/yr]	4.1E-03

B.22 M 31 WR 150

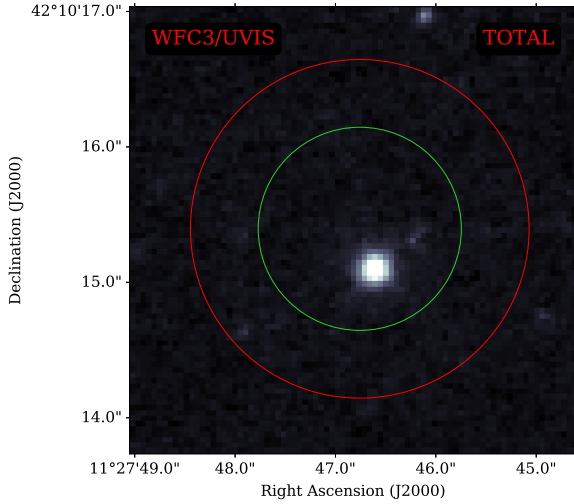


Figure 82: *HST* image of the surrounding region of WR 150. Camera and filter are noted in the image.

- WR 150 is a WC5-6 and extremely hot with very strong emission lines.
- The star shows signs of slow rotation.
- The HST image of the stellar neighborhood in Fig82 shows no bright source nearby.
- Dilution and absorption lines for $\lambda > 7000 \text{ \AA}$ indicate contamination.
- The overall quality of the spectral fit is average for a WC star.
- The spectrum shows strong nebula emissions
- Disagreements between the model spectrum and the observation can be seen, all of them are the usual problems as described above.
 - No reproduction of O VI $\lambda\lambda 3811, 34$
 - Overprediction of O III $\lambda 3961$, O IV $\lambda 3934$, and C IV $\lambda\lambda 4440 - 42$
 - The unknown emission at 4500 \AA
 - C III $\lambda 5696$ is slightly underestimated.
 - The diagnostic pair is slightly overestimated.
 - Underestimation of He II $\lambda 4338$

Table 39: Summary for M 31 WR 150

(a) General overview

Star	WR150
LGGS	J004551.12+421015.4
Spectral type	WC5-6
E(B-V)	0.1

(b) Derived stellar parameter

T_{eff}	[K]	177828
$T_{2/3}$	[K]	82207
L	[$\log L_{\odot}$]	5.4
M_*	[M_{\odot}]	13.0
R_*	[R_{\odot}]	0.5
\dot{M}	[$\log M_{\odot}/\text{yr}$]	-5.053
D		50
R_t	[R_{\odot}]	0.537
v_{∞}	[km/s]	1600
v_{rad}	[km/s]	-200
v_{rot}	[km/s]	455
v_{crit}	[km/s]	2175

(c) Derived abundances

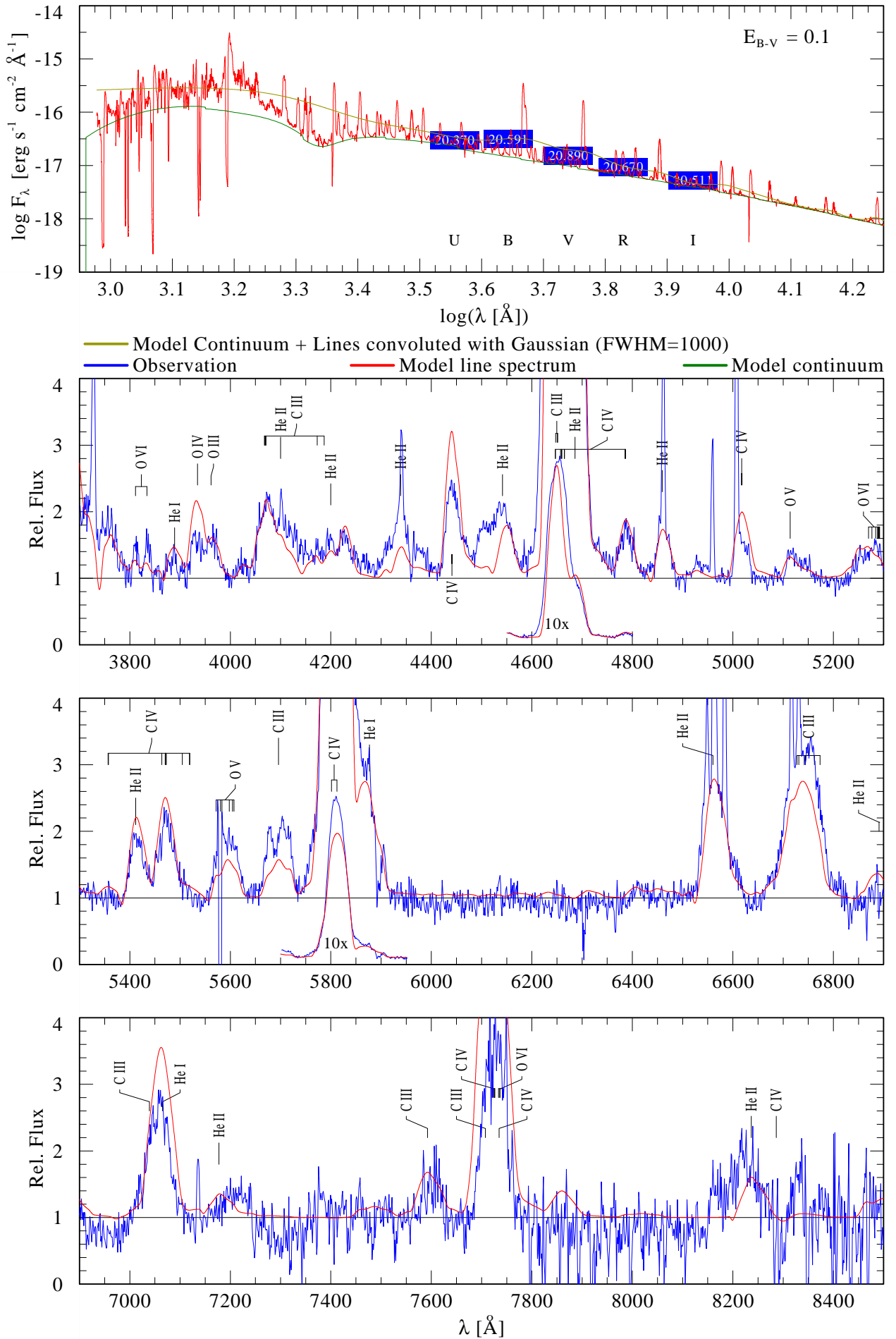
Element	mass fraction
Helium	4.7E-01
Carbon	5.0E-01
Oxygen	2.0E-02
Silicon	1.0E-03
Iron group	3.2E-03

(d) Ionizing photons, mechanical feedback, and current chemical enrichment

Ionization edge	Wavelength	$\log Q$
Hydrogen	911.6 \AA	49.21
Helium I	504.3 \AA	48.43
Helium II	227.9 \AA	38.22
Oxygen II	353.0 \AA	47.19
mechanical feedback		$1.44\text{E}+38 \text{ erg s}^{-1}$ $10^{3.57} L_{\odot}$
Chemical enrichment		
q_{He}	[M_{\oplus}/yr]	1.4E+00
q_{C}	[M_{\oplus}/yr]	1.5E+00
q_{O}	[M_{\oplus}/yr]	5.9E-02
q_{Si}	[M_{\oplus}/yr]	9.4E-03

Masterplot: M31WR150 // LGGs J004551.12+421015.4

WC5-6



B.23 M 31 WR 151

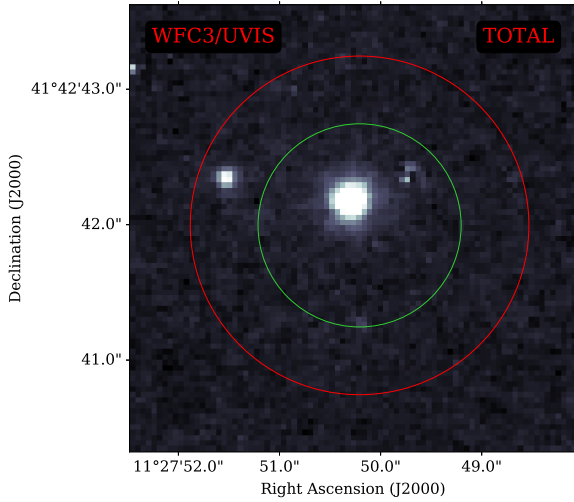


Figure 83: *HST* image of the surrounding region of WR 151. Camera and filter are noted in the image.

- WR 151 is a WC6 and extremely hot with very strong emission lines.
- The star shows no signs of rotation.
- The *HST* image of the stellar neighborhood in Fig 83 shows faint blue sources nearby.
- Dilution and absorption lines for $\lambda > 7000 \text{ \AA}$ indicate contamination. This is supported by photometry
- The overall quality of the spectral fit is average for a WC star.
- Disagreements between the model spectrum and the observation can be seen, all of them are the usual problems as described above.
 - No reproduction of O VI $\lambda\lambda 3811, 34$
 - Overprediction of O III $\lambda 3961$, O IV $\lambda 3934$, and C IV $\lambda\lambda 4440 - 42$
 - The unknown emission at 4500 \AA
 - C III $\lambda 5696$ is slightly overestimated.
 - The diagnostic pair is overestimated.
 - Underestimation of He II $\lambda 4338$

Table 40: *Summary for M 31 WR 151*

(a) *General overview*

Star	WR151
LGGS	J004551.35+41 4242.0
Spectral type	WC6
E(B-V)	0.05

(b) *Derived stellar parameter*

T_{eff}	[K]	177828
$T_{2/3}$	[K]	67489
L	[$\log L_{\odot}$]	5.3
M_*	[M_{\odot}]	11.7
R_*	[R_{\odot}]	0.5
\dot{M}	[$\log M_{\odot}/\text{yr}$]	-4.905
D		30
R_t	[R_{\odot}]	0.4898
v_{∞}	[km/s]	1800
v_{rad}	[km/s]	-250
v_{rot}	[km/s]	0
v_{crit}	[km/s]	2178

(c) *Derived abundances*

Element	mass fraction
Helium	5.7E-01
Carbon	4.0E-01
Oxygen	2.0E-02
Silicon	5.0E-03
Iron group	2.5E-03

(d) *Ionizing photons, mechanical feedback, and current chemical enrichment*

Ionization edge	Wavelength	$\log Q$
Hydrogen	911.6 \AA	49.07
Helium I	504.3 \AA	48.10
Helium II	227.9 \AA	36.51
Oxygen II	353.0 \AA	46.23
mechanical feedback		$2.56\text{E}+38 \text{ erg s}^{-1}$ $10^{3.82} L_{\odot}$
Chemical enrichment		
q_{He}	[M_{\oplus}/yr]	2.4E+00
q_{C}	[M_{\oplus}/yr]	1.7E+00
q_{O}	[M_{\oplus}/yr]	8.3E-02
q_{Si}	[M_{\oplus}/yr]	1.0E-02

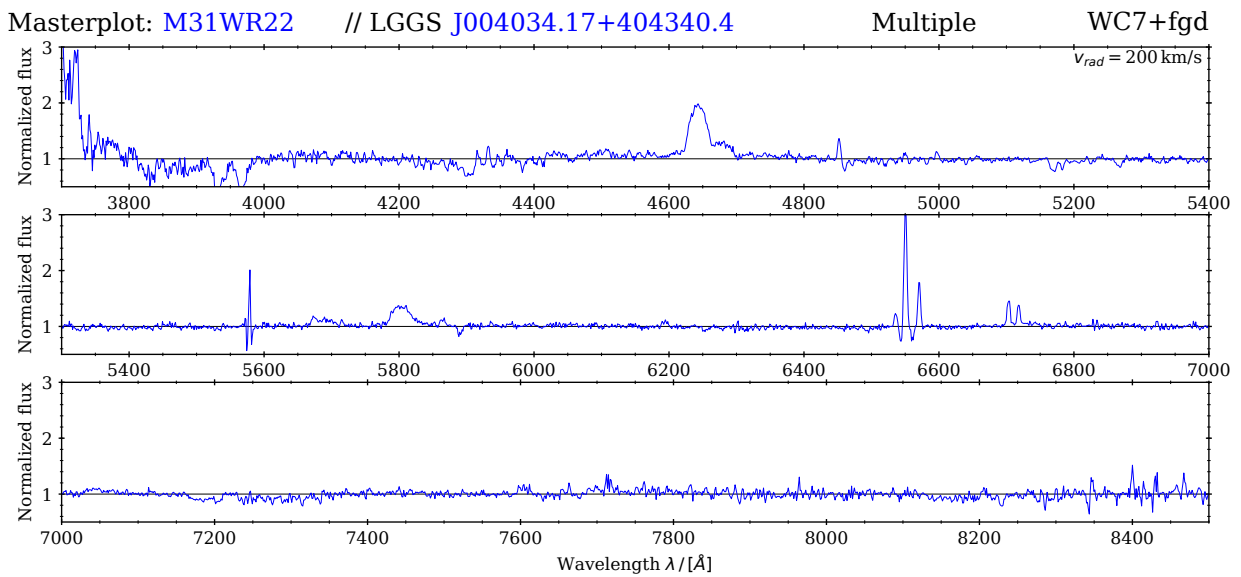
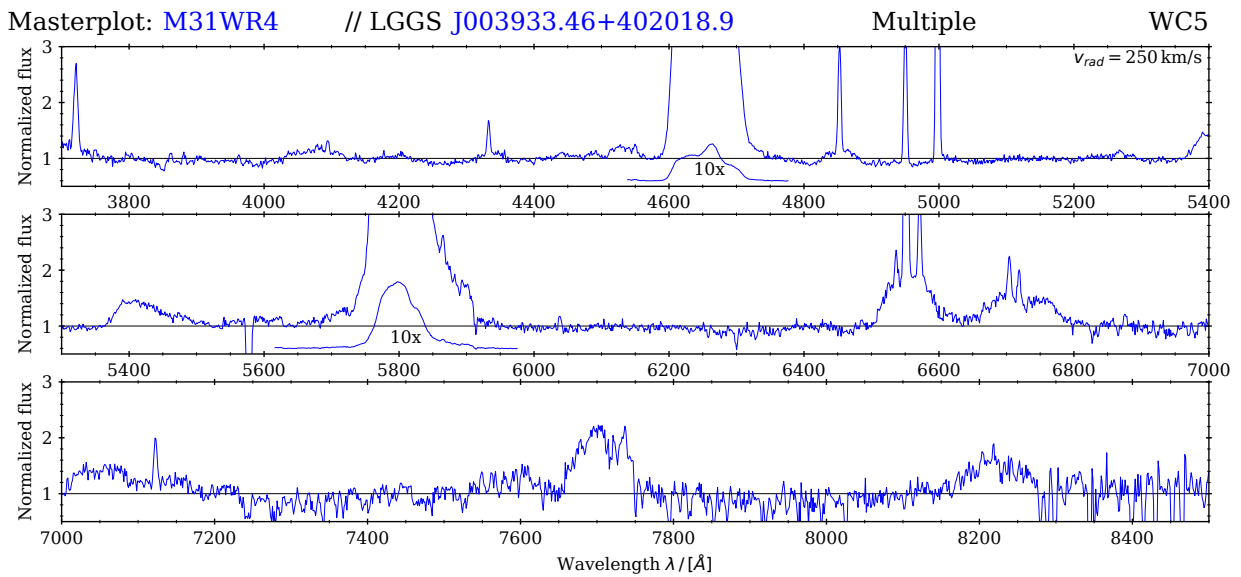
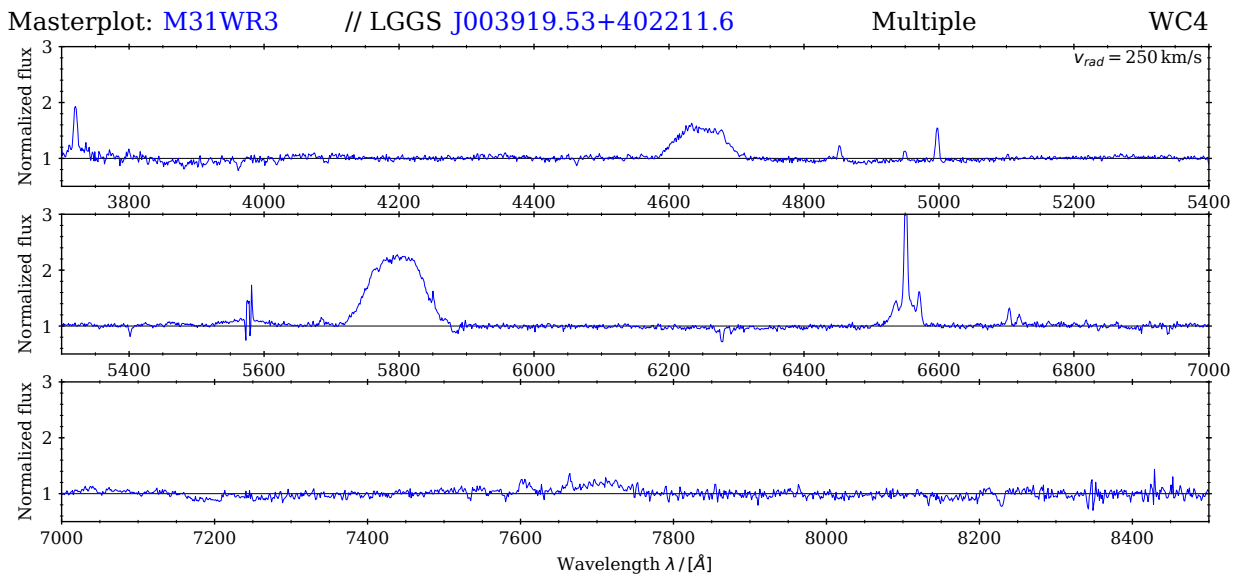
C Observed spectra of suspects and multiples

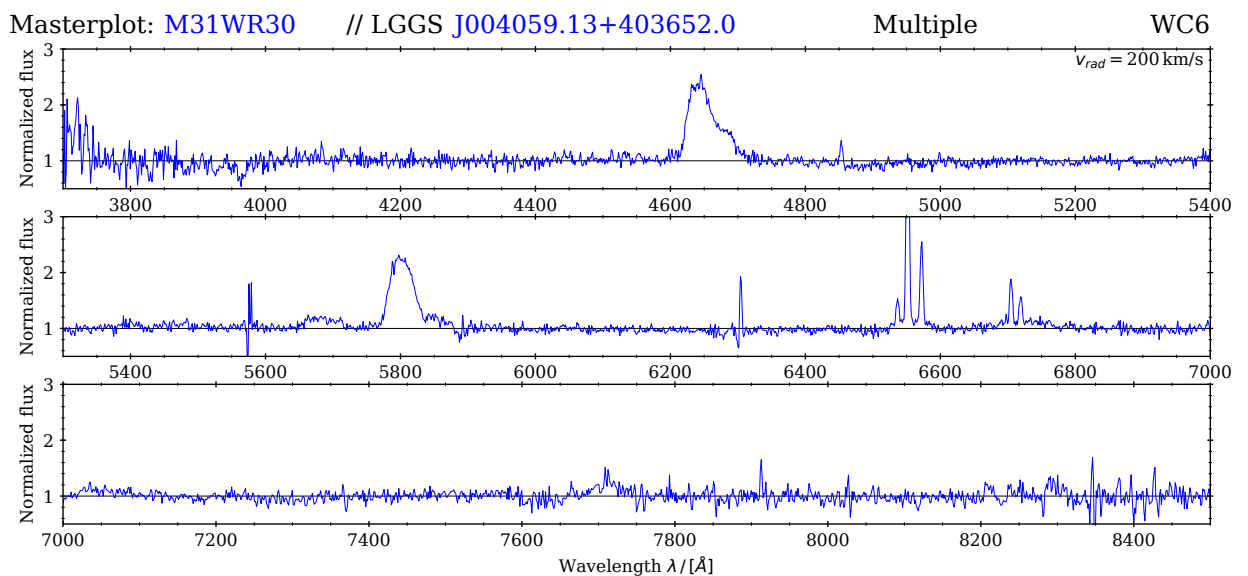
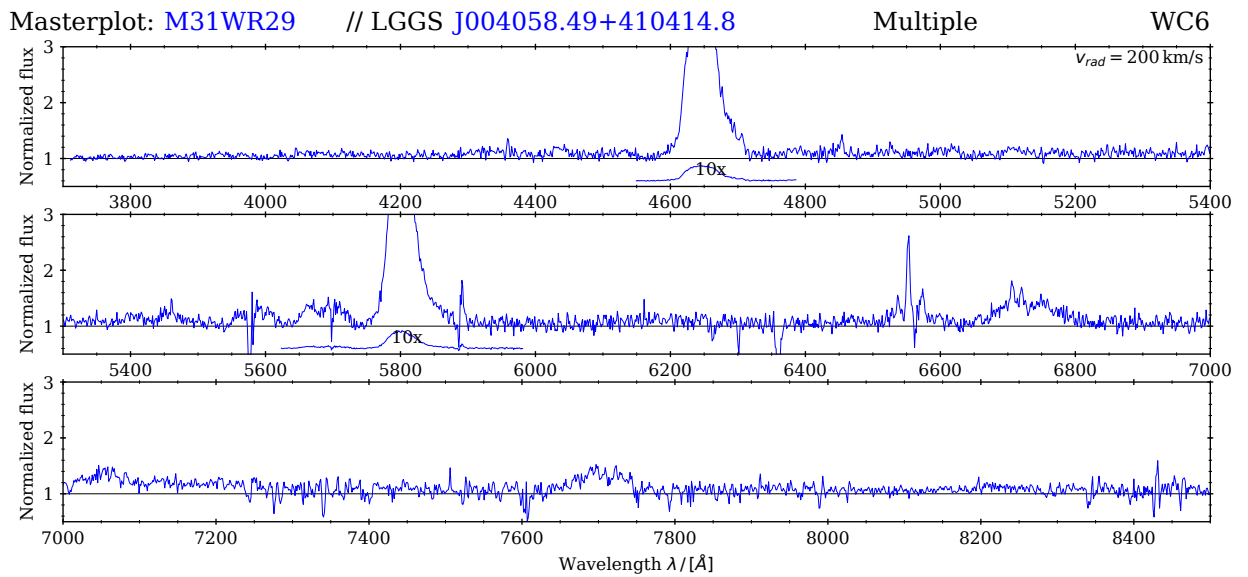
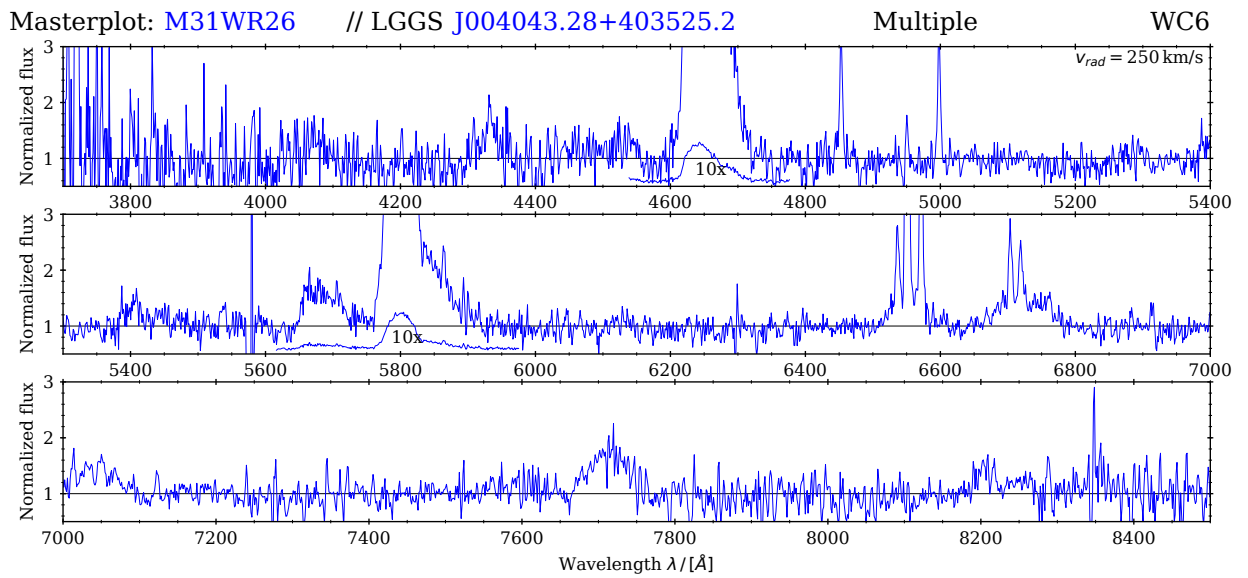
On the following pages, we will display all the stellar spectra of those stars that were identified as *suspects* and *multiples* in Sect. 5. For each star we show the observed spectrum similar to the Masterplots in Sect B. Since there are no models calculated for those stars and the photometry suffers from significant contamination, we will not show a synthetic SED compared to photometric labels. The observed spectra are shown such that they are corrected for their individual radial velocities v_{rad} . The determined value is noted in the plots. For visibility reasons, no identification marks for the individual elements are shown.

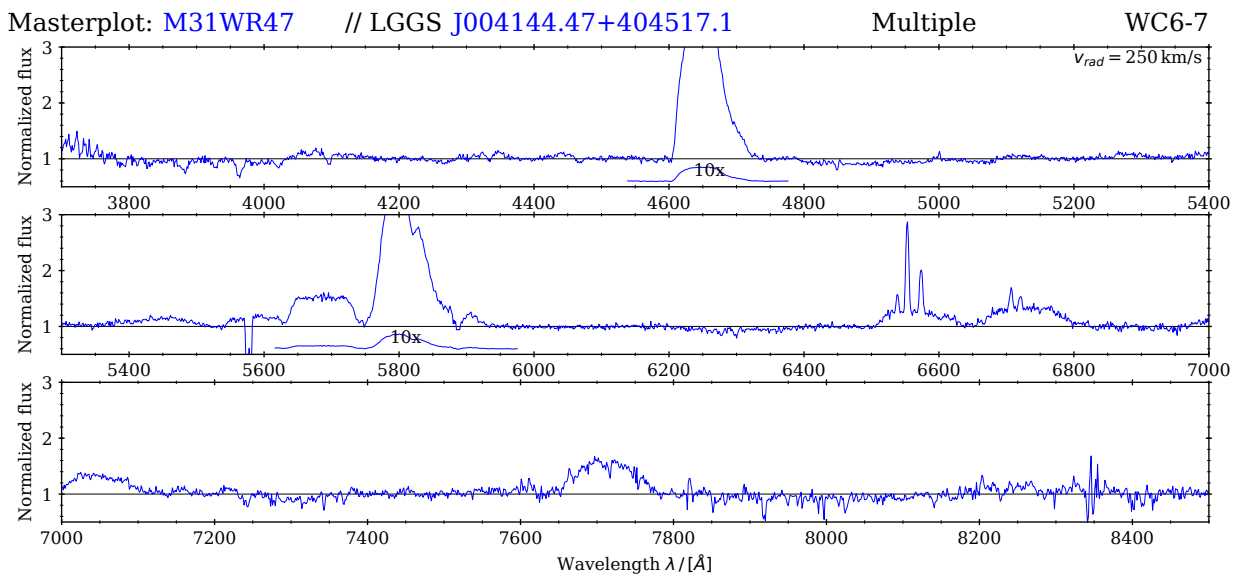
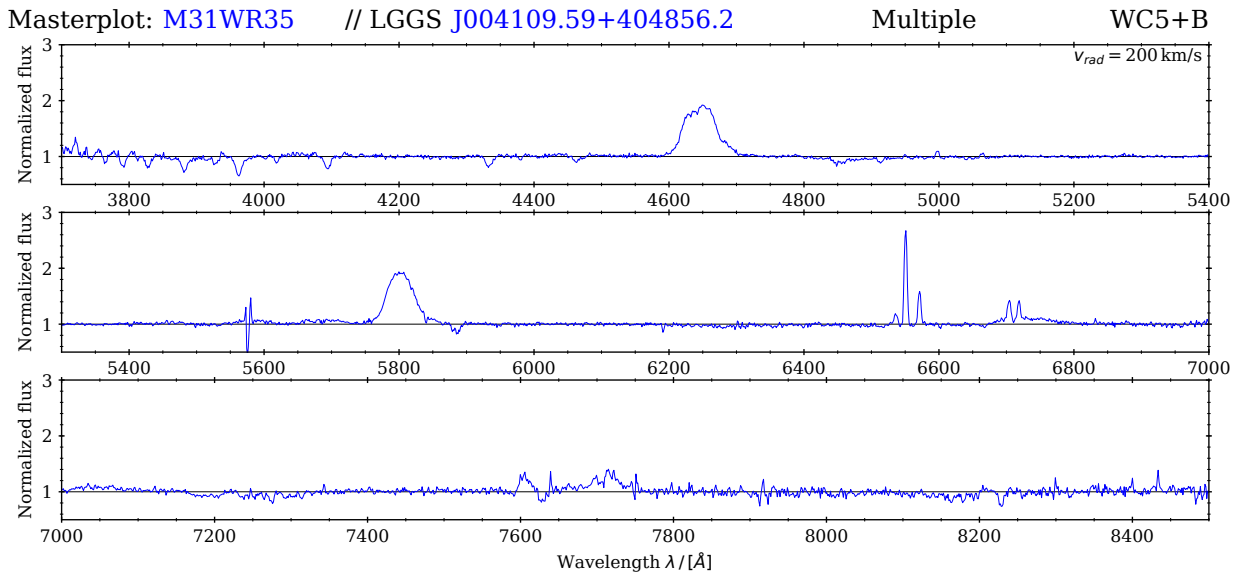
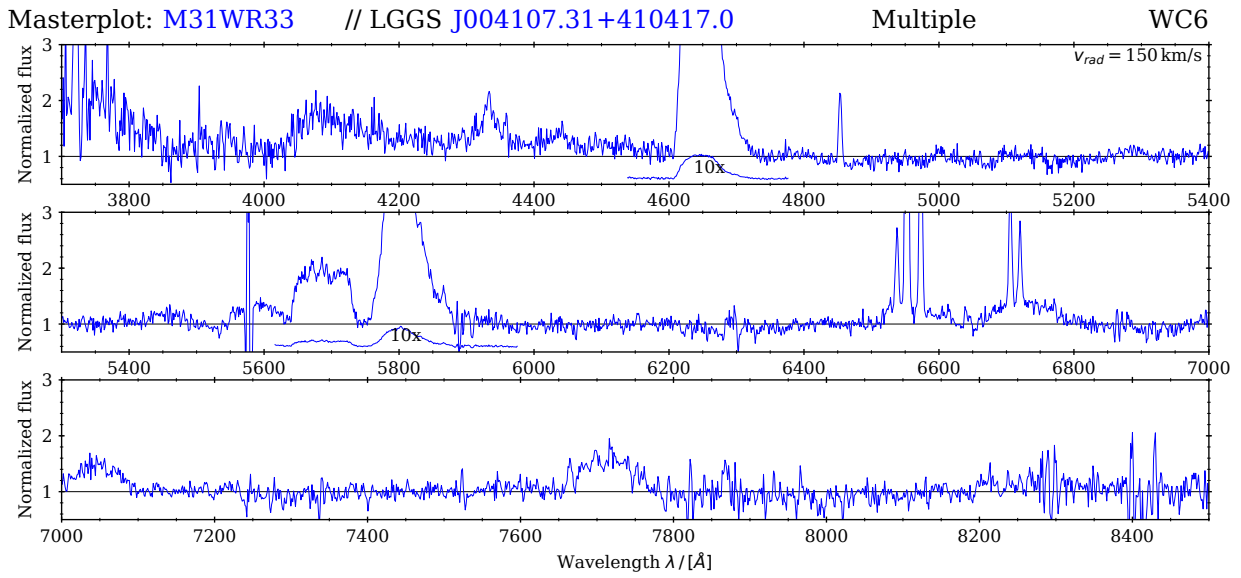
The stars are sorted numerically. Table 41 lists the multiples and suspects again, together with a page number that refers to their spectra.

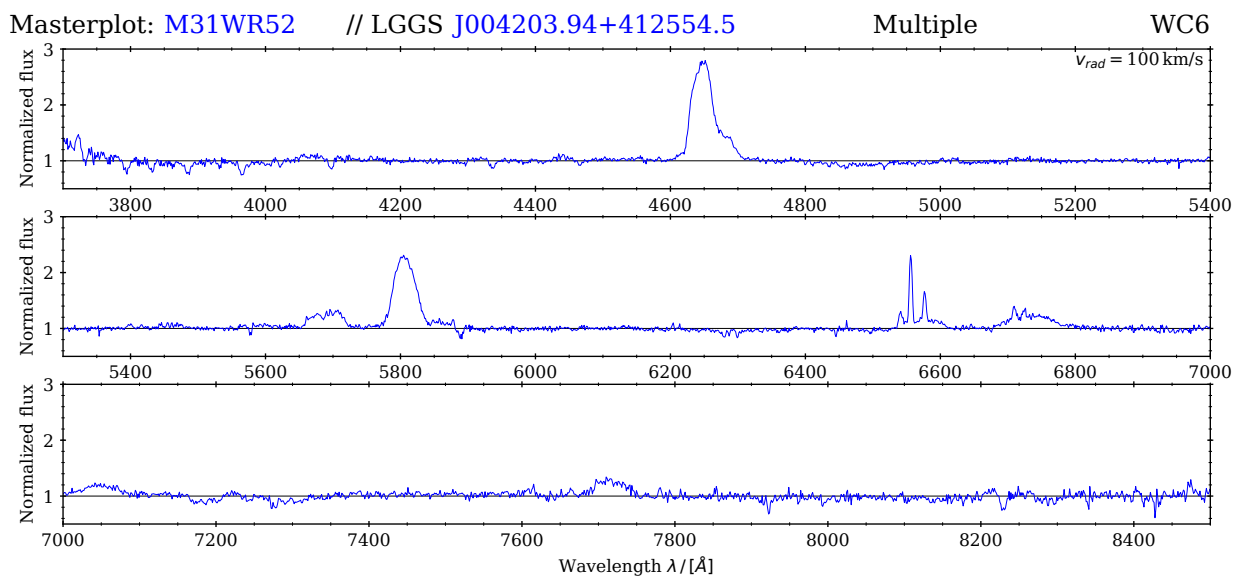
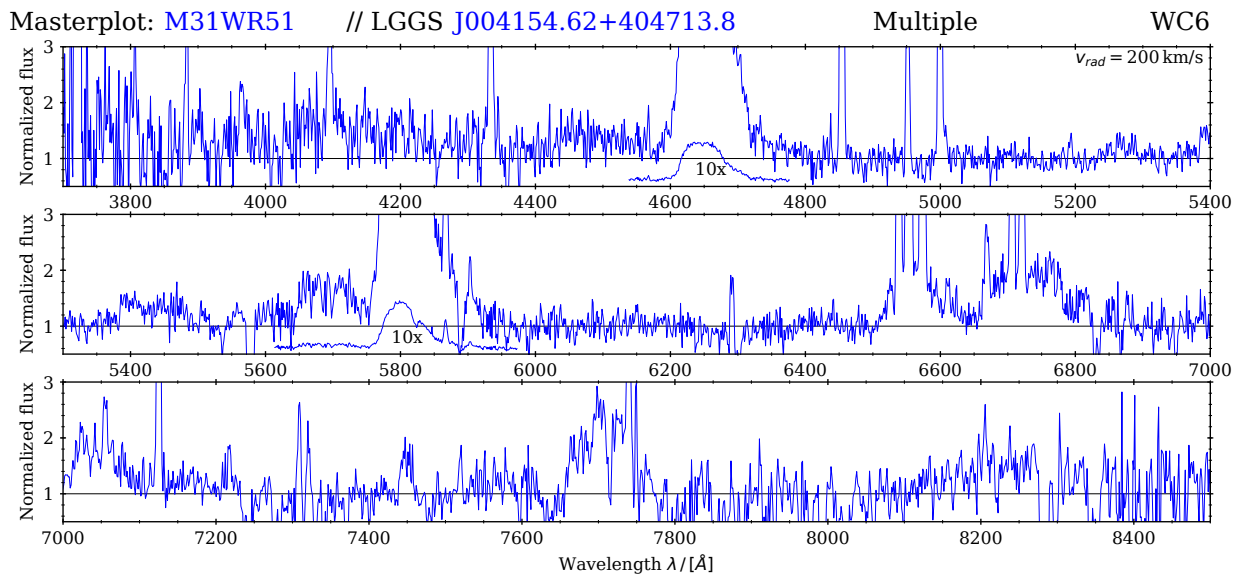
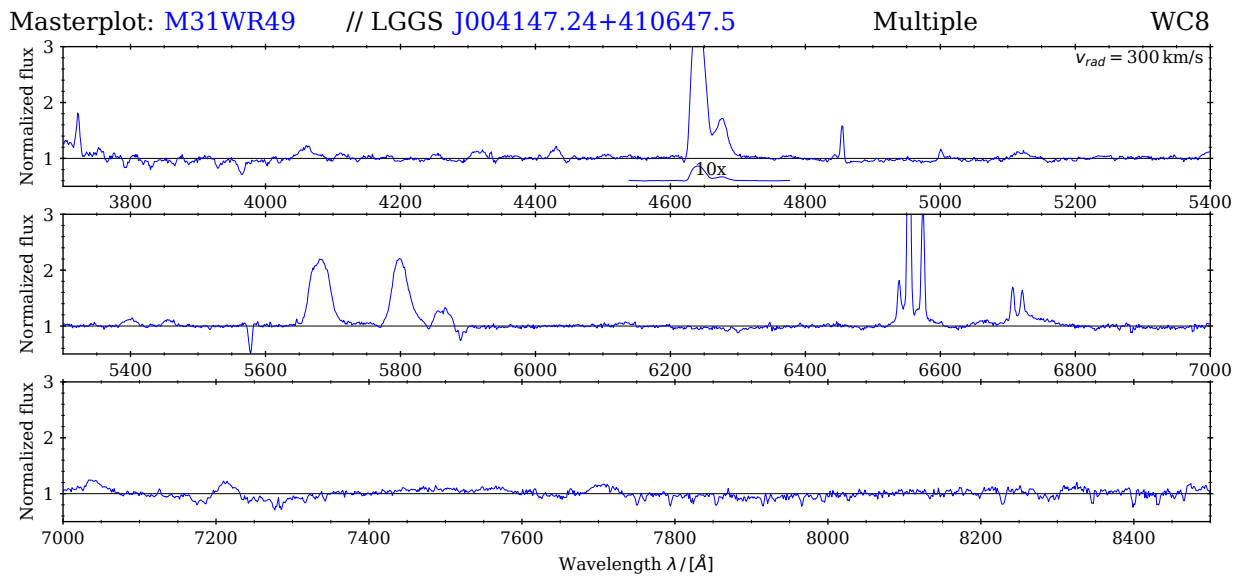
Table 41: *M31 WC stars identified multiple (upper part) and suspects (lower part). The page number indicates where to find the individual stellar spectrum.*

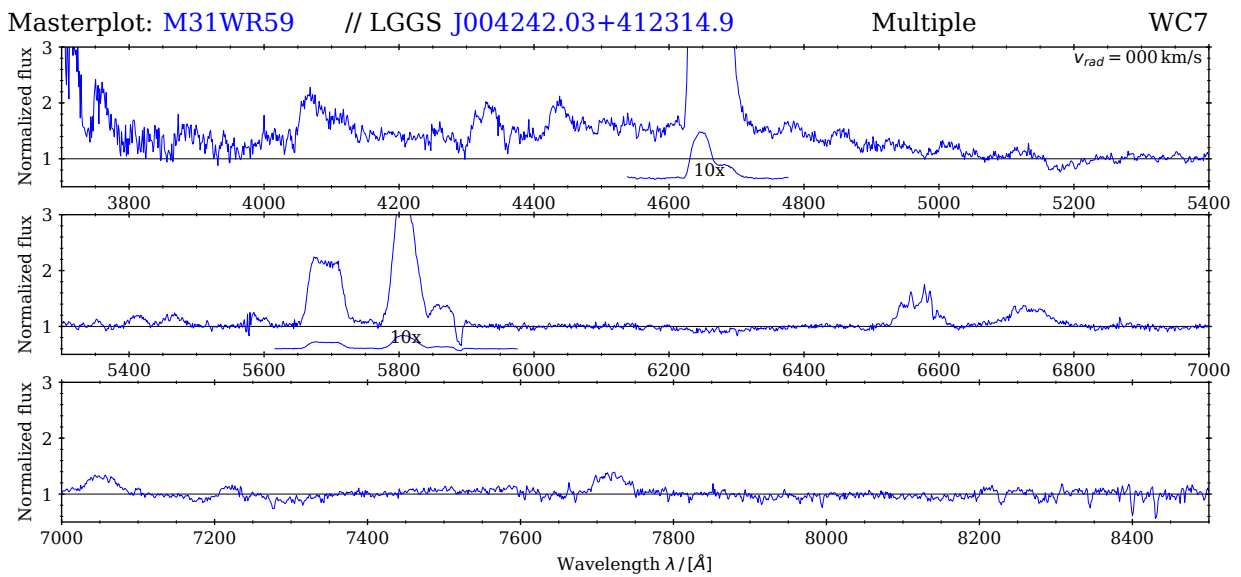
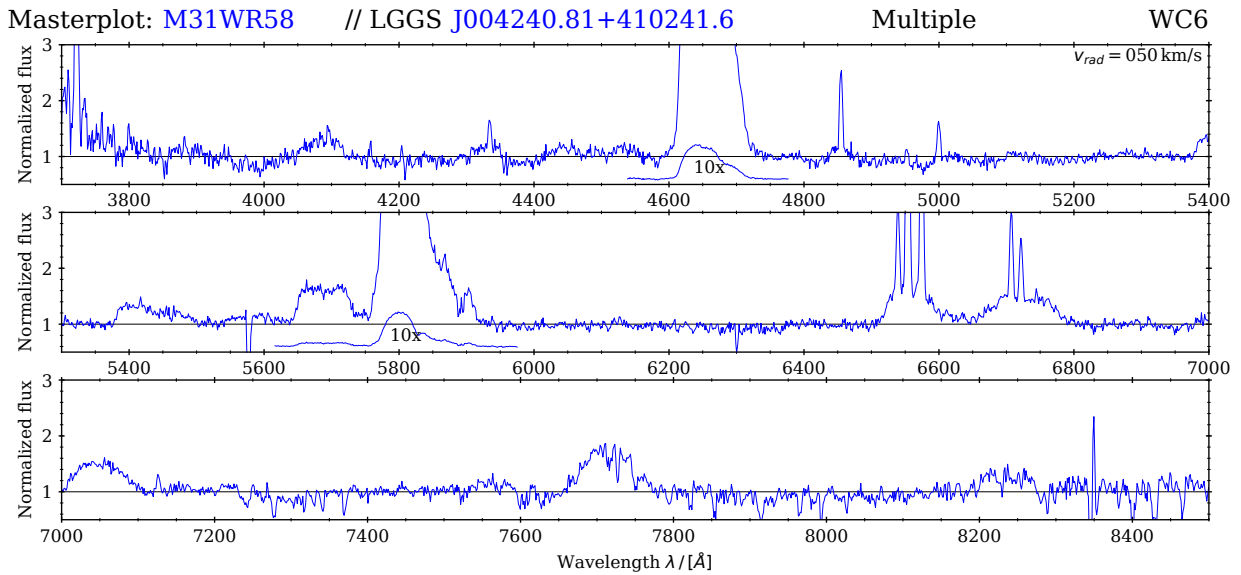
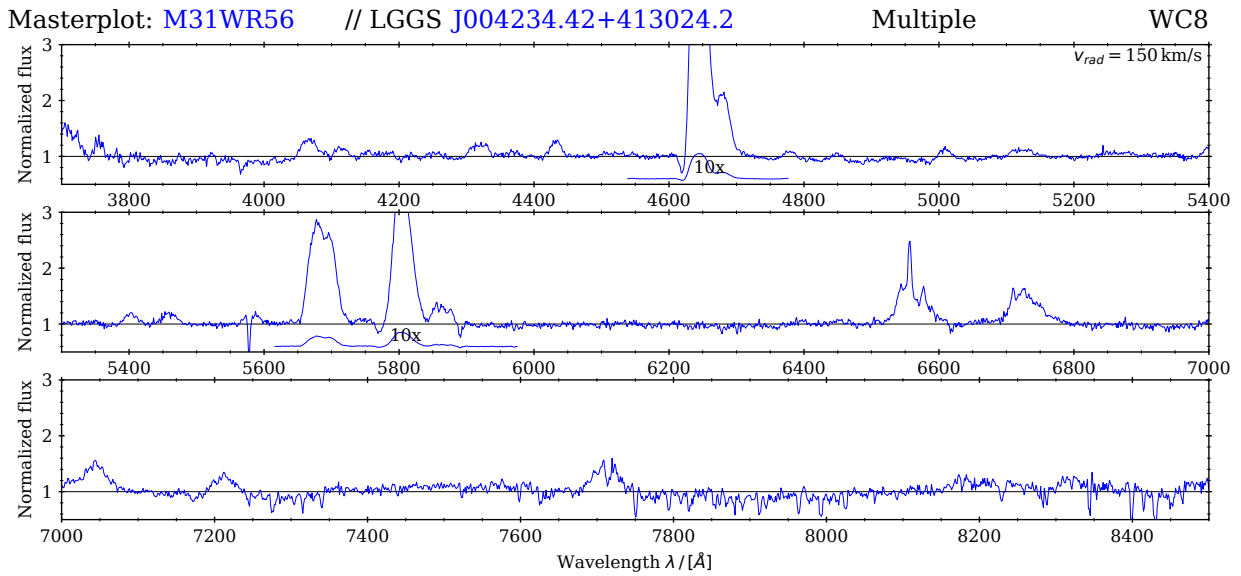
WR #	Spectral type	Page	WR #	Spectral type	Page
3	WC4	134	98	WC5	142
22	WC7+fgd	134	99	WC+B0I?	142
29	WC6	135	103	WC6+B0I	142
30	WC6	135	111	WC5	143
35	WC5+B	136	116	WC6	143
47	WC6-7	136	126	WC6	143
52	WC6	137	129	WC7	144
61	WC4	139	130	WC7+BI	144
64	WC6	139	136	WC8	144
73	WC6	140	140	WC4-5	145
77	WC6	140	143	WC6	145
91	WC6	141	146	WC5	146
4	WC5	134	59	WC7	138
26	WC6	135	62	WC5-6	139
33	WC6	136	71	WC6	140
49	WC8	137	80	WC8	141
51	WC6	137	84	WC6	141
56	WC8	138	141	WC6	145
58	WC6	138			

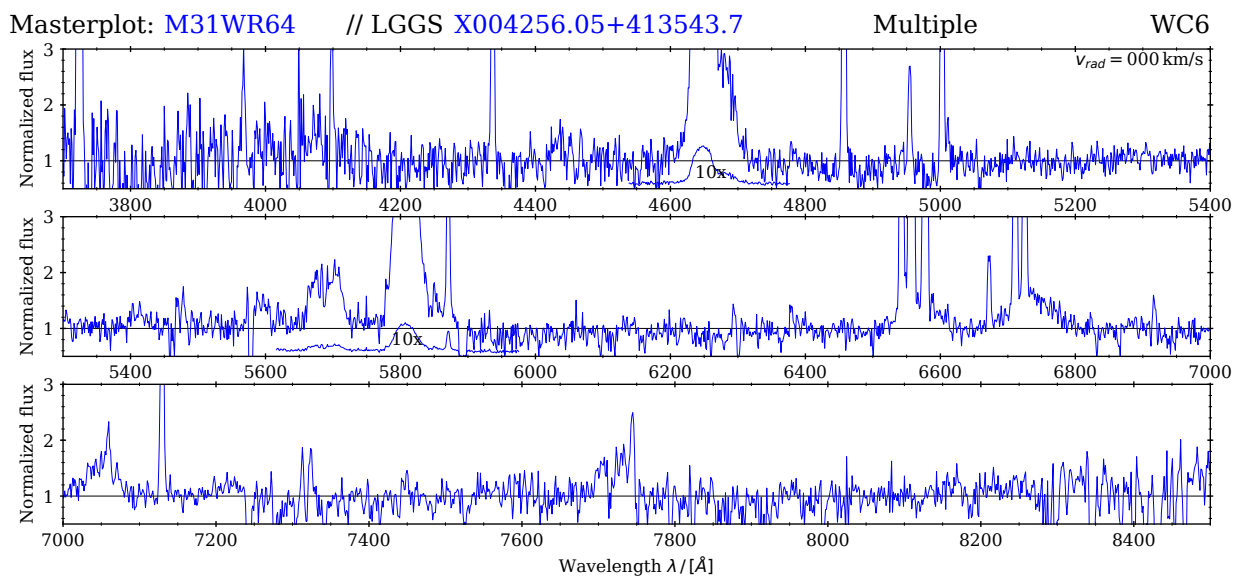
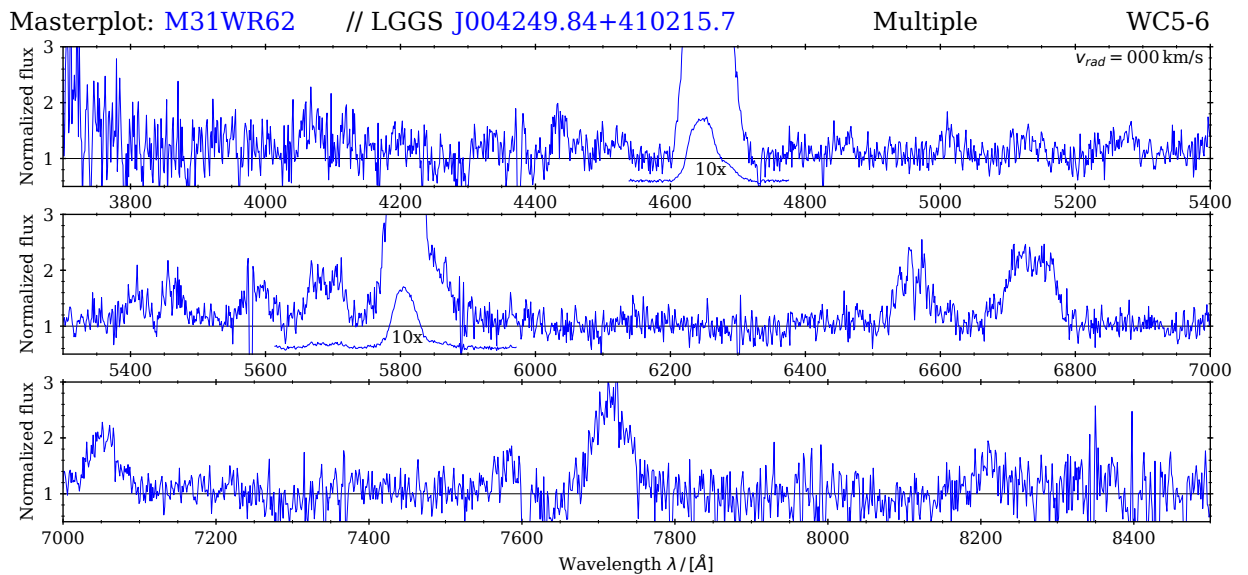
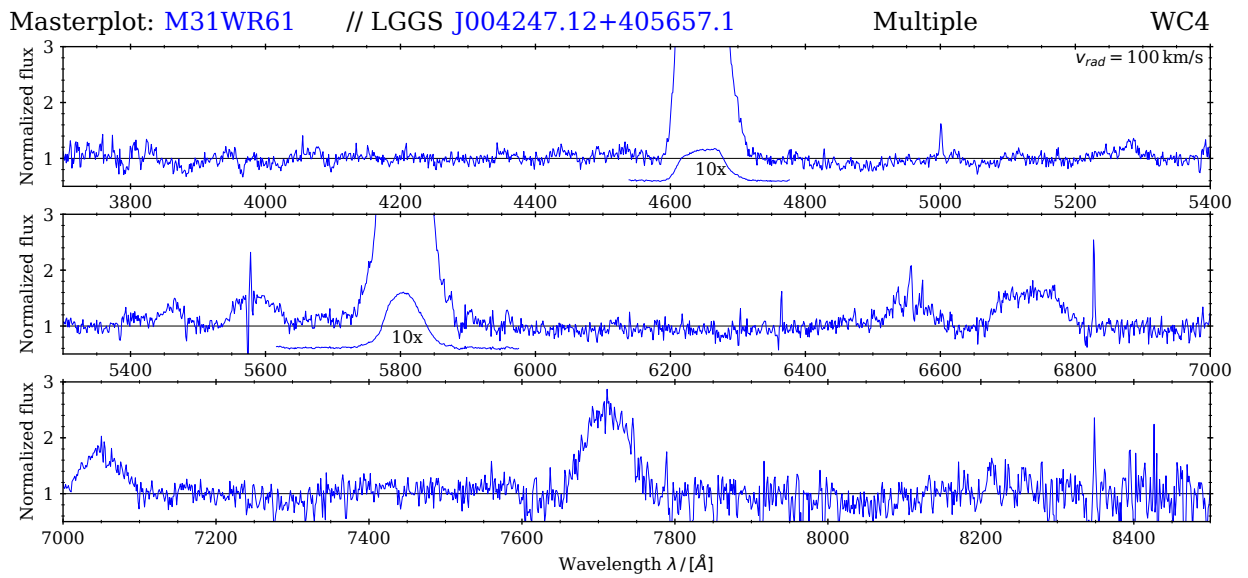


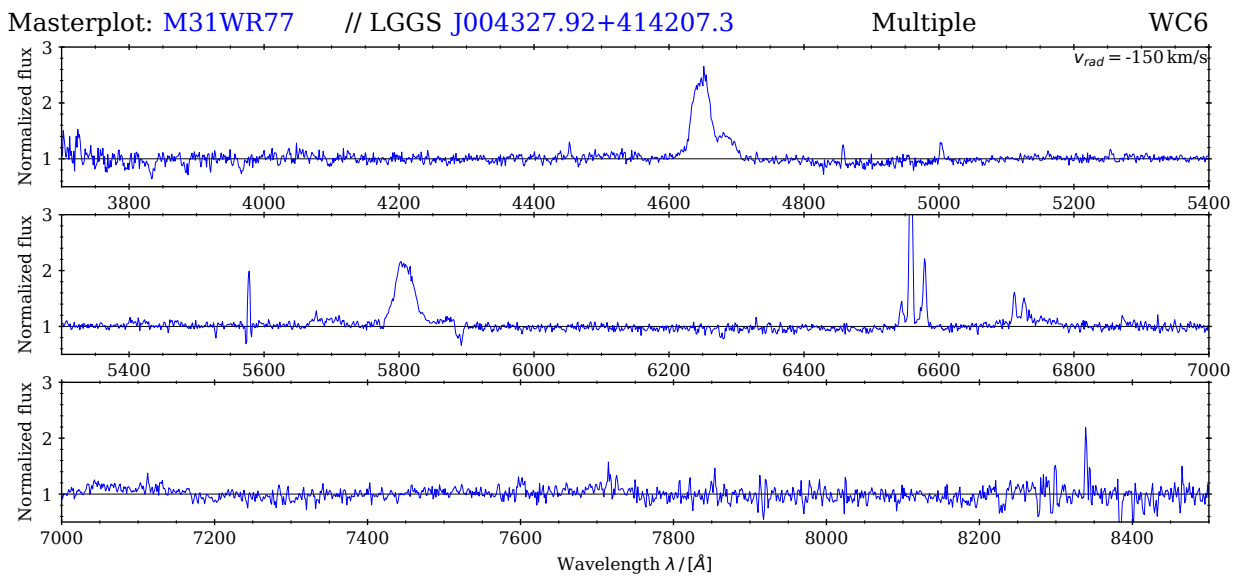
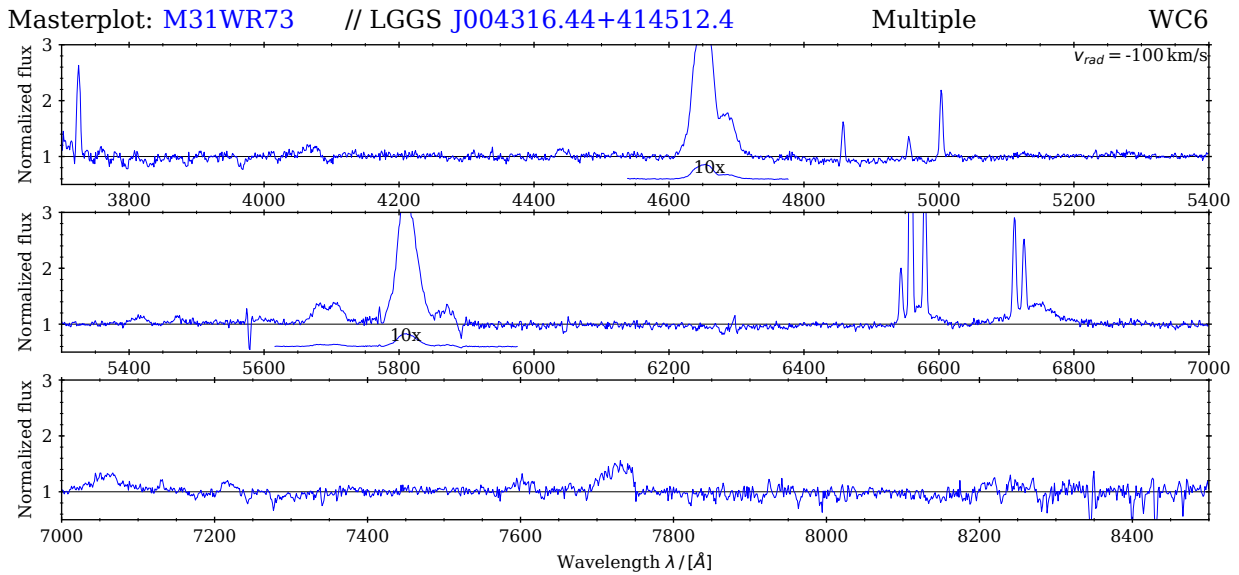
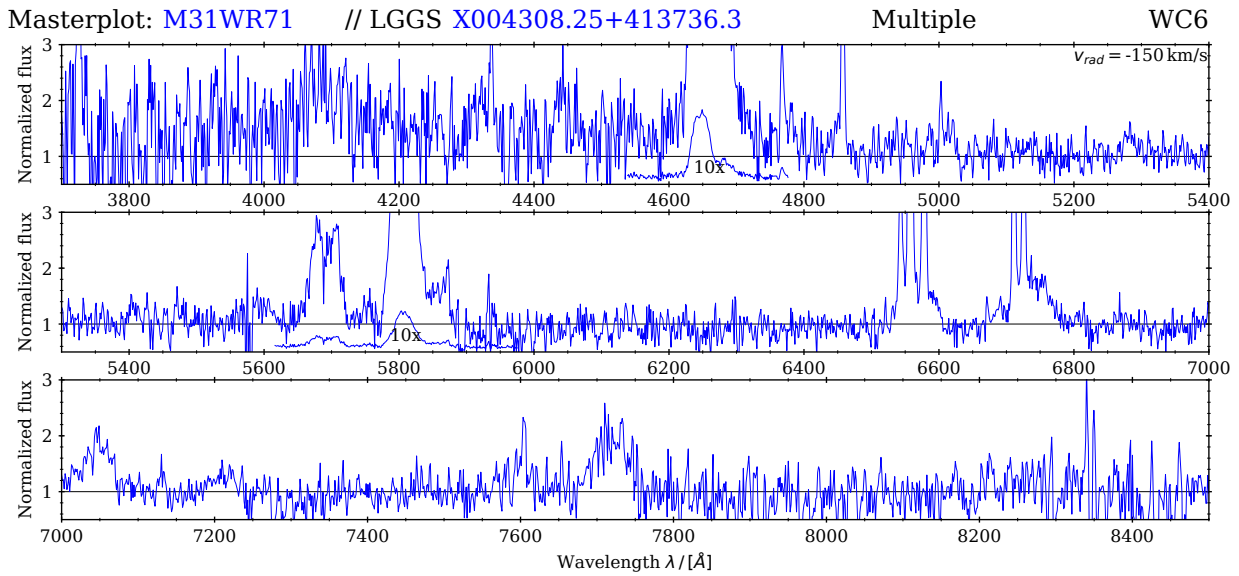


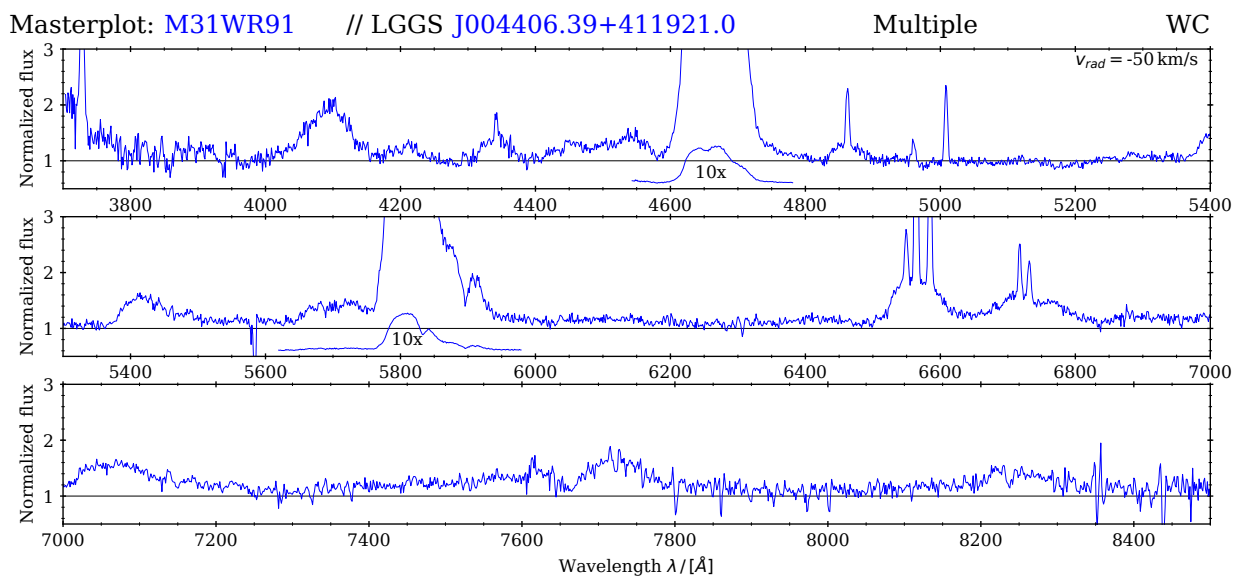
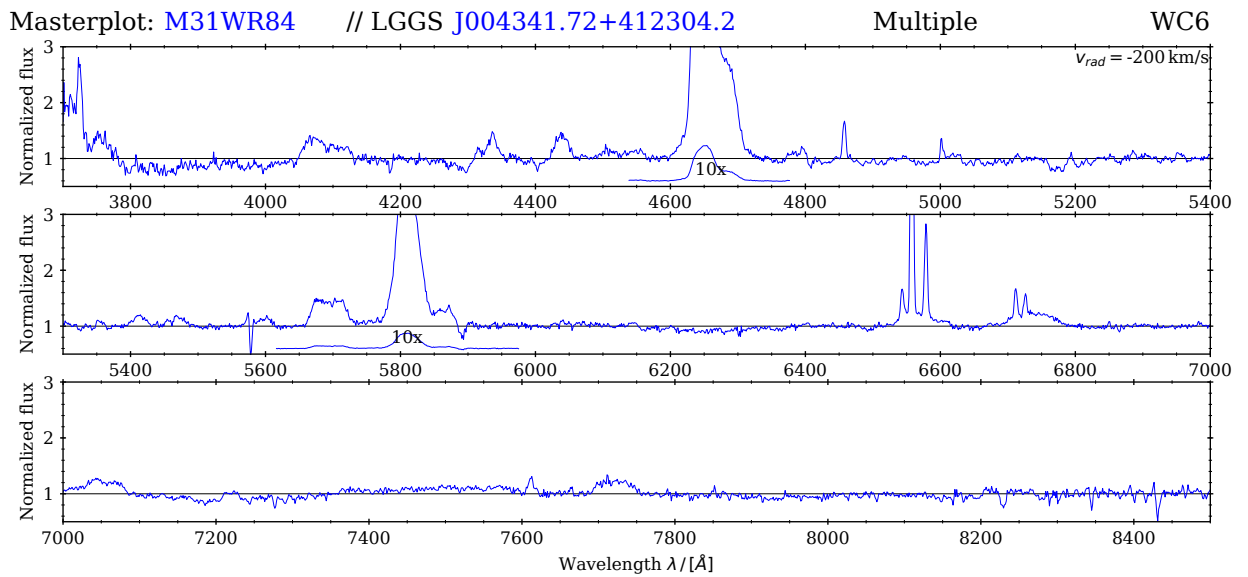
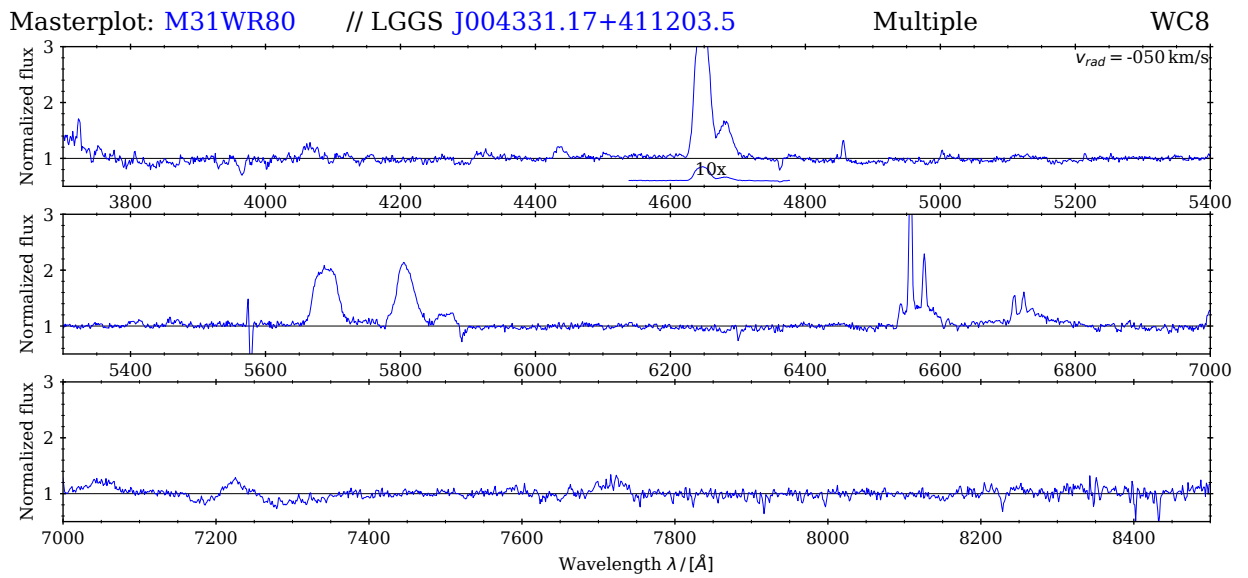


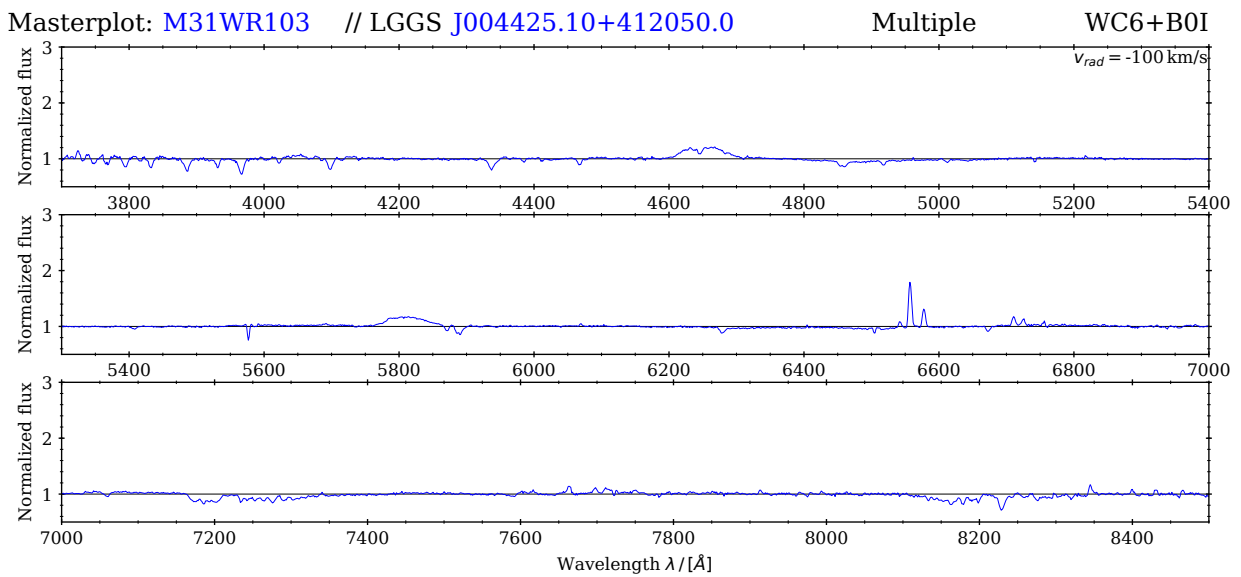
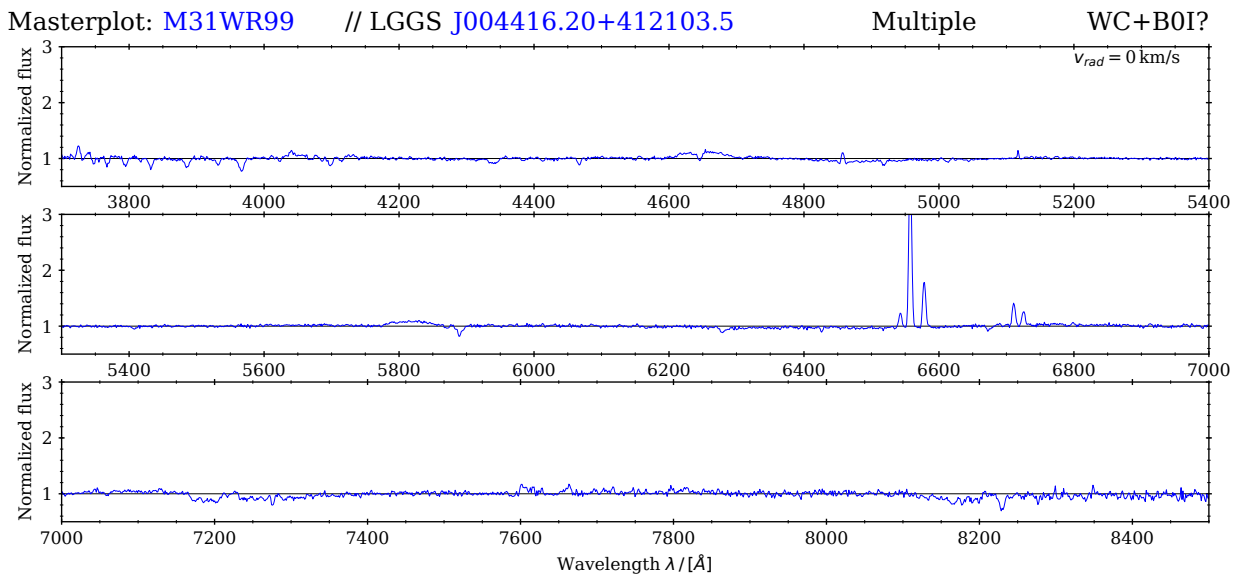
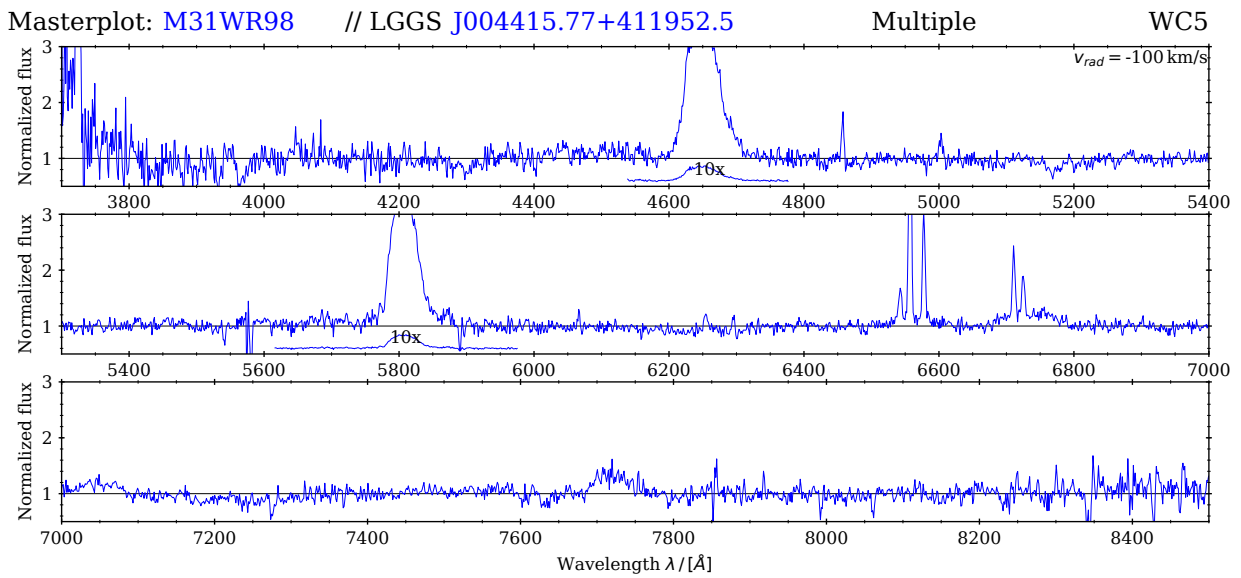


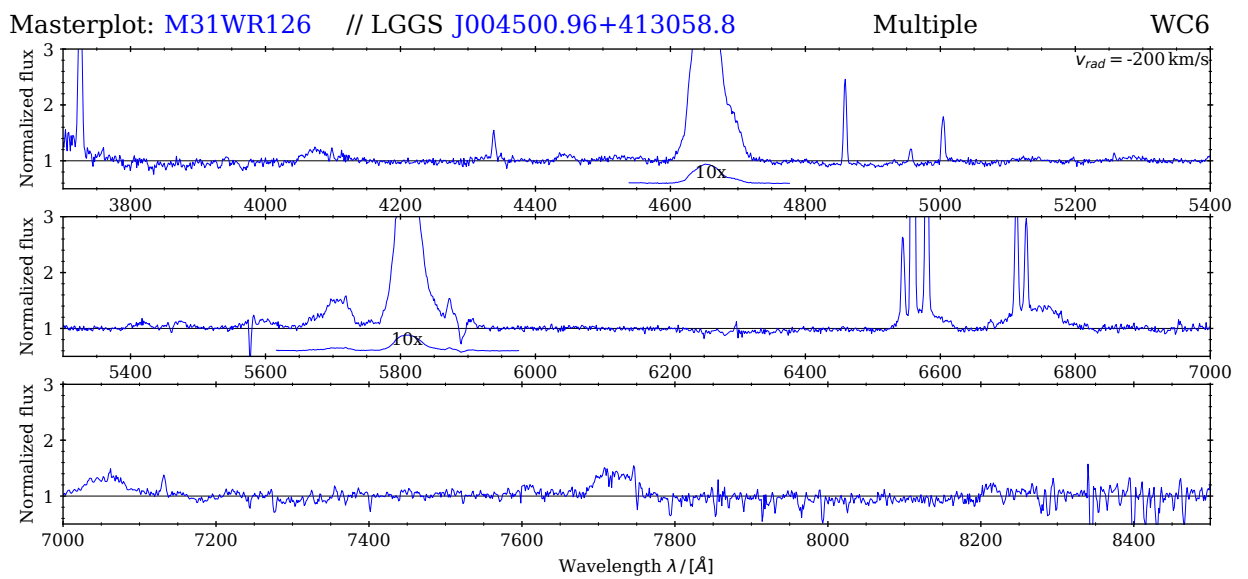
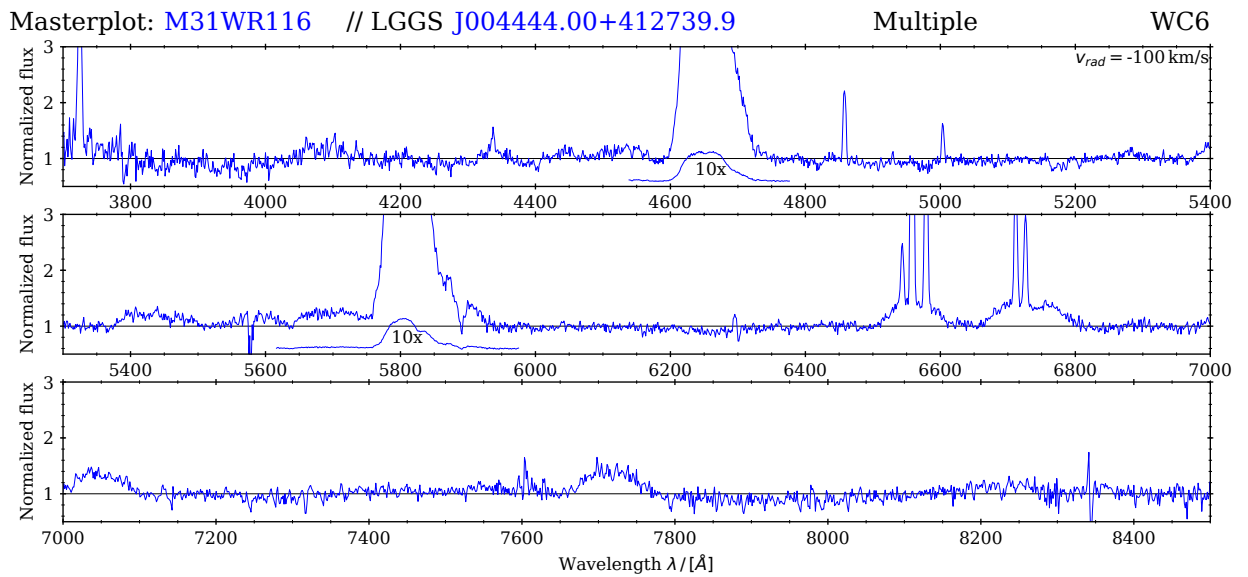
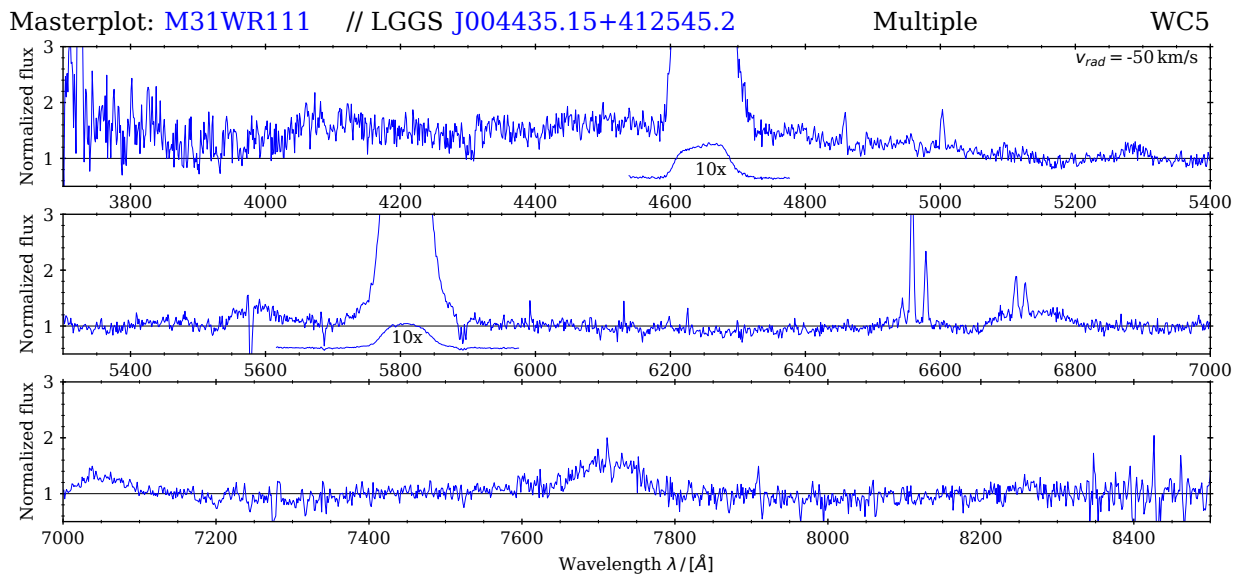


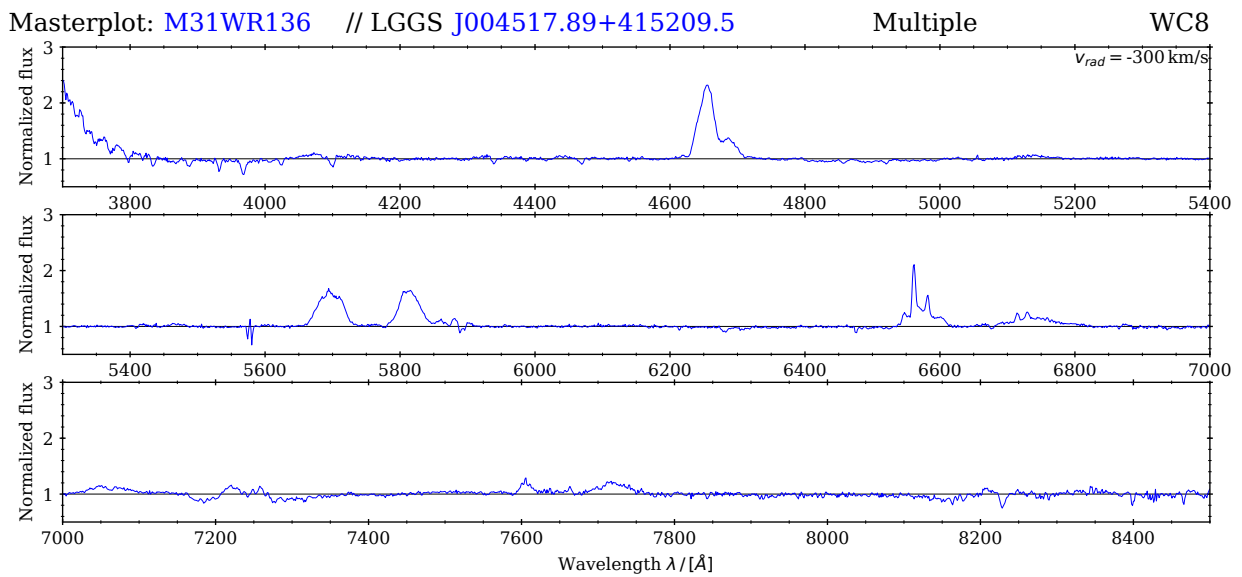
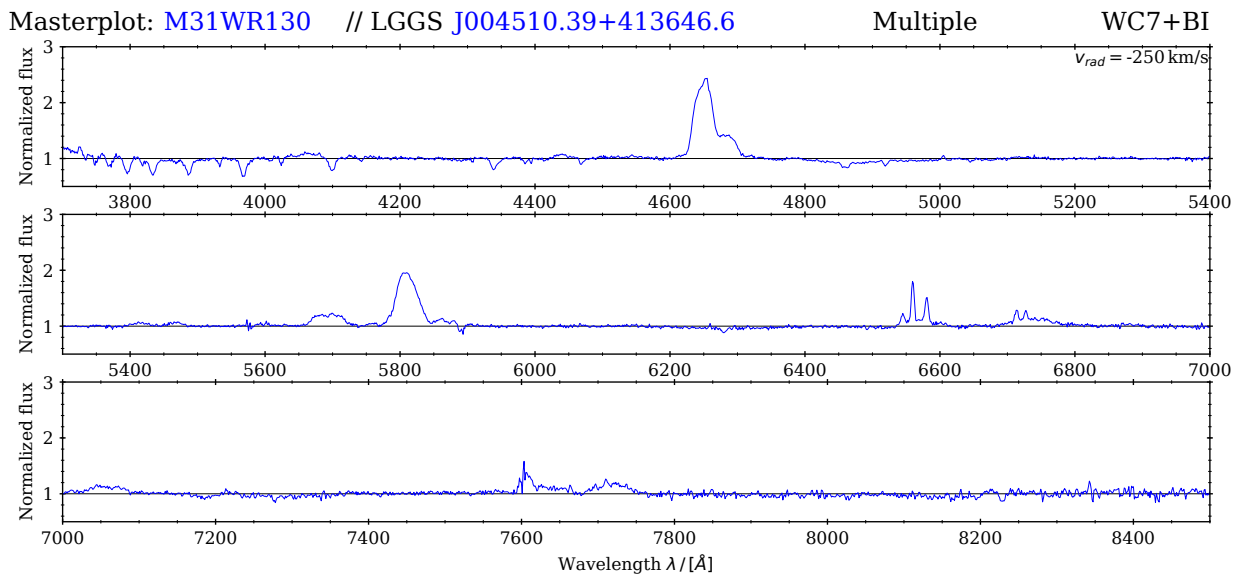
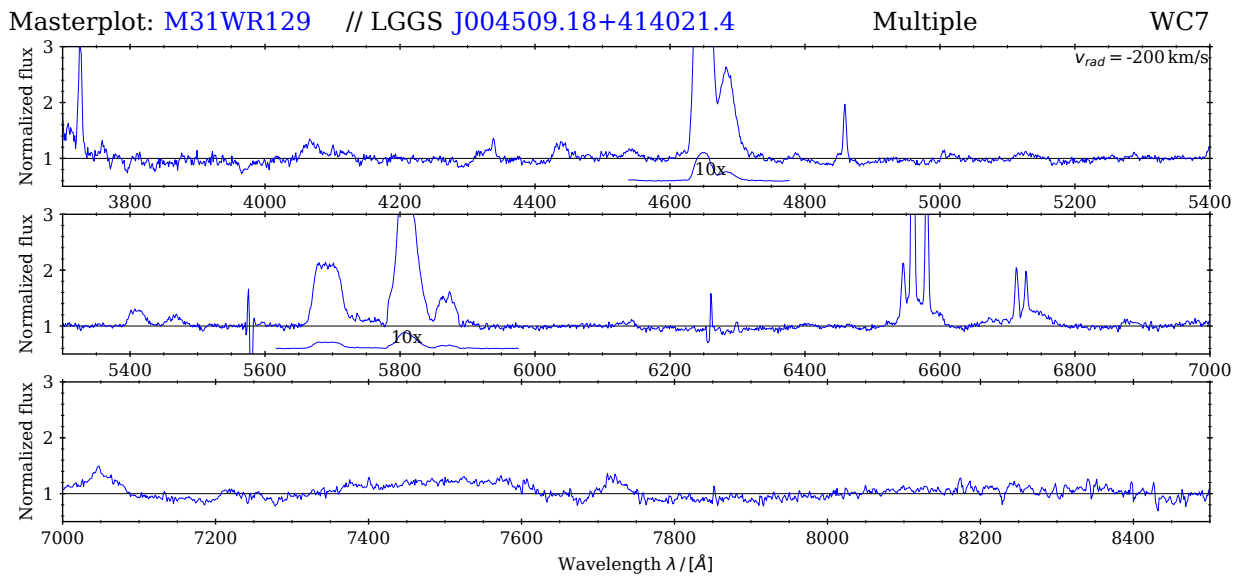


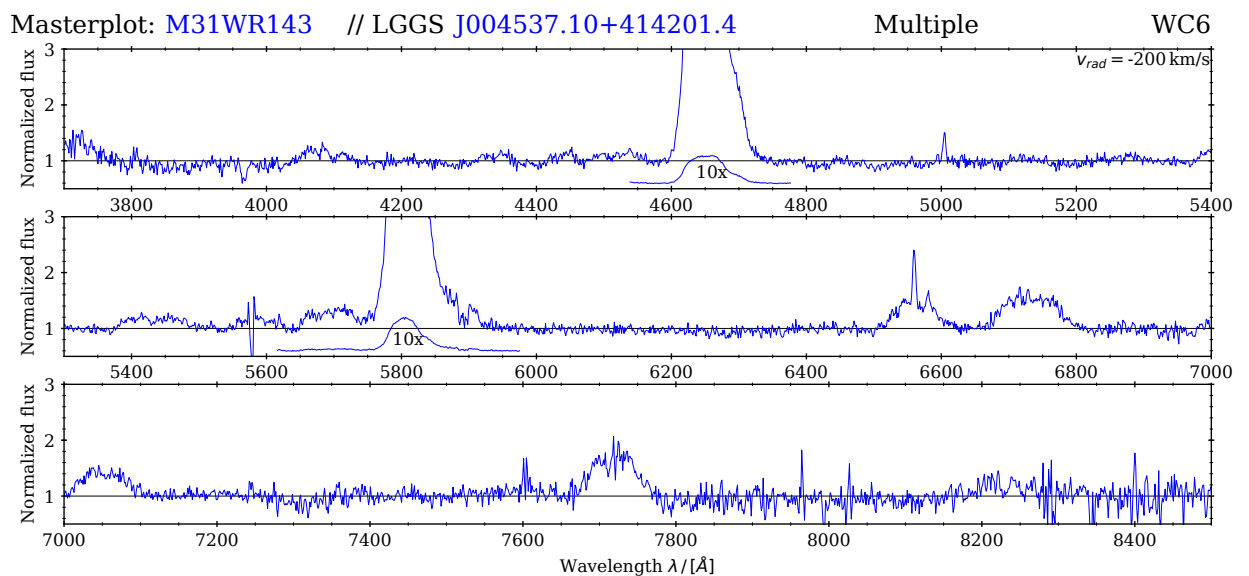
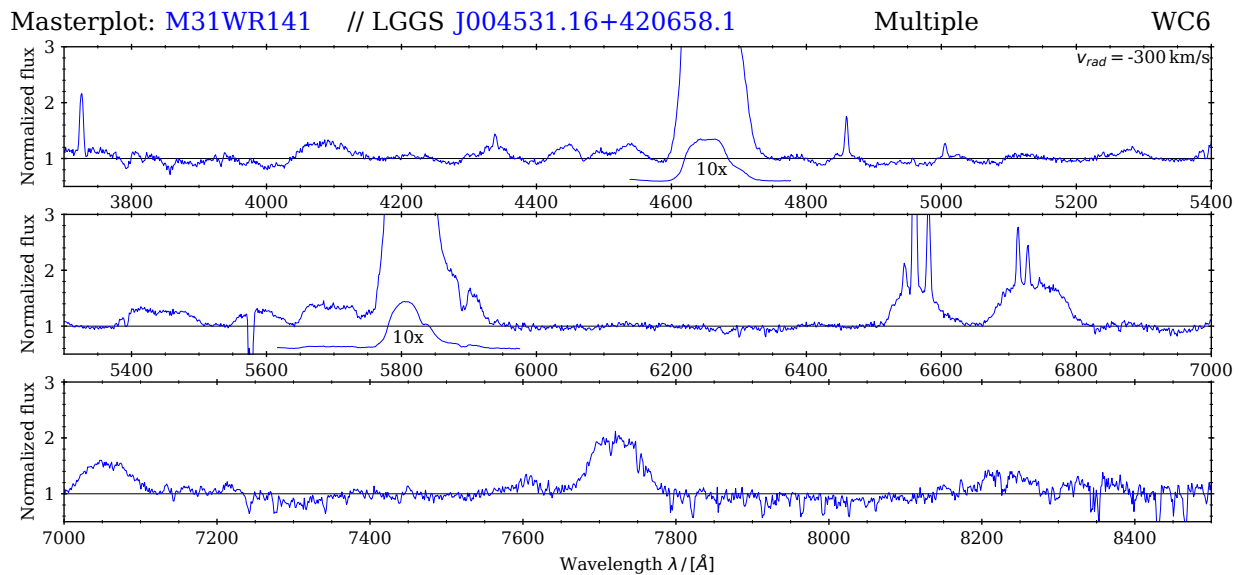
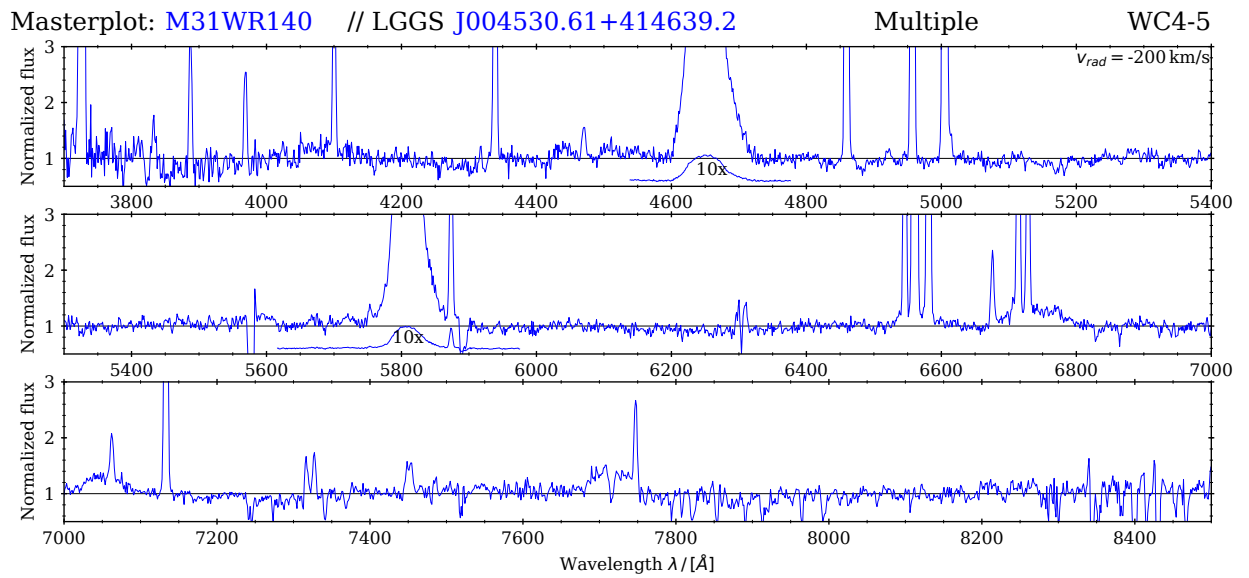




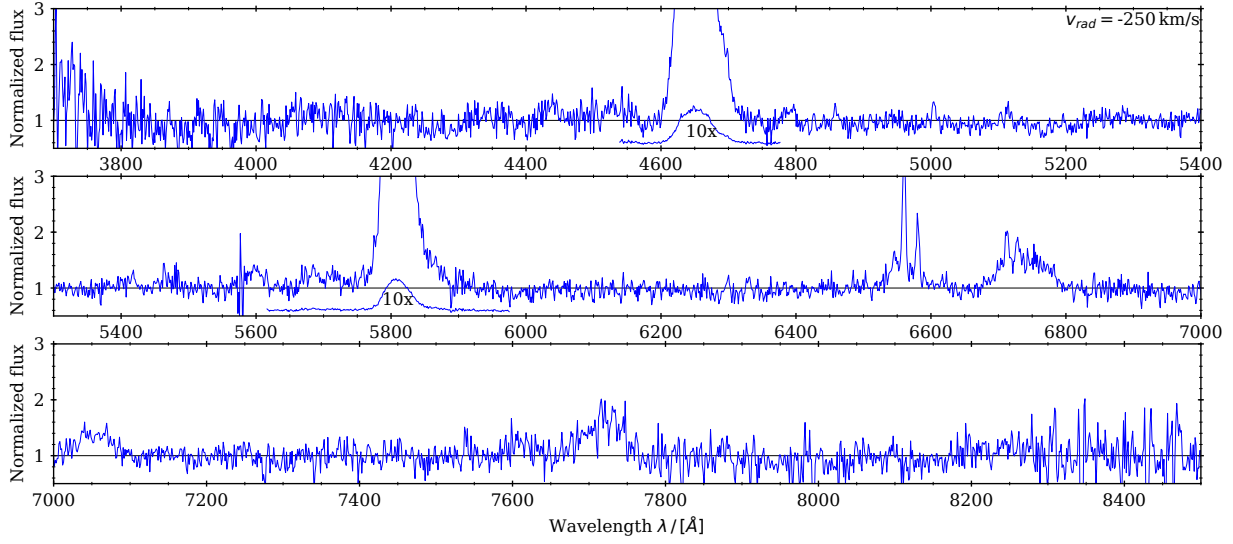








Masterplot: M31WR146 // LGG5 J004539.35+414439.8 Multiple WC5



D Deutsche Zusammenfassung

Die vorliegende Arbeit befasst sich mit einer Spektralanalyse von Wolf-Rayet Sternen der Kohlenstoffsequenz in der Andromeda Galaxie. Wolf-Rayet (WR) Sterne sind massereiche Sterne in späten Entwicklungsstadien. Durch ihre hohe Leuchtkraft erfahren massereiche Sterne einen strahlungsgetriebenen Massenverlust, gemeinhin als Sternwind bezeichnet. Dieser Sternwind sorgt einerseits dafür, dass massereiche Sterne im Laufe ihres kurzen Lebens einen Großteil ihrer Masse verlieren und gibt ihnen andererseits ihr signifikantes Spektrum, das sich rein aus Emissionslinien zusammensetzt, welche sich im Sternwind formen. Abhängig von den Elementen, deren Emissionslinien das Spektrum dominieren, sind WR Sterne weiter unterteilt. WN bezeichnet einen Stern der von Stickstoff geprägt ist, WC einen Stoff mit Kohlenstoff- und WO einen Stern mit Sauerstofflinien. Der Fokus dieser Arbeit liegt auf den WC Sternen. Grundlage der Arbeit sind optische Spektren aller 62 in der Andromeda Galaxie (M31) bekannten WC Sterne, komplementiert durch UBVRI Photometrie für selbige Sterne aus der Local Group Galaxy Survey (LGGS). Der erste Schritt ist die Überprüfung der vorhandenen Spektren auf Kontamination durch andere Objekte anhand des Vorhandenseins von Absorptionslinien und der Ausdünnung der charakteristischen Emissionslinien. Dies reduzierte die Zahl der verwendbaren Spektren auf 23. Der große Vorteil der Analyse von WR Sternen in M31 ist einerseits, dass durch die Zugehörigkeit zur Andromeda Galaxie die Unsicherheit in der Distanz zu den Sternen verringert wird und, dass andererseits M31 eine mit der Milchstraße vergleichbare Metalizität aufweist.

Für die Spektralanalyse wurde der Potsdam Wolf-Rayet Modellatmosphären (PoWR) Code genutzt. Dieser berechnet die Strahlungstransportgleichungen und non-LTE Besetzungszahlen in einer expandierenden 1D Atmosphäre und erzeugt ein emergentes und flusskalibriertes Spektrum. Dieses wird dann mit der Beobachtung verglichen um die Parameter der Sterne anhand ihrer Spektren zu bestimmen. Im Zuge der Analyse wurden für die 23 Sterne insgesamt mehr als 400 Modellatmosphärenmodelle gerechnet. Dabei wurden die Sternparameter Temperatur, Massenverlust, Leuchtkraft, die Windparameter sowie die elementaren Häufigkeiten variiert und so angepasst um die Beobachtung zu reproduzieren. Weiterhin geben die Spektren Aufschluss über die Radial- als auch Rotationsgeschwindigkeit.

Die gefundenen Parameter werden dann mit Sternevolutionsmodellen verglichen. Es zeigt sich ein vergleichbares Bild zu früheren Analysen von galaktischen WC Sternen, bei denen Evolutionsmodelle nur wenig Übereinstimmung mit den gefundenen WC Parametern haben. In der vorliegenden Arbeit wurde erstmals der Fokus auf die Reproduktion der prominenten Emissionslinien gelegt, welche in früheren Analysen häufig außen vor gelassen wurden. Es zeigt sich, dass die vorigen Arbeiten gefundene, strenge Korrelation zwischen WC Subtyp und Temperatur deutlich weniger prägnant ist. Weiterhin wurde gefunden, dass Sterne, die zwar gleich klassifiziert sind, trotzdem deutlich unterschiedliche Parameter aufweisen können. In der Konsequenz bedeutet dies, dass der Spektraltyp eines Sternes innerhalb des WC-Stadiums keine Aussage zur Natur des Sterns oder seinen Parametern zulässt.

Auch wurde gefunden, dass einige der Sterne extrem schnell rotieren. Sie übersteigen dabei zum Teil ihre kritische Rotationsgeschwindigkeit, bei der der Stern beginnt auseinander zu brechen. Dies hat zwei Konsequenzen, einerseits muss die Fliehkraft verursacht durch eine solch schnelle Rotation bei hydrodynamischen Modellen mit beachtet werden, andererseits erfordert die mit der Rotation einhergehende Verformung des Sterns ein Übergang zu 3D-Modellatmosphären. Eine detaillierte Analyse für einen Stern hat gezeigt, dass ein Teil des Windes mit dem Stern korotiert, was dazu führt, dass die Sterne nicht überkritisch rotieren $\tilde{\omega} \frac{1}{4} r_{den}$.

Die Ergebnisse dieser Arbeit sind allerdings mit Vorsicht zu behandeln. Einerseits ist die Zahl der untersuchten Sterne mit 23 gering, andererseits ist für eine Spektralanalyse von massereichen Sterne die Kombination von optischen und UV Daten empfehlenswert um Uneindeutigkeiten in der Parameterbestimmung zu vermeiden.

Selbstständigkeitserklärung

Hiermit versichere ich, dass ich die vorliegende Masterarbeit ohne fremde Hilfe angefertigt und keine anderen als die angegebenen Quellen und Hilfsmittel benutzt habe. Alle Teile, die wörtlich oder sinngemäß einer Veröffentlichung entstammen, sind als solche kenntlich gemacht. Die Arbeit wurde noch nicht veröffentlicht oder einer anderen Prüfungsbehörde vorgelegt.

Potsdam, den

.....
(Unterschrift)